

# Cortical excitability in young adults with specific phobia

-

Inauguraldissertation  
zur  
Erlangung des Doktorgrades  
der Humanwissenschaftlichen Fakultät  
der Universität zu Köln  
nach der Promotionsordnung vom 18.12.2018

vorgelegt von

Lena Pokorny  
aus  
Bad Honnef

07. Februar 2022

verfasst in englischer Sprache

Diese Dissertation wurde von der Humanwissenschaftlichen Fakultät der Universität zu Köln im Juni 2022 angenommen (Beschluss des Promotionsausschusses vom 20.10.2010).

## Acknowledgement

My first thank you goes to Prof. Stephan Bender, who accompanied and supervised me at every step of my dissertation. Thank you for the last 3.5 years, during which we discussed problems together and solved them every now and then. Thank you also for meeting my mistakes with humor and then helping me to overcome them " Help Mr. Bender, I have lost Cz".

Many thanks also to Prof. Alexander Gerlach for his supervision, opinion, and support, without which it would not have been possible for me to follow this path.

I would also like to thank my colleagues Eva Breitingner and Lea Biermann for the great cooperation, mental support and lots of gallows humor.

Another thank you goes to my parents Andrea and Stefan Pokorny, to my brother and his wife Fabian and Felicia Pokorny, and to the rest of my family, who have always been supportive and encouraging. Thanks also to my aunt Antje Pokorny Almeida, who did the proofreading of every part of my dissertation even though I often gave her little time for it.

A final and biggest thank you goes to my partner Robin Sluzalek, who celebrated both successes and failures with me, stood by my side with advice and was always my biggest fan. Thank you for your support, patience and consideration, which made this time easier for me. Thank you for never doubting me and making me feel that I can do anything. Without you, successes wouldn't have felt as good and setbacks would have been more frustrating. I am glad to have you by my side.

Thank you!

## Table of contents

1	Introduction.....	5
1.1	Specific phobias as a group of anxiety disorders .....	5
1.1.1	Classification and diagnosis criteria of specific phobias.....	5
1.1.2	Epidemiology .....	6
1.1.3	Etiology .....	6
1.1.4	Treatment options.....	9
1.2	Neurobiological foundations of anxiety .....	9
1.2.1	Processing anxiety in the brain.....	9
1.2.2	Altered neurophysiology in specific phobias.....	11
1.3	Transcranial magnetic stimulation .....	13
1.3.1	Physical basics .....	13
1.3.2	Resting motor threshold.....	16
1.3.3	The TMS-evoked potential and the TMS-evoked N100 .....	17
1.3.4	Disentangling the TMS-evoked potential: Artefacts and lateralization of the TMS-evoked potential.....	18
2	Embedding three publications of this dissertation .....	19
2.1	Study 1: Single-Pulse TMS to the Temporo-Occipital and Dorsolateral Prefrontal Cortex Evokes Lateralized Long Latency EEG Responses at the Stimulation Site.....	20
2.1.1	Introduction.....	20
2.1.2	Materials and Methods .....	22
2.1.3	Results .....	28
2.1.4	Discussion .....	40
2.2	Study 2: Topography and lateralization of long-latency trigeminal somatosensory evoked potentials.....	46
2.2.1	Introduction.....	46
2.2.2	Methods and Material.....	48
2.2.3	Results .....	57
2.2.4	Discussion .....	70
2.3	Study 3: Fearful facial expressions reduce inhibition levels in the dorsolateral prefrontal cortex in subjects with specific phobia .....	75
2.3.1	Introduction.....	75
2.3.2	Methods and Material.....	77
2.3.3	Results .....	81
2.3.4	Discussion .....	87
3	Overarching conclusion and Outlook .....	92
4	Declaration of contributions to the publications .....	97
5	References.....	98
6	Supplementary Material.....	115

## 1 Introduction

The emotion anxiety is essential for human survival, a natural phenomenon that warns of threatening situations. However, anxiety can become excessive and pathological, impairing the efficacy of this important survival mechanism. A systematic analysis of the dysfunctional cortical mechanisms in anxiety disorders is of particular benefit for understanding the pathophysiology and developing treatment techniques for this group of mental disorders. This dissertation focuses on the most common group of anxiety disorders, specific phobias, and the study of their cortical mechanisms in young adults.

A combination of transcranial magnetic stimulation (TMS) and electroencephalogram (EEG) can be used to visualize those mechanisms. TMS-EEG is a complex method that has great clinical utility when used correctly. However, the interpretation of TMS-evoked potentials (TEPs) is challenging and highly debated in the current TMS-EEG literature. For this reason, a second focus of this dissertation addresses the basics of TMS-EEG methodology. The methodological knowledge gained was then taken into account in the interpretation of our clinical research.

### 1.1 Specific phobias as a group of anxiety disorders

#### 1.1.1 Classification and diagnosis criteria of specific phobias

In the DSM-5, specific phobias, together with generalized anxiety disorder, panic disorder, agoraphobia, social anxiety disorder, and separation anxiety disorder are classified as anxiety disorders. Five related disorders are also classified as anxiety disorders (post-traumatic stress disorder, acute stress disorder, obsessive-compulsive disorder, adjustment disorder and selective mutism), which are not discussed in detail (American Psychiatric Association, 2022). Specific phobias are described as a severe and persistent fear of a particular object, situation or activity that is usually not dangerous to an extent, that the fear would be justified. A phobia is characterized by the phobic stimulus almost always causing anxiety for a period longer than 6 months. The confrontation with the phobic stimulus is either avoided or only overcome with great fear, so that the avoidance behavior or the fear leads to significant impairments in the affected person's life. Furthermore, a specific phobia may only be coded if the symptoms cannot be better explained by another mental disorder, such as another anxiety or related

disorders. The following different subtypes of specific phobia are distinguished: animal type (e.g. insects, dogs), blood-injection-injury type, natural environment type (e.g. flood, storm), and situational type (e.g. lift, plane) (Meermann & Okon, 2005).

### 1.1.2 Epidemiology

Anxiety-, trauma- and stressor-related disorders have with 16% the highest lifetime prevalence among the mental disorders (Beesdo-Baum & Knappe, 2012; Kessler et al., 2009). Their origin can often be identified already in childhood or adolescence (Paus et al., 2008; Zimmermann et al., 2019). Specific phobias have the highest lifetime prevalence rates among anxiety disorders of around 12% (Beesdo-Baum & Knappe, 2012; Kessler et al., 2005; Stinson et al., 2007), with the subtype of animal phobia being most prevalent (approximately 3-5%), followed by the situational type, blood-injection-injury type, and the rather rare natural environment type (Becker et al., 2007; Wardenaar et al., 2017). Meta-analytic data have suggested that after separation anxiety disorder, specific phobia has the earliest onset of all anxiety disorders at 11.0 years [95%CI 8.25 to 13.65] (de Lijster et al., 2017).

Furthermore, comorbidity rates between specific phobia and other mental disorders have been estimated to be 81.0%, with specific phobia predominantly preceding the comorbid disorder (Magee et al., 1996; Wardenaar et al., 2017).

Gender differences have also been discussed, with women being more than twice as likely as men to develop a specific phobia (15.7% vs. 6.7%) (McLean et al., 2011). However, women not only show higher prevalence rates but also tend to be more often comorbid with another anxiety disorder or depression (McLean et al., 2011).

### 1.1.3 Etiology

Despite their high prevalence, current literature has described that the development and maintenance of specific phobias have not yet been fully understood (Adams et al., 2014; Mineka & Oehlberg, 2008). Nevertheless, there are different theories that have been discussed to best explain the phenomena observed in specific phobias. Some researchers have suggested that phobias are primarily the product of associative conditioning processes. Others rely on biological explanations. The following is a non-exhaustive description of different etiological approaches.

The oldest and long most convincing model for the development of phobias is Mowrer's two-factor theory, which combines classical and operant conditioning (Mowrer, 1947). The two-factor theory distinguishes between two components: fear acquisition and maintenance (Mowrer, 1947). Fear acquisition follows the principle of classical conditioning in which a fear-inducing situation (unconditioned stimulus (US)) that leads to an unconditioned fear response (UCR) is coupled with a previously neutral stimulus (conditioned stimulus (CS)). By coupling, the CS then leads to a conditioned fear response (CR) when presented alone (Mowrer, 1939, 1956). An example of the acquisition of a specific phobia through classical conditioning would be that a person in a crowded lift experiences an excessive proximity of other people (UCS), which evokes an unconditioned aversive feeling of fear (UCR). Using the lift is now bound to this aversive feeling (CS) what results in fear when riding in a lift (CR) (Mowrer, 1947, 1960; Wittchen & Hoyer, 2011). Maintenance, on the other hand, works according to the principle of operant conditioning, introduced by Skinner in the 1930s (Skinner, 1938). The conditioned stimulus (CS) is coupled with the expectation that aversive feelings will be evoked (C-). Therefore, the CS, in our example the lift, is avoided, which leads to an omission of the expected negative reaction (C-). Due to the avoidance behavior, the coupling between CS and UCS cannot be extinguished by relearning (Mowrer, 1960; Wittchen & Hoyer, 2011).

A reformulation of the classical conditioning theory came from Seligman (1971), who has highlighted that there are stimuli that trigger more often phobias than others. He explained this with a biological preparedness for evolutionarily relevant stimuli that facilitates the learning of fear in response to these stimuli.

A critique of the classical conditioning paradigms came from Rachman, who has described in his three-way theory that phobias can be acquired not only through classical conditioning, but also through vicarious exposure and the transmission of information and instructions (Rachman, 1977). Vicarious conditioning and information transmission can also take place without direct contact with the phobic stimulus (Rachman, 1977). In vicarious conditioning, a phobia is acquired through modelling, such as by observing models behaving fearfully towards a stimulus (Coelho & Purkis, 2009; Cook & Mineka, 1990; Rachman, 1977). As a third way of fear acquisition, Rachman has suggested the transmission of information and instruction by

family members or peers, through which we learn to distinguish dangerous from harmless situations (Rachman, 1977).

Furthermore, the theory of non-associative account emerged as an explanatory model for specific phobias, based on the observation that phobias can occur without prior learning experience (Menzies & Clarke, 1995). Menzies and Clarke (1995) have proposed that Rachman's three pathways need to be supplemented by a fourth non-associative pathway. The theory of non-associative accounts assumes, according to Charles Darwin's assumptions about natural selection, that there is a set of evolutionary relevant stimuli that trigger fear at first encounter (Menzies & Clarke, 1995; Poulton & Menzies, 2002). These include, for example, fear of heights, water or loud noises (Menzies & Clarke, 1995).

Further biological approaches came from Öhman and Mineka (2001) who have proposed a fear module, a system that has evolved evolutionarily for adaptive problem solving in life-threatening situations (Coelho & Purkis, 2009). The relevance of biological approaches is supported by studies on the heritability of specific phobias. A moderate heritability that varies between the subtypes of specific phobia has been discussed (Hettema et al., 2001; Van Houtem et al., 2013) with blood-injury-injection and animal type having the highest inheritance rates (33% and 32%) followed by situational type with 25% (Van Houtem et al., 2013).

A multifactorial theory, known as the vulnerability-stress model, represents an integrative approach in which various approaches of phobia acquisition can be found (Muris et al., 2002; Wittchen & Hoyer, 2011). The vulnerability-stress model (or diathesis-stress model) assumes a certain vulnerability that varies according to intra-individual differences such as gender, age, genetics, and social factors such as attachment, economic class, or family support. In specific phobias, vulnerability may consist of greater activation of the behavioral inhibition system (Gray, 1990; Wittchen & Hoyer, 2011), preparedness, a fear module (Öhman & Mineka, 2001; Seligman, 1971) or the transmission of information and instruction (Rachman, 1977). Exposure to stressful or personal life events present challenges that require an adaptive response to adequately cope with a challenging situation. Psychological factors such as resilience, coping, social support and developmental factors such as impulse control or performance skills subsequently influence the success of an adaptive response to a stressor (Schiele et al., 2020).

If vulnerability persists and psychological and developmental resources are low, the development of a specific phobia is facilitated. As a consequence, phobias can cause acute and long-term effects (Wittchen & Hoyer, 2011).

#### 1.1.4 Treatment options

Generally, a combination of psychotherapy and medication such as serotonin reuptake inhibitors (SSRIs) is recommended for the treatment of anxiety disorders (Bandelow et al., 2021). However, the S3 guideline on the treatment of anxiety disorders does not recommend pharmacological treatment for specific phobias due to an insufficient data basis, but only psychotherapeutic procedures (Bandelow et al., 2021). In particular, extinction-based methods such as exposure therapy (ET) are proposed as psychotherapeutic treatment for specific phobias (Böhnlein et al., 2020). In ET, the CS is repeatedly presented without the US, which leads by systematic desensitization to an extinction of the learned fear response (Craske et al., 2014). With the help of different techniques, patients learn to cope with their anxiety (Adams et al., 2014). Coping methods include relaxation, breathing, or cognitive techniques as summarized by Meuret et al. (2012). The influence of individual coping skills has also been investigated in a recent study, which has described that efficient coping can break the interaction between vulnerability and stressful experiences (Schiele et al., 2020). ET can take place in different forms such as graduated, flooding, virtual or real form (Craske et al., 2014). Interestingly, meta-analytic data have shown that virtual reality exposure is similarly effective compared to real confrontation with the fear-conditioned stimulus (Powers & Emmelkamp, 2008).

## 1.2 Neurobiological foundations of anxiety

### 1.2.1 Processing anxiety in the brain

Every threatening stimulus is processed in the brain and results in a specific fear response. Several brain areas are involved in the processing of fear (Figure 1). Current research has described a two-way framework that distinguishes between a cortical and a subcortical anxiety circuit (LeDoux & Pine, 2016). Whereas the cortical circuit involving the lateral and medial prefrontal cortex produces the conscious feeling of fear, the subcortical circuit involving the amygdala, superior colliculus, basal ganglia, and pulvinar controls behavioral and physiological responses to threat (Carr, 2015; Tao et al., 2021).

The amygdala has been described as the center for the initiation of a fear response and is mostly responsible for the acquisition and storage of fear memories (LeDoux, 2000). The amygdala can be divided into a basolateral nucleus (BLA), a central nucleus (CE), and intercalated cell masses (ICT) (Pape & Pare, 2010). The BLA, which consists of the lateral (LA) and basal (BL) nuclei, is considered the crucial input structure. The LA has been suggested to be responsible for fear learning (Paré et al., 2004). Sensory and auditory information on the threatening stimulus enter the BLA and are transmitted by the LA via ICTs to the CE (Paré et al., 2004). The CE forms the central output structure of the amygdala and is thereby considered the command center for initiating the fear response (Paré et al., 2004; Sotres-Bayon & Quirk, 2010).

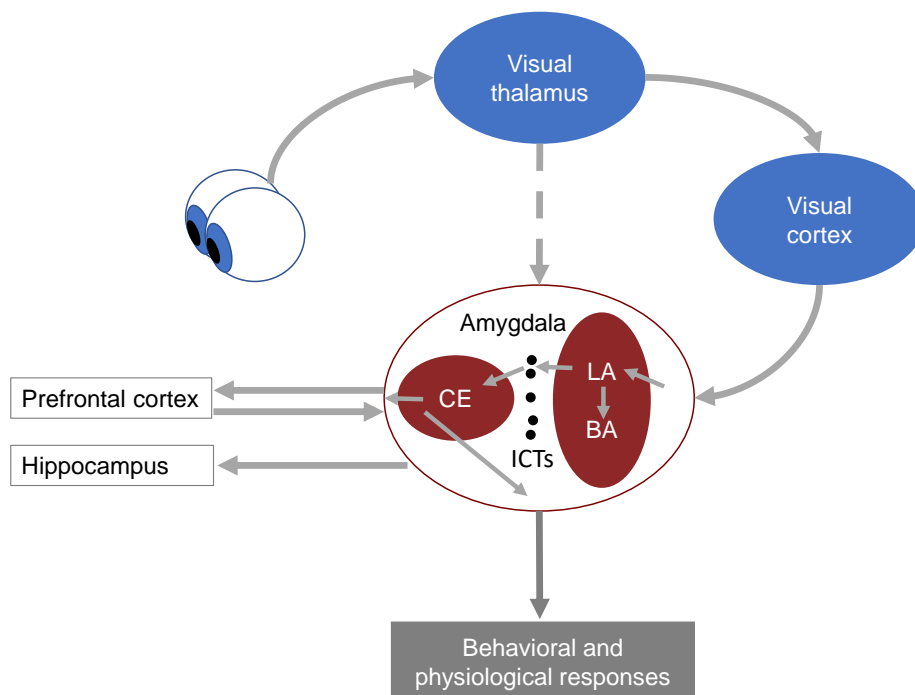


*Figure 1.* A simplified illustration of fear processing using the example of a threatening visual stimulus. The visual thalamus sends information about the stimulus to the visual cortex, where the information is fully processed and then transmitted to the amygdala. The visual thalamus sends rough, unprocessed information directly to the amygdala to allow fast preparation of the body for the threat. The information enters the amygdala via the basolateral nucleus consisting of the lateral nucleus (LA) and basal nucleus (BA) and is then transmitted via intercalated cell masses (ICT) to the central nucleus (CE). In the CE, the behavioral and physiological body response is initiated and information are transmitted to prefrontal areas and the hippocampus (figure according to LeDoux, 2000; Nuss, 2015; Paré et al., 2004)

Furthermore, the dorsal anterior cingulate cortex (DACC), medial and dorsolateral prefrontal cortex (MPFC, DLPFC) have been suggested to play a role in the regulation of fear. The DACC and MPFC receive and transmit glutamatergic projections to and from the amygdala (Nuss, 2015). While the MPFC has been thought to be involved in the experience of fear by modulating activity in the amygdala, the DLPFC has been said to play a crucial role in attentional control (Grace & Rosenkranz, 2002). The DLPFC has been suggested to be responsible for enabling goal-directed behavior through the successful shielding of threatening and interfering stimuli (Sagliano et al., 2016). Neuroimaging studies have shown a functional connectivity between the amygdala and prefrontal areas with top-down and bottom-up pathways of communication (Stujenske & Likhtik, 2017). In this context, the DLPFC has been said to be responsible for top-down regulation of the amygdala during fear processing (Bishop, 2009; Hariri et al., 2000). This is supported by studies that have described an association between DLPFC activation and a decrease of bottom-up limbic-amygdala responses (Ganella et al., 2017; Hariri et al., 2000). Furthermore, the DLPFC has been said to be responsible for shielding the attention from interfering or irrelevant information by selectively suppressing the amygdala (Grace & Rosenkranz, 2002). Studies have suggested that the prefrontal top-down regulation of the amygdala works via activation of GABAergic interneurons (Garcia, 2017; Grace & Rosenkranz, 2002; Paré et al., 2004).

Another structure, relevant for fear processing is the hippocampus. The hippocampus has been said to be crucial for the modulation and storage of contextual information of a threatening situation. Through its connection with the basal nucleus of the amygdala, this contextual information can gain emotional significance (LeDoux, 2000; Quirk & Mueller, 2008).

### 1.2.2 Altered neurophysiology in specific phobias

Individuals with a specific phobia show increased activity levels in the amygdala and limbic system in response to threat compared to controls (summarized by Garcia, 2017). For the prefrontal cortex, on the other hand, imaging studies showed reduced activation with increasing anxiety levels (Bishop et al., 2004). The functional balance of activity between the prefrontal and limbic systems thus appears to be unbalanced in individuals with specific phobia. Limbic areas predominate and counteract a relatively weak prefrontal activity. This imbalance is supported by studies on specific phobias that have described deficits in cognitive

control in form of an impaired ability of the DLPFC to inhibit interfering information (Bishop et al., 2007; Del Casale et al., 2012). Hariri et al. (2000) have also suggested that deficits in the ability to modulate the emotional response prefrontally through cognitive labelling and reasoning, may be crucial for the development of a specific or other anxiety disorder.

Furthermore, a reduction in working memory capacity has been discussed with anxiety. It has been said that threat-related thinking may claim a large part of the working memory resources, leaving little for the actual task (Fales et al., 2008). This leads to a deficient functional cognition and impairs goal-directed behavior. This has been supported by studies describing an attentional bias with increased brain activation response in spider phobic individuals to phobic-relevant information (Schienle et al., 2005; Straube et al., 2004). Inhibitory interneurons may contribute to the affected ability of goal-directed behavior, as inhibitory interneurons in the DLPFC have been thought to be responsible for shielding the behavioral goal from the influence of interfering stimuli (Grace & Rosenkranz, 2002; Rosenkranz & Grace, 2001).

On a neurochemical level, various neurotransmitters are discussed with specific phobias. It is well known that phobic stimuli increase the cortisol level in individuals with specific phobia (Alpers et al., 2003; Fredrikson et al., 1985; Garcia, 2017) what leads to norepinephrine release in the amygdala. A norepinephrine sensitization has been suggested to be associated with a deficient GABAergic inhibitory control resulting in a hyperactivation of the amygdala (Garcia, 2017). Furthermore, Bhagwagar et al. (2004) have described an increased GABA-concentration in the brain after the administration of SSRIs. Additionally, threatening stimuli has been said to increase the dopamine level in the amygdala which suppressed GABAergic inhibition (Garcia, 2017; Marowsky et al., 2005; Nikolaus et al., 2010). Serotonergic dysfunction and its influence on the GABAergic system has also been a recurring theme with regard to specific phobias (Freund et al., 1990). Especially in the context of fear extinction, serotonin has been suggested to play a crucial role (Garcia, 2017). A dysfunction of the serotonergic system could thus be connected to a deficient ability of fear extinction and decoupling of CS and CR in specific phobias.

Overall, various neurochemical dysfunctions in specific phobia have been associated with altered GABA transmission. GABA thus appears to be a crucial factor in the development and maintenance of specific phobias as well as other anxiety disorders. For this reason, its function in phobias is described in more detail below.

### 1.2.2.1 $\gamma$ -Aminobutyric acid and its role in specific phobias

$\gamma$ -Aminobutyric acid (GABA) is the main inhibitory neurotransmitter in the brain and thus influences various physiological and psychological processes (Cryan & Kaupmann, 2005; Mombereau et al., 2004). It is crucial in both presynaptic and postsynaptic inhibition of neurons and is synthesized from glutamate (Bandelow et al., 2017). Ligand-gated ionotropic GABAA and GABAC receptors and metabotropic GABAB receptors are distinguished (Mombereau et al., 2004). Whereas GABAA and GABAC receptors have integral chloride channels and lead to quick inhibition, GABAB receptors are coupled to separate  $K^+$  or  $Ca^{2+}$  channels via G-protein and result in slower but prolonged inhibition (Enz & Cutting, 1998; Jie et al., 2018).

The role and mechanisms of action of GABA in specific phobias are not yet fully understood. Nevertheless, there are already studies that have investigated the role of GABA in relation to anxiety disorders. For example, reduced GABAA receptor binding has been found in patients with generalized anxiety disorder (Pollack et al., 2005) and panic disorders (Malizia et al., 1998). Anxiolytic drugs like benzodiazepines have been said to bind to GABAA-receptors and thus quickly increase the release of GABA (Schandry, 2016). The comorbidity of anxiety disorders and alcohol abuse has also been suggested to be due to the anxiolytic effect of alcohol through its GABAA receptor binding (Kushner et al., 2000).

GABAB receptors have been suggested to be highly concentrated along the dendrites of pyramidal neurons in the basolateral amygdala (McDonald et al., 2004). For this reason, GABAB has been discussed to play an important role in the regulation of emotional behavior (Cryan & Kaupmann, 2005). Furthermore, animal studies have indicated that the prefrontal cortex might reduce anxiety by GABAB-mediated top-down control of the amygdala (Cryan & Kaupmann, 2005; Garcia, 2017; Paré et al., 2004).

## 1.3 Transcranial magnetic stimulation

### 1.3.1 Physical basics

TMS, first introduced by Barker and colleagues (Barker et al., 1985), is a non-invasive method of neurostimulation. Over the last few years, TMS has become increasingly important in the research of biomarkers and therapy of various diseases like depression or anxiety disorders, as TMS can be used to investigate cortical excitability (Croarkin et al., 2011; Teng et al., 2017). TMS is based on Faraday's law of electromagnetic induction (Galili et al., 2006) and can be

used to investigate dynamic changes in brain activity (Massimini et al., 2005; Rogasch & Fitzgerald, 2013). According to the principle of electromagnetic induction, an electric current produced by a coil induces a magnetic flux. This magnetic field in turn induces an electric field in the conductor, here the brain, that is aligned perpendicular to the magnetic field (Figure 2) (Hallett, 2007). If the induced transcellular current exceeds the stimulus threshold of horizontally running axons, a depolarization of cortical neurons occurs. Crucial for the magnetic stimulation of axons is the parallel orientation of the induced electric field to the skull because horizontally oriented axons are thus best stimulated (Kammer & Thielscher, 2018). The neuron depolarization triggers an action potential and due to the connectivity of the activated neurons, a transaxonal current flow is produced (Reti, 2015). Magnetic fields can pass non-conductive structures such as bone, so that neurons can be stimulated without invasive intervention (Kammer & Thielscher, 2018; Merton & Morton, 1980). This is the main difference to electrical stimulation, which can only stimulate superficially.

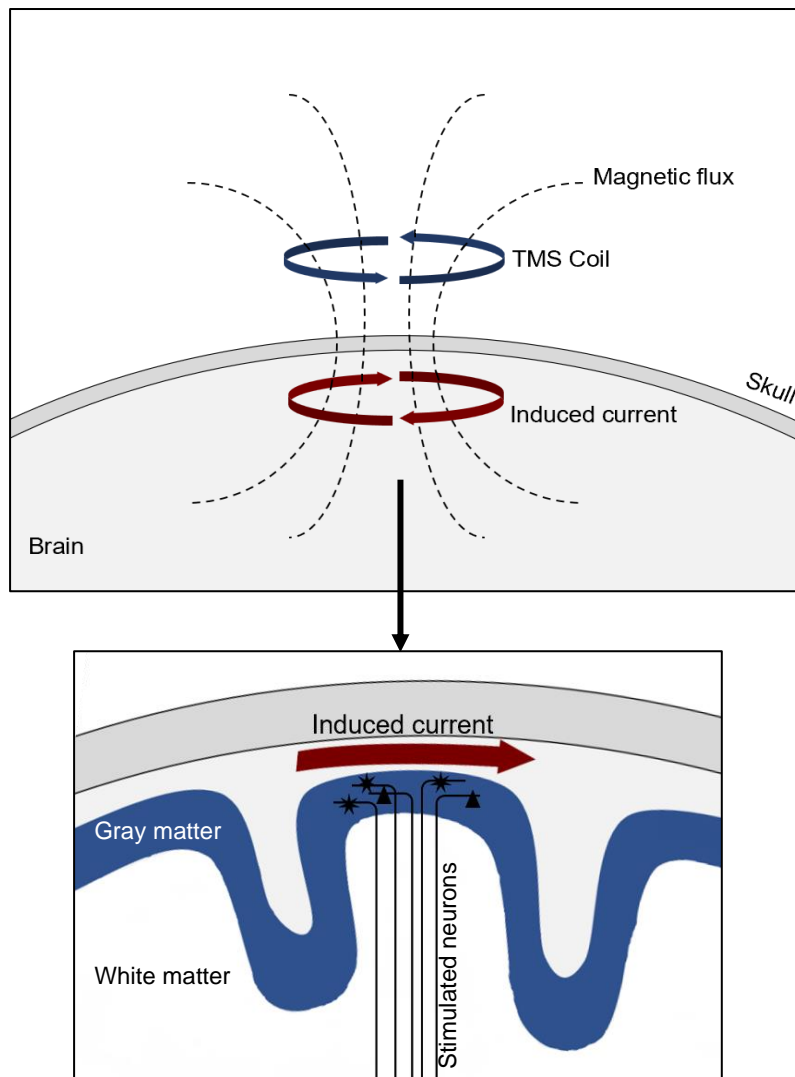


*Figure 2.* Transcranial Magnetic Stimulation (TMS). According to the principle of electromagnetic induction, an electric current generated by a coil induces a magnetic flux, which in turn induces an electric field in the brain. Neurons aligned parallel to the coil are stimulated (figure according to Hallett, 2000).

There are different types of TMS coils. With simple round coils, the intensity of the induced electric field decreases towards the center and there is no current in the center of the field (Hallett, 2007) (Figure 3). In contrast, double coils, so-called figure-of-eight coils, are used for focal, punctual stimulation (Figure 3). Here, two coils are placed next to each other through which the current flows in opposite directions. This leads to a summation in the middle and thus to an increase in the strength of the magnetic field, which can reach a flux density of up to 2 tesla in conventional magnetic coils and last for about 100  $\mu$ s (Hallett, 2007; Kammer & Thielscher, 2018; Weyh & Siebner, 2007). In our studies, we used a focal figure-of-eight coil as described in the methods and material sections of the studies.

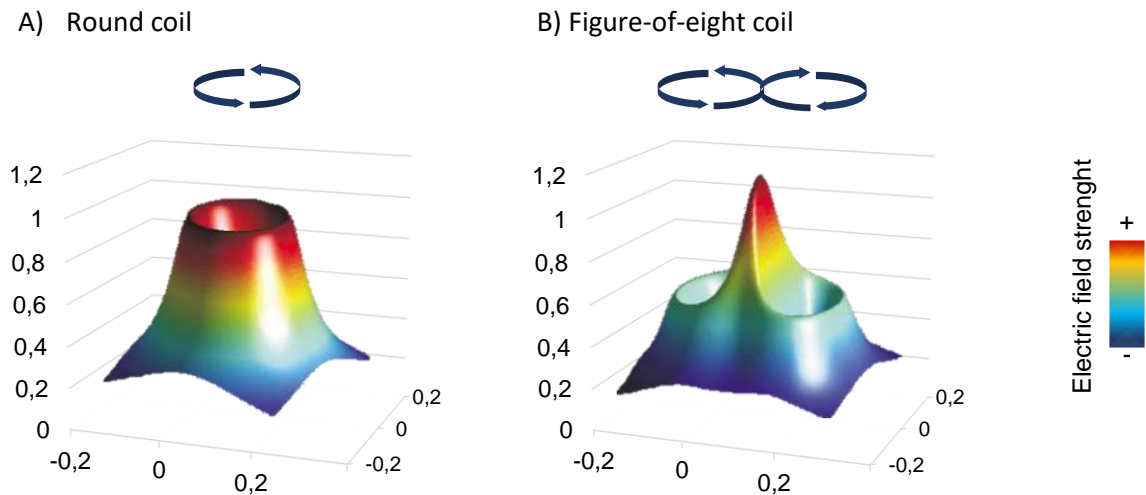


*Figure 3.* Different types of TMS coil, produces different electrical fields. (A) With a simple round coil, there is no current in the center. (B) The figure-of-eight coil enables a focal stimulation with a maximum intensity in the center (figure according to Kammer & Thielscher, 2018).

### 1.3.2 Resting motor threshold

As described above, the excitability of cortical neurons can be measured with TMS, although, excitability varies significantly between individuals. Thus, it is important to use a stimulation intensity that corresponds to the individual's excitability threshold. To determine individual excitability, the threshold in the motor cortex (M1) is often used since M1 is the only region where TMS results in a directly measurable physiological output in the form of a motor evoked potential (MEP) (Kammer et al., 2001). According to the International Federation of Clinical Neurophysiology (IFCN), the resting motor threshold (RMT) corresponds to the stimulation intensity sufficient to evoke an MEP in the resting muscle of the hand of about 100  $\mu\text{V}$  in 10 out of 20 cases (Rossini et al., 1994). Later, it has been described that a MEP has to exceed 50  $\mu\text{V}$  in 10 out of 20 stimulations (Rothwell et al., 1999; Westin et al., 2014; Ziemann, 2003). In 2-5% steps, the TMS intensity has to be increased successively until the MEP exceeds 50  $\mu\text{V}$  (Rossini et al., 1994).

Further procedures for RMT hunting refer to the maximum likelihood method (Awiszus, 2003) and replace the 10 out of 20 stimulations procedure.

### 1.3.3 The TMS-evoked potential and the TMS-evoked N100

When stimulating with TMS, time-locked neuronal responses are called TMS-evoked potentials (TEP) and can be visualized via a simultaneously running EEG recording. TEP deflections reflect both the activity of the transcranially stimulated neuron populations of the stimulated brain region and the indirect activation of other functionally coupled neurons. TEPs are characterized by positive or negative peaks in the EEG signal that has been suggested to be a summation of synchronous excitatory and inhibitory post-synaptic potentials (Kirschstein & Köhling, 2009; Rogasch & Fitzgerald, 2013) (Figure 4). In the literature, several positive and negative components have been described to occur reliably within approximately 300ms after a TMS pulse. Often studied components are the TMS-evoked N15, P30, N45, N100, and P180 after TMS of M1 and the N40, P60, N100 and P185 as reliable peaks after TMS of the DLPFC (Hill et al., 2016; Komssi & Kähkönen, 2006). The N100 represents the most frequently investigated component, especially in M1 but has also been described in the DLPFC (Bender et al., 2005; Lioumis, Kicić, et al., 2009; Tallus et al., 2013), and represents the target parameter for this dissertation. The N100 has been said to reflect GABAB-mediated inhibitory processes (Premoli, Castellanos, et al., 2014; Rogasch et al., 2015). Thus, the amplitude of the TMS-evoked N100 can be used as a direct parameter for intracortical inhibition in the DLPFC and M1, which is relevant when aiming to investigate inhibitory mechanisms in the DLPFC in anxiety disorders.

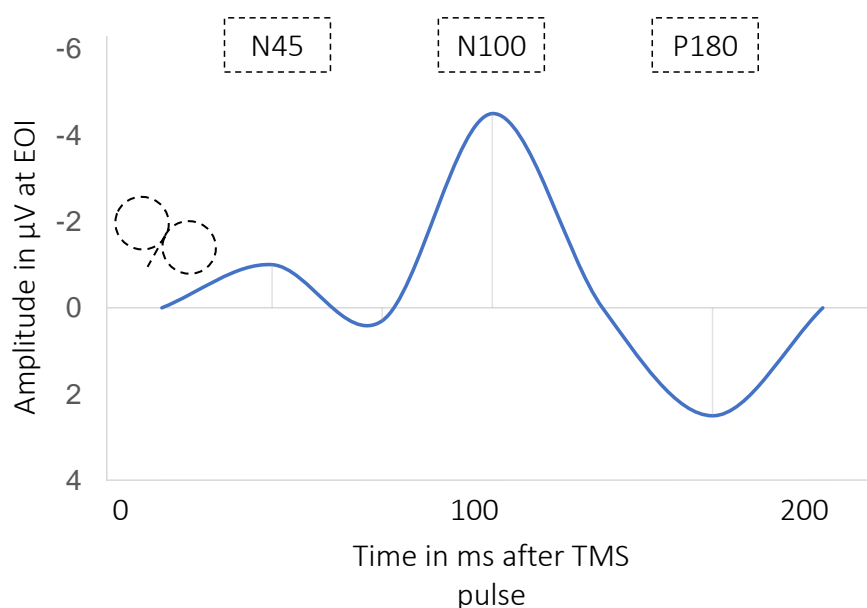


*Figure 4.* Schematic illustration of an EEG-wave complex at an electrode of interest (EOI) that depends on the stimulated area following a TMS pulse.

#### 1.3.4 Disentangling the TMS-evoked potential: Artefacts and lateralization of the TMS-evoked potential

TMS is a complex method that requires a lot of knowledges about the correct application. There has been a discussion on how TMS-EEG studies should be designed to best generate reliable data (Belardinelli et al., 2019; Conde et al., 2019). With TMS, not only cortical neurons, but also nerve afferents like V1 of the trigeminal nerve are excited what leads to a tapping sensation on the surface of the scalp. The resulting potentials are called trigeminal somatosensory evoked potentials (SSEPs). Furthermore, the discharge of the TMS coil is accompanied by a clicking sound, that results in auditory processing and produces auditory evoked potentials (AEPs) (Ilmoniemi & Kičić, 2010; Rogasch & Fitzgerald, 2013). Thus, not all recorded EEG data that build the TEP represent real transcranially evoked activity when TMS is applied.

There have been different approaches to disentangle sensory and transcranially evoked activity and to develop techniques to remove artifacts like AEPs or SSEPs in EEG data preprocessing (Rocchi et al., 2021; Rogasch et al., 2014). Furthermore, sensory masking has been discussed to eliminate possible confounders. However, a complete sensory masking has been described to be difficult to apply and/or to result in an impairment of the signal (Lioumis et al., 2018). Another approach is the systematical analysis of the lateralization and latency of sensory potentials to be able to differentiate them from transcranially evoked activity. While there has been a lot of research on AEPs (Hine & Debener, 2007; Nikouline et al., 1999; ter Braack et al., 2015), there is unfortunately a lack of data on trigeminal SSEPs in time windows that are relevant for the often-used TMS-evoked N100. The trigeminal nerve innervates a large part of the sculp and forehead and can thus contribute to the TEP when TMS is applied to different brain areas like the DLPFC or M1 (Fillmore & Seifert, 2015).

Furthermore, to be able to distinguish sensory from transcranial activity by lateralization and latency, knowledge about the lateralization and latency of transcranially evoked potentials is necessary. The TMS-evoked N100 has been suggested to have its maximum ipsilateral to the TMS stimulation side (Bender et al., 2005; Bonato et al., 2006). However, there is also literature that has described the N100 to be constant and symmetrical at the vertex during the stimulation of different brain areas (Du et al., 2017). Furthermore, some authors have argued that the N100 could be related to sensory processes. For this reason, more studies are

needed on both the lateralization and latency of the TMS-evoked N100 as well as on co-evoked potentials such as trigeminal SSEPs.

## 2 Embedding three publications of this dissertation

This dissertation is embedded in the overarching study "Cortical excitability and anxiety disorders in children, adolescents and young adults", which addresses the pathophysiological mechanisms in anxiety disorders. Within the framework of this study, six different samples were recruited, subdivided according to age and/or group of anxiety disorder (Table 1).

This dissertation represents a partial evaluation of the sample of young adults with specific phobias (Table 1, blue) compared to the group of young adults without any mental disorder (Table 1, green). Through this comparison, cortical mechanisms are to be investigated regarding their relevance for the pathophysiology of specific phobias.

Table 1. *Overview of all planned samples within the study called "Cortical Excitability and Anxiety Disorders in Children, adolescents and young Adults".*

Samples	Age	
	8-17 years	18-25 years
Comprehensive anxiety disorders <ul style="list-style-type: none"> <li>• generalized anxiety disorder</li> <li>• separation anxiety disorder</li> <li>• social anxiety disorder</li> </ul>	Children and adolescents with anxiety disorders	Young adults with anxiety disorders
Specific phobias	Children and adolescents with specific phobia	Young adults with specific phobia
Control group	Children and adolescents without any mental disorder	Young adults without any mental disorder

*Note.* The two samples that were evaluated for this dissertation are marked in blue and green columns.

Since we have learned that TMS-EEG can be used to visualize cortical mechanisms but is a complex method in which the interpretation of TEPs is challenging, two preliminary studies were conducted in this dissertation to address the basics of TMS-EEG methodology. The knowledge gained about the best possible interpretation of TEPs was then applied to the interpretation of the results on patients with specific phobia compared to controls.

Thus, three papers have been written and published in scientific journals within the framework of this cumulative dissertation: two methodological papers and one with a clinical sample.

## 2.1 Study 1: Single-Pulse TMS to the Temporo-Occipital and Dorsolateral Prefrontal Cortex Evokes Lateralized Long Latency EEG Responses at the Stimulation Site

The N100 as a marker of cortical inhibition has been discussed for the investigation of dysfunctions in various mental disorders. Since we have learned that it can be difficult to differentiate between sensory and transcranially evoked activity, the N100 should be further analyzed in terms of its lateralization and property to vary with the side of stimulation. Therefore, a study was conducted in which late components of TMS over the DLPFC were compared with those of TMS over the temporo-occipital cortex regarding systematically lateralized components.

### 2.1.1 Introduction

Since the introduction of transcranial magnetic stimulation (TMS) (Barker et al., 1985), there have been considerable efforts to extend its scope as a clinical and research tool. Repetitive TMS (rTMS) is used in the clinical treatment of depression (Perera et al., 2016). Also, rTMS (George, 2019) and other brain stimulation techniques such as transcranial direct current stimulation (tDCS) (Venkatasubramanian & Narayanaswamy, 2019) are increasingly evaluated as experimental treatments in a variety of neuropsychiatric conditions. The combination of TMS with concurrent electroencephalography (TMS-EEG) allows for the measurement of neural activity resulting directly from the TMS procedure with high temporal resolution in both motor and non-motor cortical regions (Cracco et al., 1989; Ilmoniemi et al., 1997; Tremblay et al., 2019). In the context of neuropsychiatric disorders, TMS-EEG has been used to measure cortical excitability in functionally relevant brain areas such as the primary motor cortex (M1) (Bruckmann et al., 2012) and the dorsolateral prefrontal cortex (DLPFC) (Noda et al., 2017; Voineskos et al., 2018) in attempts to identify biomarkers for cortical dysfunctions. Therapeutic neuromodulation of cortical excitability through brain stimulation techniques could potentially be made more effective if it was possible to measure the activity and monitor the functional changes in the targeted brain region throughout the treatment course. For example, rTMS to the DLPFC for the treatment of depression may benefit from the possibility

to measure and monitor the excitability of the target cortical area with TMS-EEG. However, despite promising attempts to monitor the effects of rTMS and tDCS using TMS-EEG (Alyagon et al., 2020; Helfrich et al., 2012; Moliadze et al., 2018), there is no clear consensus among researchers about which TMS-EEG parameters reflect functions of the targeted brain region. This hinders the further development of TMS-EEG basic research and its translation into clinical practice.

In TMS-EEG, the EEG signal time-locked to the TMS pulse is averaged to obtain TMS-evoked potentials (TEPs). TEP deflections reflect the activity of the targeted populations of neurons resulting from transcranial effects of the changing magnetic field and secondary activation of other functionally connected neurons (transcranially evoked activity). However, TMS also indirectly evokes cortical activity through the unintended activation of sensory peripheral nerves (sensory evoked activity) including auditory activity associated with the coil click and somatosensory activity caused by activation of afferent cranial nerves (Conde et al., 2019; Gordon et al., 2018). Yet, while compound TEPs are a summation of several neural processes, there is no consensus regarding the spatiotemporal pattern reflecting the actual transcranially evoked activity.

The second prominent negative TEP peak, often referred to as TMS-evoked N100 in motor cortex and DLPFC stimulation, is one of the most robust and often studied TEP peaks (Bender et al., 2005; Bonato et al., 2006; Du et al., 2017; Nikulin et al., 2003; Premoli, Castellanos, et al., 2014; Rogasch et al., 2015). It is the TEP deflection with the highest retest reliability (Kerwin et al., 2018). The N100 in TMS applied to M1 has a lateralized maximum over the ipsilateral M1 (Bender et al., 2005; Bonato et al., 2006; Paus et al., 2001), is modulated by the activational state of M1 (Bruckmann et al., 2012) and can be used to successfully monitor excitability changes resulting from rTMS of M1 (Helfrich et al., 2012). These findings are consistent with the notion that the N100 is site-specific and reflects local intracortical excitability–inhibition networks in the targeted brain region. By contrast, other studies found the TMS-evoked N100 to be uniform across several different stimulated brain areas with a stereotypical symmetrical distribution over the vertex irrespective of the targeted cortex region, therefore interpreting it as an unspecific response representing global properties of the brain or even an artifact (Du et al., 2017; Freedberg et al., 2020). In order to use TEPs in neuropsychiatric research and to adequately translate findings into applications as a neurostimulation biomarker, it is crucial to determine which TEP components reflect local cortical properties evoked by direct transcranial effects. Evoked components with a lateralized

site-specific topography (i.e., varying with the stimulated brain region) are most likely transcranially evoked (Conde et al., 2019) and would thus be suitable parameters to study cortical excitability.

Therefore, we studied the spatiotemporal distribution of TEPs during the stimulation of the temporo-occipital cortex (TOC) and the DLPFC of both hemispheres. Although there is still uncertainty regarding late deflections (>80 ms), early TEPs (<80 ms) are more widely recognized to reflect activity of the stimulated cortex (Conde et al., 2019; Du et al., 2017; Herring et al., 2015; Rogasch et al., 2020). We thus focused on late negative deflections corresponding to the N100 in motor cortex stimulation and expected to identify lateralized site-specific components over the stimulated brain region.

## 2.1.2 Materials and Methods

### 2.1.2.1 Ethics Statement

The study protocols were approved by the Ethics Committee of the Faculty of Medicine, University of Cologne, Germany, for DLPFC stimulation (document no. 15-432) and the Ethics Committee of the Technical University Dresden, Germany, for TOC stimulation (document no. EK 184052011). All participants provided written consent after being informed about the study.

### 2.1.2.2 Experimental Design

We integrated the samples of two separate studies. One sample received TMS to the TOC; the other sample received TMS to the DLPFC. For both targeted brain areas, TMS was performed over the left and the right hemisphere sequentially in a counterbalanced order. A quantitative assessment of hemispheric lateralization of TEPs in the stimulated brain region was accomplished through within-subject comparison of left- versus right-sided TMS. As there were some methodological differences between the two studies, we did not intend to make any direct quantitative comparisons (e.g., amplitude differences) between TOC and DLPFC TMS. Therefore, only major differences in the topographies of lateralized TEP (LatTEP) components that cannot be explained by differences between the subjects or methods of the two studies are reported.

### 2.1.2.3 Subjects

Participants were healthy adults who reported no history of neurological or psychiatric disorders and were free of medication at the time of testing. Before participation we screened for exclusion criteria according to established safety guidelines (Rossi et al., 2009). Persons with epilepsy in close relatives were also excluded for safety reasons. The TOC stimulation sample included 17 subjects (mean age,  $24.7 \pm 6.1$  years; 11 female, 6 male subjects; mean, IQ  $113.4 \pm 9.1$ ). The DLPFC stimulation sample included 26 subjects (mean age,  $22.6 \pm 1.8$  years; 23 female and 3 male; mean IQ,  $115.1 \pm 10.1$ ). All participants were right-handed according the Edinburgh Handedness Inventory (Oldfield, 1971).

### 2.1.2.4 Electroencephalography

A 64-channel DC-EEG was recorded concurrently with a TMS procedure. The EEG signal was amplified by a BrainAmp DC amplifier and recorded with a sampling rate of 5,000 Hz using the BrainVision Recorder 1.20 (both Brain Products, München, Germany). Custom-made EEG caps, which were equipped with TMS-compatible Ag/Ag-Cl electrodes, were used for both TOC and DLPFC (EasyCap GmbH, Herrsching, Germany). Electrodes were arranged in equidistant montages on five concentric rings around Cz with electrodes on the horizontal and vertical central line corresponding to the 10–10 system (Chatrian et al., 1985). Other electrodes were named according to the nearest corresponding electrodes in the 10–10 system. Electrode layouts of caps used for TOC and DLPFC were identical, except for additional bilateral supraorbital electrodes and an electrode at the nasion for DLPFC stimulation. For TOC stimulation, Fpz served as reference electrode, whereas for DLPFC stimulation, Cz served as reference electrode during recording. EEG data were re-referenced to an average reference offline, in order to ensure independence of topographies from the reference electrode. Impedances were kept below 10 k $\Omega$ .

### 2.1.2.5 Transcranial Magnetic Stimulation

For TOC stimulation, the TMS procedure was performed using a PowerMAG 100 Stimulator (Mag & More GmbH, München, Germany) with a figure-of-8 coil with an outer diameter of each wing of 70 cm. As the procedure was performed as part of an experiment in which TMS was used to perturb visual working memory processes, the exact placement of the coil was individually determined resulting in some interindividual variation of the locus of stimulation. The site was determined by localizing the visual N700 event-related potential component reflecting visual working memory processes (Bender et al., 2008). The targeted region was

thus in secondary visual areas (V2) located in lower parts of the occipital lobe bordering the temporal lobe (visual “what” pathway) (Clark et al., 2010). The exact procedure used to determine the locus of stimulation is described in the [Supplementary Material](#). In all subjects, the locus of stimulation was located between P7 and P11 for left-sided TMS and between P8 and P12 for right-sided TMS. The interindividual variation of the stimulation location had only a small nonsystematic effect on the TEP topography ([Supplementary Figures 1, 2](#)). The TEPs recorded at the homologous electrodes P9 and P10 were used for further analysis, which best reflected the grand average topographic maximum for the two stimulation sides.

During the stimulation procedure, the coil was held manually by a trained examiner. The coil was placed tangentially to the skull over the stimulated region. The stimulator was externally triggered by a PC running Presentation software 18.1 (NeuroBehavioral Systems, Berkley, CA, United States), which generated transistor–transistor–logic triggers that were also registered in the recording software. A total of 20 TMS single pulses were administered over each hemisphere. High reliability of the data indicated a sufficient signal-to-noise ratio with the amount of trials (see section “*Preprocessing*” and [Supplementary Table 1](#) and [Supplementary Figure 1](#)). The interstimulus intervals varied evenly between 5 and 7 s (mean, 6 s). The participants were instructed to sit upright and still in a chair and to fixate a cross located on a computer screen in front of them in order to reduce movement and eye artifacts.

For DLPFC stimulation, the TMS procedure was applied using a MagPro X100 MagOption stimulator and a figure-of-8 coil with a diameter of 2 × 75 mm (MagVenture, Farum, Denmark). The coil was placed over electrodes F5 for left-sided stimulation and F6 for right-sided stimulation as this method has been recommended as the most accurate to target the DLPFC when individual structural MRI data are not available (Rusjan et al., 2010). The coil was held manually by a trained examiner. Like for TOC stimulation, the stimulator was triggered by the Presentation software. The protocol encompassed a total of 45 TMS single pulses for each hemisphere with interstimulus intervals varying evenly between 5 and 8 s (mean, 6.5 s). High reliability of the data indicated a sufficient signal-to-noise ratio with the amount of trials (see section “*Preprocessing*” and [Supplementary Table 1](#) and [Supplementary Figure 1](#)). The participants were instructed to sit upright and still in a chair and to fixate a cross located on a computer screen.

The stimulation intensity for the stimulation protocol in both groups was set to 120% of resting motor threshold (RMT). To measure the individual RMT in both groups, an electromyogram was recorded from the first dorsal interosseus muscle of the contralateral hand with self-

adhesive electrodes (H207PG/F; Covidien, Mansfield, MA, United States). The active electrode was placed over the first dorsal interosseus muscle; the reference electrode was placed over the basic phalanx of digit III for DLPFC and the proximal interphalangeal joint of digit II for TOC. Motor-evoked potentials (MEPs) were amplified with a Brain Amp ExG MR amplifier (Brain Products, München, Germany). Single pulses were applied at the position over the left primary motor cortex where the most consistent and highest MEP peak-to-peak amplitudes were recorded (hot spot). For TMS to the TOC, RMT was defined as the intensity that evoked an MEP of over 50  $\mu$ V in 5 of 10 stimuli at the hot spot. For the DLPFC, RMT was determined by applying single TMS pulses at the hot spot in varying intensities according to the maximum likelihood method (Awiszus, 2003) using the software TMS Motor Threshold Assessment Tool (MTAT 2.0<sup>1</sup>). Mean RMT was  $65.9\% \pm 7.0\%$  stimulator output for TOC and  $51.6 \pm 10.0$  stimulator output for DLPFC. As TEP amplitudes are affected by the stimulation intensity, a comparison of amplitudes across groups is not possible, and only amplitude comparison within subjects can be interpreted. Notably, shifts of topographies do not result from changes of stimulation intensities.

Previous studies suggesting that TMS evokes invariable potentials located at the vertex were performed without white noise or somatosensory masking (Du et al., 2017). Also, it is uncertain whether masking procedures can eliminate sensory input completely from the overall evoked potentials (Biabani et al., 2019; Conde et al., 2019; Siebner et al., 2019). As our aim was to identify lateralized site-specific components in compound TEPs including sensory activity, we performed TMS without masking procedures.

#### 2.1.2.6 EEG Data Analysis

##### *Preprocessing*

The EEG was analyzed offline with Brain Vision Analyzer 2.1 software (Brain Products, München, Germany). The EEG data were re-referenced to the average reference. The sampling rate was reduced to 500 Hz. As down-sampling in Brain Vision Analyzer includes an automatic filtering process (low-pass filter 225 Hz, 24 db/oct), a slight broadening of the high amplitude TMS pulse artifact occurred. In order to prevent a contamination by the pulse artifact, the time segments from -10 to 40 ms in TOC stimulation and from -10 to 20 ms in DLPFC stimulation around the TMS pulse were removed and then linearly interpolated (Thut et al., 2011) different time segments were interpolated, because the duration of the high-amplitude TMS artifact differed slightly between groups). The EEG was then segmented into epochs of -500 to 500 ms relative to the TMS pulse. A baseline correction procedure was

performed with the interval of –110 to –10 ms serving as the baseline (the last 10 ms before the onset of TMS were not included in the baseline to exclude contamination of the baseline by a distortion of the TMS artifact). Epochs were visually inspected for artifacts and were removed if artifacts severely affected further analysis of the segment. Further artifacts were subsequently removed in an independent component analysis. Later, linear DC trends were removed. All available epochs were averaged to create TEPs.

As the amount of trials per condition was different across the two stimulated brain regions, we assessed the reliability of TEPs to establish that the signal-to-noise ratio was sufficient. To this end, we calculated averages for odd and even TMS trials separately. Preprocessing and peak measurements were performed using the same methodology as reported for the overall TEP averages. The intraclass correlation coefficients for odd and even trials were found to be very high (Supplementary Table 1) (Cicchetti, 1994). The time courses and topographies of odd and even trials were highly consistent in all stimulation conditions (Supplementary Figure 3), indicating a sufficient signal-to-noise ratio.

#### *LatTEP Analysis*

In order to test our hypothesis that TMS evokes activity localized at the stimulation site, we aimed at extracting systematically lateralized activity from the TEPs. To this end, we performed a calculation analogous to the lateralized readiness potential (LRP) (Coles, 1989; Eimer, 1998) with TEPs of homologous electrodes for both stimulation sides. The signals of each pair of homologous electrodes for both stimulation sides are used to calculate a single measure named LatTEP, e.g., for homologous electrode pairs F5 and F6:  $\text{LatTEP F5/F6} = [\text{F5(TMS left)} - \text{F6(TMS left)} + \text{F6(TMS right)} - \text{F5(TMS right)}] / 2$  (analogous to Coles, 1989). The channels resulting from the LatTEP calculation were named LatTEP P9/P10 (temporo-occipital brain region) and LatTEP F5/F6 (frontal brain region). This procedure integrates measurements over both hemispheres (i.e., ipsilateral electrodes and homologous contralateral electrodes) for TMS to both sides. It eliminates processes that are either symmetrical to the midline or asymmetrical but localized in the same hemisphere irrespective of the side of stimulation (e.g., left-sided preponderance for both left- and right-sided TMS). The procedure retains systematically lateralized activity from the original evoked potentials, i.e., activity that changes hemispheres depending on the side of stimulation.

### *Peak Detection*

We aimed at measuring the peak amplitude of the long-latency negative peak of the TEP. Peaks were detected automatically and confirmed by visual inspection in both regular TEPs and LatTEPs. In order to determine the search window for peaks, we inspected the grand average latencies at electrodes overlying the respective site of stimulation and compared the results with latencies reported in the literature.

For DLPFC stimulation, we searched for the maximum amplitude in the time window from 80 to 140 ms following the TMS pulse in agreement with previous reports (Kerwin et al., 2018; Lioumis, Kicić, et al., 2009). As LatTEP latencies tended to be shorter, a slightly broader peak detection window of 60–140 ms was used for LatTEPs. For TOC stimulation, the second prominent peak showed a markedly longer peak latency and a broader peak, which was in agreement with previous studies (Belardinelli et al., 2019; Herring et al., 2015; Rosanova et al., 2009; Samaha et al., 2017). We thus searched for the maximum amplitude in the time window from 140 to 230 ms. Peak latencies were determined in the reference channel overlying the site of stimulation for each stimulation condition (F5: left DLPFC, F6: right DLPFC, P9: left TOC, P10: right TOC). For the analysis of LatTEPs, the reference channels LatTEP F5/F6 for DLPFC and LatTEP P9/P10 for TOC were used. Amplitudes in all electrodes were measured at this peak latency  $\pm 10$  ms of the respective stimulation condition in all analyzed channels. For the comparison of amplitudes across stimulation sites, we used the amplitudes of all channels overlying the stimulation sites in one of the four stimulation conditions (F5, F6, P9, P10). Additionally, amplitudes in electrode Cz were analyzed as a control location, since a topographic maximum at the vertex has previously been reported (Du et al., 2017). As we analyzed a negative deflection, we henceforth use the term *higher amplitudes* to refer to higher negative voltage values.

#### 2.1.2.7 Statistical Analysis

Statistical analyses were performed using the IBM SPSS Statistics versions 23 and 25 (IBM Corp., Armonk, NY, United States).

TEPs were screened for outliers ( $>3$  standard deviations from the mean), and the Shapiro–Wilk test was used to test for a normal distribution of the data. For DLPFC stimulation, TEP amplitudes included two outliers that caused a violation of normality. These were a result of artifacts that could not be removed adequately through the artifact rejection procedure. After the removal of the two subjects, all variables were normally distributed. The removal of the two subjects did not induce any systematic effects and did not, in particular, produce the

presented results. In the TOC stimulation condition, there were no outlier values, and all parameters were normally distributed.

We tested whether TEP peaks and LatTEP peaks localized at the stimulation sites were significantly different from the baseline with a one-sample *t*-test against the value 0. For TOC and DLPFC stimulation, repeated-measures analyses of variance (ANOVAs) were calculated to test whether the maximum of the TEP was localized at the site of stimulation. The two separate ANOVAs with the dependent variables N100 and N180 amplitudes included the factors TMS SIDE (TMS applied to left side vs. TMS applied to right side), HEMISPHERE (left hemisphere electrodes vs. right hemisphere electrodes), and BRAIN REGION (temporo-occipital electrodes/P9 and P10 vs. frontal electrodes/F5 and F6).

To compare amplitudes at the respective site of stimulation to amplitudes at electrode Cz, repeated-measures ANOVAs were conducted for each dependent variable (N100 and N180 amplitudes) with the factors, TMS SIDE and ELECTRODE LOCALIZATION (factor levels: “electrode at the site of stimulation” and “electrode Cz”).

In order to compare LatTEP amplitudes in the stimulated vs. the non-stimulated cortical region, repeated-measures ANOVAs with the dependent variables LatTEP N100 and LatTEP N180 amplitudes and the factor BRAIN REGION (levels: LatTEP F5/F6 vs. LatTEP P9/P10) were conducted for TOC and DLPFC stimulation.

Significant interaction effects were followed up by further ANOVAs of reduced complexity.

### 2.1.3 Results

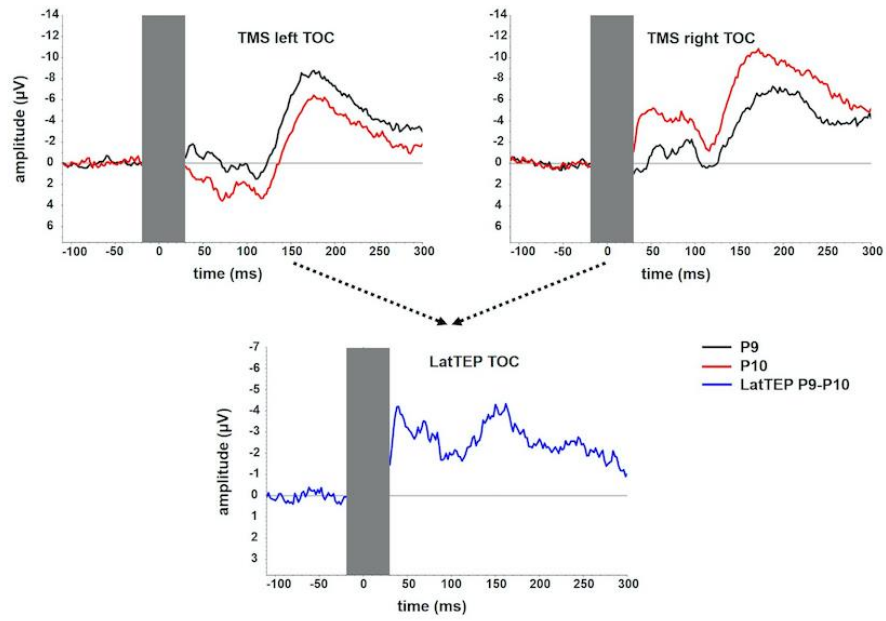
#### 2.1.3.1 Temporo-Occipital Stimulation

##### *TEP Time Course*

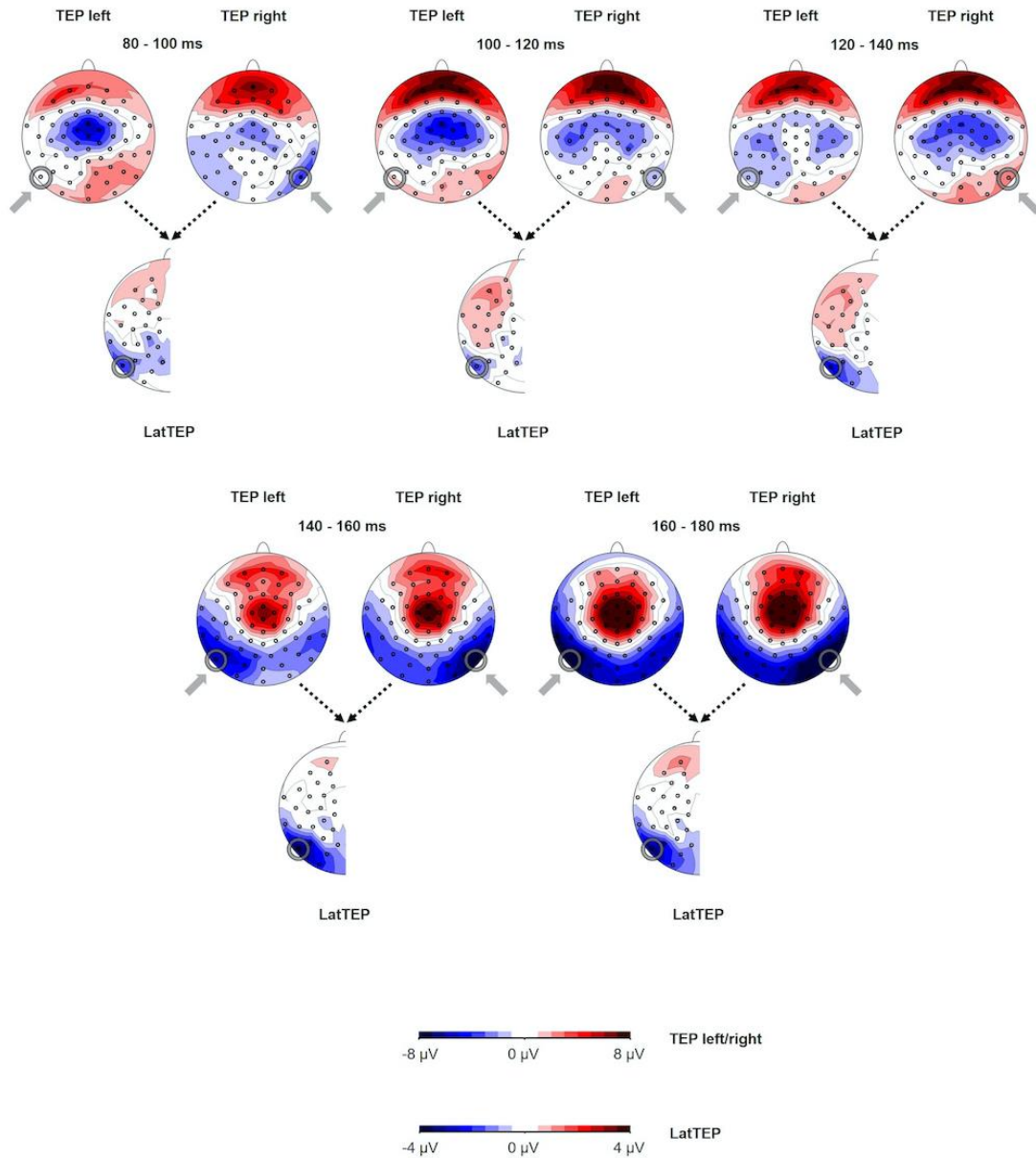
The TEP time course in the electrodes overlying the sites of stimulation showed a first negative deflection at approximately 40 ms, a positive deflection peaking at approximately 110 ms and a more prominent and broader negative deflection peaking at approximately 180 ms (N180). The amplitude of the N180 at the site of stimulation was significantly different from the baseline [at electrode P9 for left TMS:  $t(16) = -5.72$ ;  $p < 0.001$ ; at electrode P10 for right TMS:  $t(16) = -9.37$ ;  $p < 0.001$ ]. The LatTEP time course showed a negative deflection with a peak at approximately 40 ms and another prominent negative peak at approximately 170 ms (LatTEP N180) ([Figure 1A](#)). LatTEP N180 amplitude at electrode LatTEP P9/P10 was significantly different from the baseline [ $t(16) = -5.60$ ;  $p < 0.001$ ].

Study 1: Single-Pulse TMS to the Temporo-Occipital and Dorsolateral Prefrontal Cortex Evokes Lateralized Long Latency EEG Responses at the Stimulation Site

**A**



**B**



*Study 1 Figure 1. (A)* TEP time course at electrodes P9 and P10 for TMS to the left (TMS left TOC) and the right (TMS right TOC) temporo-occipital cortex. The extent to which TEPs are higher (more negative) ipsilateral than contralateral to the side of stimulation is reflected in LatTEP amplitudes. Lateralization of evoked activity from both stimulation sides is condensed in one measure (LatTEP P9/P10). The LatTEP peaks at approximately 170 ms after the TMS pulse. Note the different scaling of the y axis between TEPs and LatTEPs. *(B)* Topographical plots of TEPs in time segments of 20-ms length for TMS to the left (TMS left TOC) and right (TMS right TOC) temporo-occipital cortex. LatTEP topographies are derived from TEP maps of both stimulation sides with each channel calculated according to the LatTEP formula. LatTEP maps show a topographical maximum around electrode LatTEP P9/P10 seen most prominently in the time range from 140 to 180 ms. Note that the color-coding scales differ between TEPs and LatTEPs.

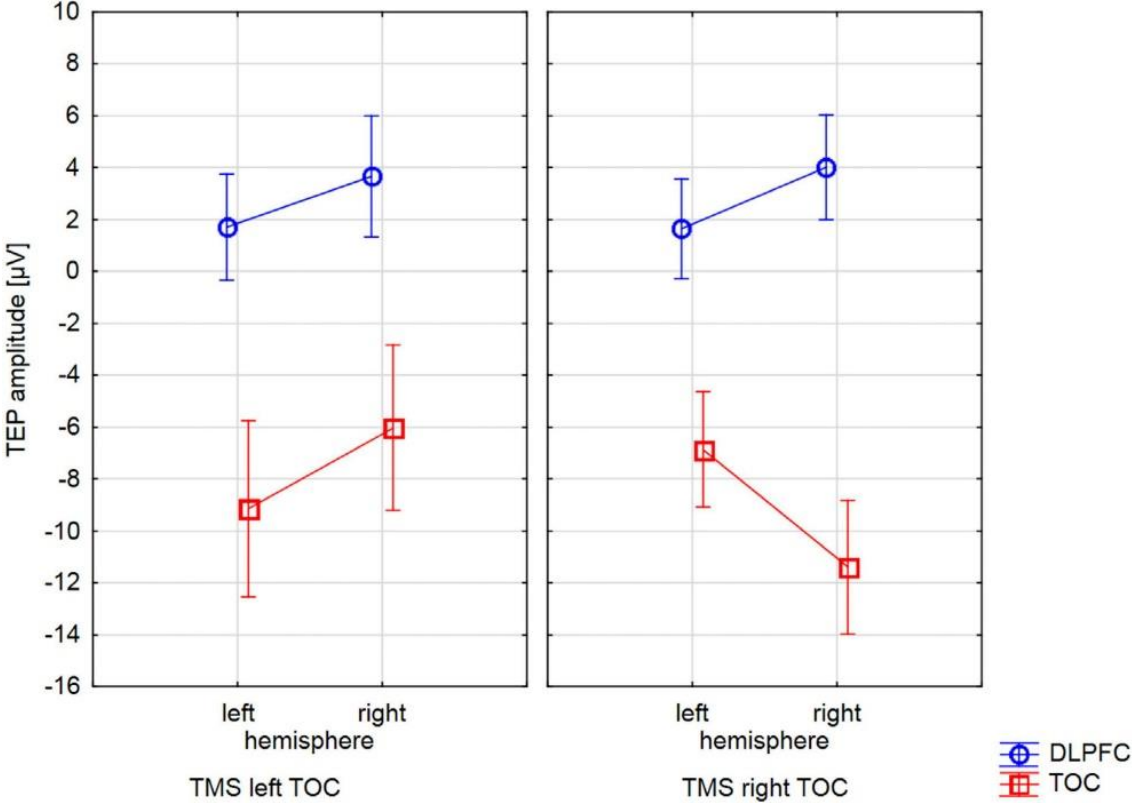
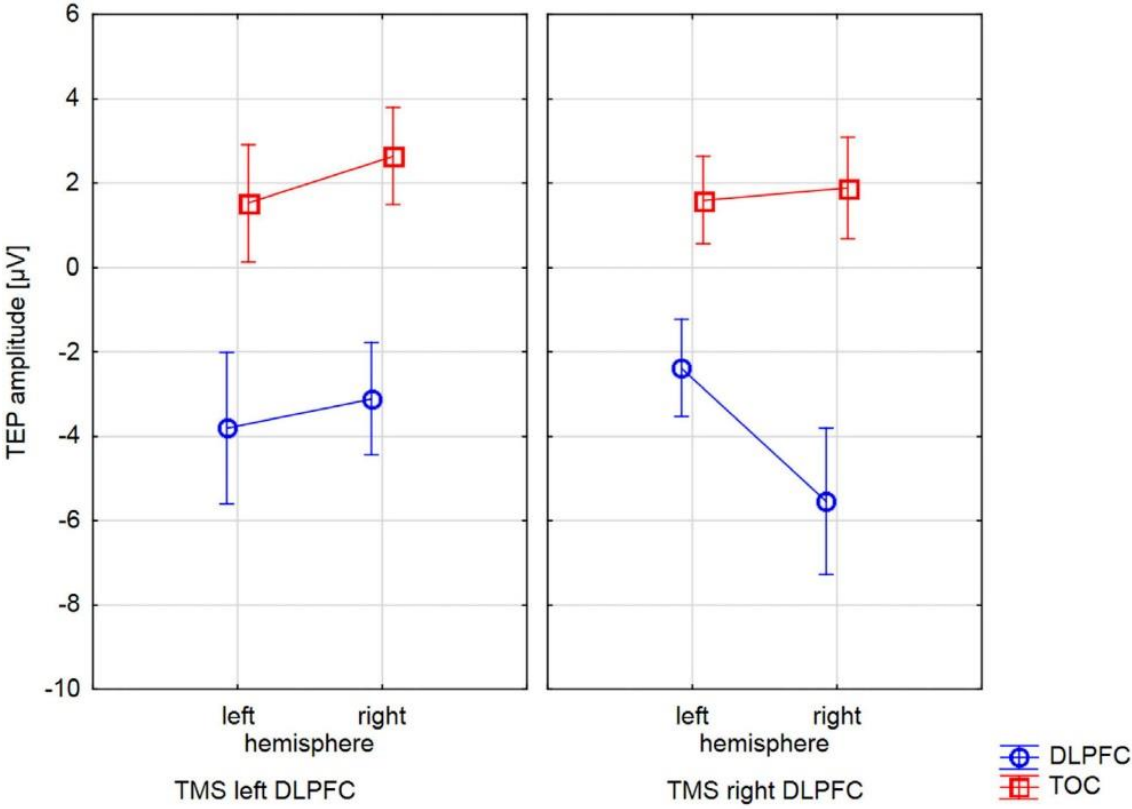
### *TEP Topography*

In the topographical distributions of the TEPs, there was a pronounced negativity around electrode P9 for left-sided TMS and around P10 for right-sided TMS, which is visible most clearly in the time window from 140 to 180 ms. In the time window from 80 to 120 ms, a central symmetrical negativity (located around Cz and FCz) was present. Furthermore, there was a symmetrical positivity located at the vertex and a broad posterior negativity visible in the time range from 140 to 180 ms. To the extent that this activity is identical in homologous electrodes of both hemispheres (i.e., symmetrical to the midline) for both stimulation sides, it is canceled out in LatTEPs. LatTEPs show a posterior negativity with a clear maximum around electrode LatTEP P9/P10 in the same time window. No prominent lateralized negativity was found over other brain regions ([Figure 1B](#)).

### *Lateralized Site-Specific Activity at the Stimulation Site for TOC TMS*

For TOC stimulation, in the repeated-measures ANOVA with the dependent variable N180 amplitude and the factors TMS SIDE, HEMISPHERE, and BRAIN REGION, there was a three-way interaction effect TMS SIDE  $\times$  HEMISPHERE  $\times$  BRAIN REGION [ $F(1,16) = 18.17$ ;  $p < 0.001$ ;  $\eta_p^2 = 0.53$ ; [Figure 2](#)]. There was also a main effect for BRAIN REGION [ $F(1,16) = 48.61$ ;  $p < 0.001$ ;  $\eta_p^2 = 0.75$ ] with higher amplitudes at temporo-occipital electrodes compared to frontal electrodes ([Table 1](#)). The results of all effects of the ANOVA are presented in [Table 2](#).

Study 1: Single-Pulse TMS to the Temporo-Occipital and Dorsolateral Prefrontal Cortex Evokes Lateralized Long Latency EEG Responses at the Stimulation Site



*Study 1 Figure 2.* Interactions of TMS SIDE X HEMISPHERE area for all four BRAIN REGIONS. The diagrams present TEP amplitude values at one of the electrodes of interest (TOC left hemisphere: P9, TOC right hemisphere: P10, DLPFC left hemisphere: F5, DLPFC right hemisphere F6). Error bars represent 95% confidence intervals. Each diagram refers to one stimulation condition (i.e., target site), with the upper diagrams presenting left and right DLPFC stimulation and the lower diagrams presenting left and right TOC stimulation. TEP amplitudes at the site of stimulation are lateralized with higher (more negative) amplitudes over the stimulated hemisphere. This effect was statistically significant for the stimulation of the left ( $p = 0.007$ ) and right ( $p = 0.005$ ) temporo-occipital cortex and the right DLPFC ( $p = 0.001$ ). For left DLPFC stimulation, TEPs over the stimulated brain lateralization were not significant. The brain region that was not stimulated did not show systematic lateralization.

This three-way interaction was followed up by two-way repeated-measures ANOVAs. As we expected a change of the direction of TEP lateralization at the stimulation site depending on the level of the factor TMS SIDE, these ANOVAs were conducted with the factors HEMISPHERE and BRAIN REGION separately for left-sided TMS and right-sided TMS.

The two-way ANOVA for stimulation applied to the right side yielded a HEMISPHERE  $\times$  BRAIN REGION [ $F(1,16) = 30.34$ ;  $p < 0.001$ ;  $\eta_p^2 = 0.66$ ] interaction effect and a main effect for BRAIN REGION [ $F(1,16) = 56.36$ ;  $p < 0.001$ ;  $\eta_p^2 = 0.78$ ]. The main effect is based on higher amplitudes in temporo-occipital electrodes compared to frontal electrodes ([Table 1](#)). The two-way interaction was followed up by univariate ANOVAs. In the univariate ANOVA with the factor HEMISPHERE for temporo-occipital electrodes there was a main effect HEMISPHERE [ $F(1,16) = 10.74$ ;  $p = 0.005$ ;  $\eta_p^2 = 0.40$ ], showing that amplitudes were higher in P10 (ipsilateral to TMS) compared to P9 (contralateral to TMS). In the univariate ANOVA with the factor HEMISPHERE for frontal electrodes, there was a main effect for HEMISPHERE [ $F(1,16) = 10.25$ ;  $p = 0.006$ ;  $\eta_p^2 = 0.39$ ], here amplitudes were lower ipsilateral to TMS compared to contralateral. The highest N180 amplitude values for right-sided stimulation were found near the locus of stimulation (ipsilateral temporo-occipital; see [Table 1](#) and [Figure 3](#)).

The two-way ANOVA for TMS applied to the left side showed a main effect for HEMISPHERE [ $F(1,16) = 9.47$ ;  $p = 0.007$ ;  $\eta_p^2 = 0.37$ ], which was explained by higher amplitudes over the hemisphere ipsilateral to the side of stimulation ([Table 1](#)). Furthermore, there was a main effect for BRAIN REGION [ $F(1,16) = 26.26$ ;  $p < 0.001$ ;  $\eta_p^2 = 0.62$ ], reflecting higher amplitudes at temporo-occipital electrodes compared to frontal electrodes ([Table 1](#)). There was no interaction effect for left-sided stimulation. Again, the highest N180 amplitudes were found near the locus of stimulation (ipsilateral temporo-occipital; see [Table 1](#) and [Figure 3](#)).

Study 1 Table 1. *Descriptive values of the N180 and LatTEP N180 component peak latencies and amplitudes in various channels for TMS applied to the temporo-occipital cortex.*

Variable	Mean	SD
Latency left (ms)	178.8	20.0
F5 left ( $\mu\text{V}$ )	1.7	4.0
F6 left ( $\mu\text{V}$ )	3.7	4.5
P9 left ( $\mu\text{V}$ )	-9.2	6.6
P10 left ( $\mu\text{V}$ )	-6.0	6.2
Cz left ( $\mu\text{V}$ )	9.4	7.5
Latency right (ms)	183.1	20.4
F5 right ( $\mu\text{V}$ )	1.6	3.7
F6 right ( $\mu\text{V}$ )	4.0	3.9
P9 right ( $\mu\text{V}$ )	-6.9	4.3
P10 right ( $\mu\text{V}$ )	-11.4	5.0
Cz right ( $\mu\text{V}$ )	10.3	5.4
Latency LatTEP (ms)	171.9	21.6
LatTEP F5/F6 ( $\mu\text{V}$ ) LatTEP	0.0	1.6
P9/P10 ( $\mu\text{V}$ )	-4.3	3.1

*Note.* Left and right refer to the respective side of stimulation. SD, standard deviation.

Study 1 Table 2. *Results of the repeated-measures ANOVA for TOC stimulation with the dependent variable N180 amplitude.*

Effect	$F$	$df$	$p$	$\eta_p^2$
TMS SIDE	0.95	1,16	0.35	0.06
HEMISPHERE	1.26	1,16	0.28	0.07
BRAIN REGION	48.61	1,16	< .001	0.75
TMS SIDE X HEMISPHERE	9.88	1,16	0.006	0.38
TMS SIDE $\times$ BRAIN REGION	0.96	1,16	0.34	0.06
HEMISPHERE $\times$ BRAIN REGION	8.66	1,16	0.01	0.35
TMS SIDE $\times$ HEMISPHERE $\times$ BRAIN REGION	18.17	1,16	0.001	0.53

#### *Comparison of the N180 Peak Between the Locus of Stimulation and Cz*

In the repeated-measures ANOVA with the dependent variable N180 amplitude and the factors TMS SIDE and ELECTRODE LOCALIZATION (factor levels: “ipsilateral temporo-occipital electrode” vs. “Cz”) a main effect for the factor ELECTRODE LOCALIZATION was found [ $F(1,16) = 52.64$ ;  $p < 0.001$ ;  $\eta_p^2 = 0.77$ ]. Amplitudes at Cz were lower than the amplitudes at the

ipsilateral temporo-occipital electrodes (site of stimulation; [Table 2](#)). There were no other main effects or interaction effects.

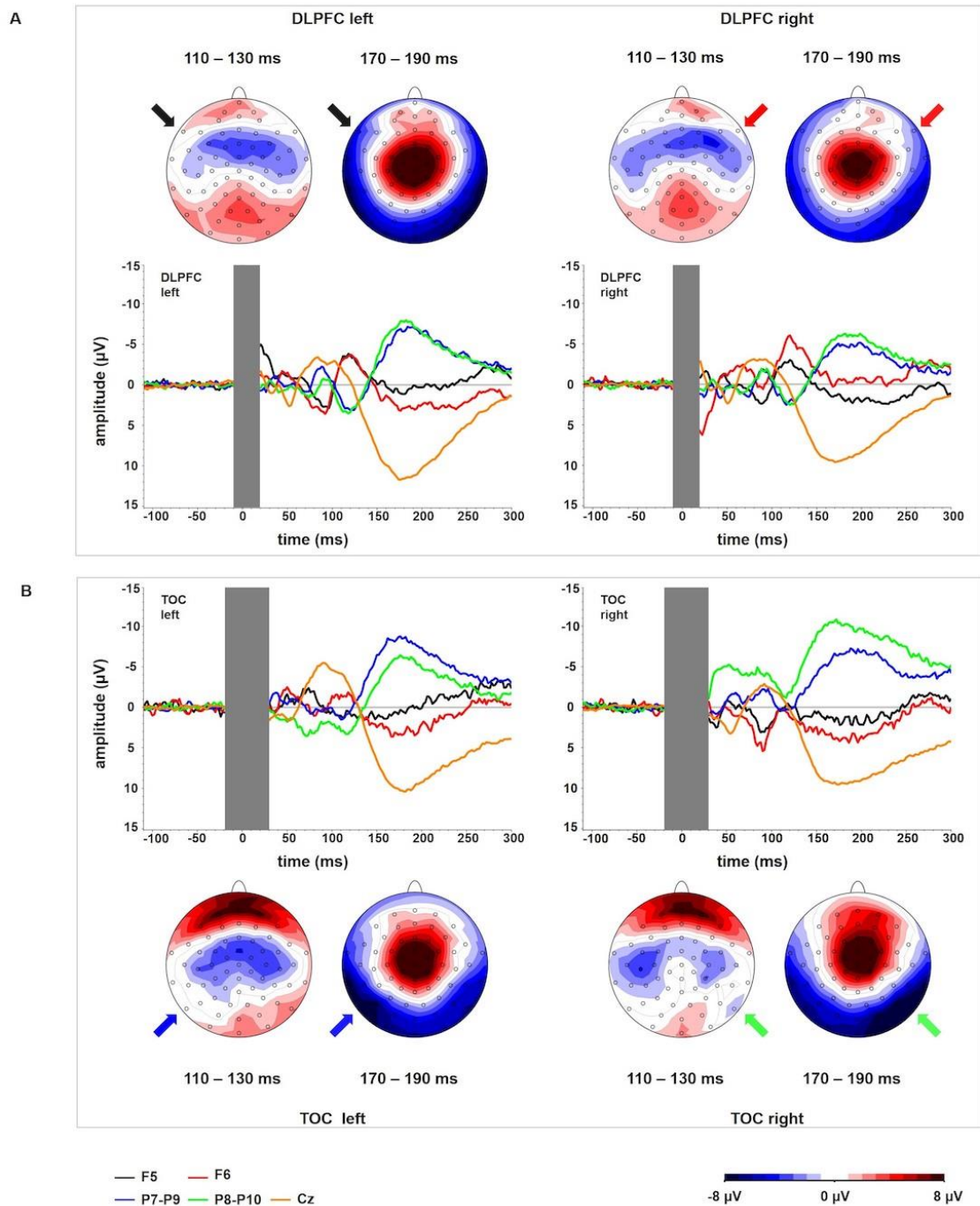
#### *Comparison of the LatTEP N180 Peaks Across Brain Regions*

A univariate repeated-measures ANOVA with the dependent variable LatTEP amplitude and the factor BRAIN REGION (LatTEP F5/F6 vs. LatTEP P9/P10) yielded a main effect [ $F(1,16) = 31.6$ ;  $p < 0.001$ ;  $\eta_p^2 = 0.66$ ]. LatTEPs were higher at parieto-occipital electrodes compared with frontal electrodes ([Table 2](#)).

#### 2.1.3.2 DLPFC Stimulation

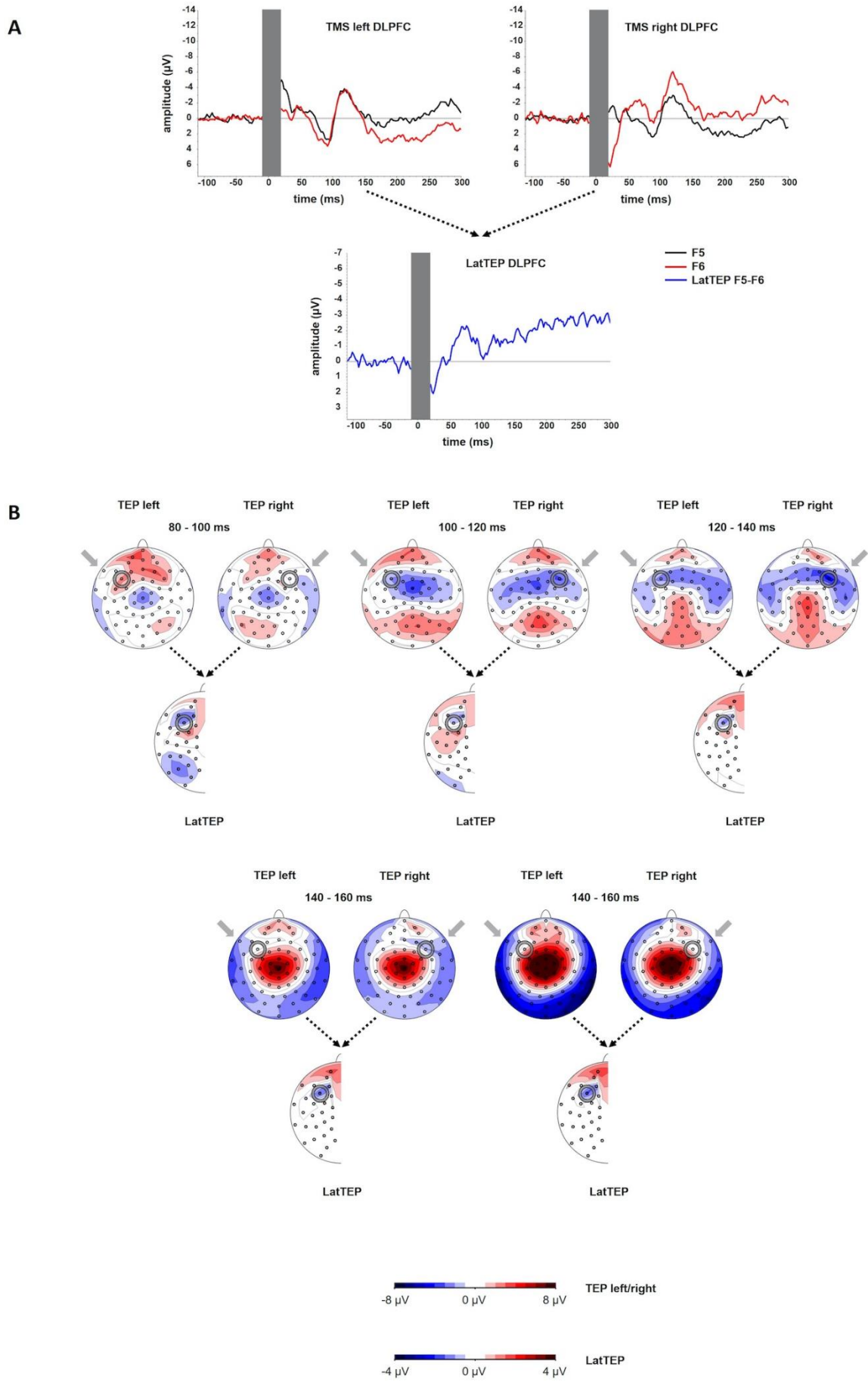
##### *TEP Time Course*

The grand averages of the TEPs at electrodes overlying the site of stimulation showed a first negative deflection at approximately 50 ms, a positive deflection peaking at approximately 90 ms and a more prominent negative deflection peaking at approximately 120 ms (N100). The amplitude of the N100 was significantly different from the baseline [at electrode P5 for left TMS:  $t(23) = -4.39$ ;  $p < 0.001$ ; at electrode P10 for right TMS:  $t(16) = -6.60$ ;  $p < 0.001$ ]. The LatTEP curve included a negative deflection with a peak at approximately 80 ms (LatTEP N100; [Figure 4A](#)). The LatTEP N100 amplitude at electrode LatTEP F5/F6 was significantly different from the baseline [ $t(23) = -5.72$ ;  $p < 0.001$ ].



*Study 1 Figure 3.* TEP time course for each of the channels corresponding to one of the stimulation locations (F5, F6, P9, P10) and channel Cz. The (top panel, **A**) represents DLPFC stimulation; the (bottom panel, **B**) represents OCC stimulation. The corresponding topographical plots show the time windows in which local stimulation site-specific TEPs peak in each of the stimulation conditions. For DLPFC, there is no activity systematically lateralized toward the stimulated hemisphere in temporo-occipital electrodes in the time window around 180 ms. For TOC, there is no activity systematically lateralized toward the stimulated hemisphere in frontal electrodes around 120 ms. In all conditions, a relatively uniform time course in electrode Cz can be observed.

Study 1: Single-Pulse TMS to the Temporo-Occipital and Dorsolateral Prefrontal Cortex Evokes Lateralized Long Latency EEG Responses at the Stimulation Site



*Study 1 Figure 4. (A)* TEP time course at electrodes F5 and F6 for TMS to the left (TMS left DLPFC) and the right (TMS right DLPFC) dorsolateral prefrontal cortex. The extent to which TEPs are higher (more negative) ipsilateral than contralateral to the side of stimulation is reflected in LatTEP amplitudes. Lateralization of evoked activity from both stimulation sides is condensed in one measure (LatTEP F5/F6). The LatTEP peaks at approximately 80 ms after the TMS pulse. Note the different scaling of the y axis between TEPs and LatTEPs. *(B)* Topographical plots of TEPs in time segments each of 20-ms length for TMS to the left (TMS left DLPFC) and right (TMS right DLPFC) temporo-occipital cortex. LatTEP topographies are derived from TEP maps of both stimulation sides with each channel calculated according to the LatTEP formula. LatTEP maps show a topographical maximum around electrode LatTEP F5/F6 seen most prominently in the time range from 80 to 100 ms. Note that the color-coding scales differ between TEPs and LatTEPs.

### 2.1.3.3 TEP Topography

For right DLPFC stimulation, the topographic distribution showed a distinct negativity around electrode F6 most prominently in the time window 100–140 ms but no apparent lateralized maximum for left DLPFC stimulation. In the time window from approximately 80–120 ms, a central symmetrical negativity (Cz and FCz) was present that resembles the symmetrical negativity found in the corresponding time window of the TOC stimulation. For right DLPFC stimulation, this negativity overlaps and conflates with the lateralized negativity around F6 in the time window from 100 to 120 ms. For left DLPFC stimulation, this negativity extends to both frontal lobes including electrodes F5 and F6 ([Figure 4B](#)).

Beginning at a latency of approximately 140 ms, a positivity at the vertex and a posterior bilateral negativity are apparent. The posterior negativity has a slightly asymmetrical topography with a preponderance of the right hemisphere for both left- and right-sided TMS (i.e., the topographic maximum is not systematically located in the stimulated hemisphere). Its topographic distribution corresponds to the pattern seen in TOC stimulation except for the additional systematically lateralized activity around P9 and P10 observed in TOC stimulation.

In LatTEP maps, symmetrical evoked activity and also asymmetrical activity that is not systematically lateralized with respect to the side of stimulation are canceled out. Consequently, a negativity with a maximum at electrode LatTEP F5/F6 is visible most prominently in the time window from 80 to 100 ms ([Figure 4B](#)).

*Lateralized Site-Specific Activity at the Stimulation Site for DLPFC TMS*

For DLPFC stimulation, the repeated-measures ANOVA with the dependent variable N100 amplitude and the factors TMS SIDE, HEMISPHERE, and BRAIN REGION showed a strong trend toward a three-way interaction effect TMS SIDE × HEMISPHERE × BRAIN REGION [ $F(1,23) = 4.05$ ;  $p = 0.056$ ;  $\eta_p^2 = 0.15$ ]. Furthermore, there was a main effect for BRAIN REGION [ $F(1,23) = 59.37$ ;  $p < 0.001$ ;  $\eta_p^2 = 0.72$ ] due to higher amplitudes in frontal compared to temporo-occipital electrodes (Table 3). The results of all effects of the ANOVA are presented in Table 4.

Study 1 Table 3. *Descriptive values of the N100 and LatTEP N100 component peak latencies and amplitudes in various channels for TMS applied to the dorsolateral prefrontal cortex.*

Variable	Mean	SD
Latency left (ms)	115.9	15.3
F5 left ( $\mu V$ )	-3.8	4.2
F6 left ( $\mu V$ )	-3.1	3.2
P9 left ( $\mu V$ )	1.5	3.3
P10 left ( $\mu V$ )	2.6	2.7
Cz left ( $\mu V$ )	0.4	3.1
Latency right (ms)	113.7	16.1
F5 right ( $\mu V$ )	-2.4	2.7
F6 right ( $\mu V$ )	-5.5	4.1
P9 right ( $\mu V$ )	1.6	2.5
P10 right ( $\mu V$ )	1.9	2.9
Cz right ( $\mu V$ )	0.7	3.8
Latency LatTEP (ms)	83.8	20.0
LatTEP F5/F6 ( $\mu V$ )	-2.6	3.3
LatTEP P9/10 ( $\mu V$ )	-0.8	1.6

Note. Left and right refer to the side of stimulation. SD, standard deviation. SD

Study 1 Table 4. Results of the repeated-measures ANOVA for DLPFC stimulation with the dependent variable N100 amplitude.

Effect	<i>F</i>	<i>df</i>	<i>p</i>	$\eta_p^2$
TMS SIDE	1.55	1,23	0.23	0.06
HEMISPHERE	0.02	1,23	0.50	0.02
BRAIN REGION	59.47	1,23	< .001	0.72
TMS SIDE X HEMISPHERE	9.76	1,23	0.005	0.30
TMS SIDE × BRAIN REGION	0.03	1,23	0.87	0.001
HEMISPHERE × BRAIN REGION	5.66	1,23	0.026	0.20
TMS SIDE × HEMISPHERE × BRAIN REGION	4.05	1,23	0.056	0.15

As the trend toward a three-way interaction is consistent with our *a priori* hypothesis, we used two-way repeated-measures ANOVAs to follow up this interaction. Again, as a change of the direction of TEP lateralization at the stimulation site depending on the level of the factor TMS SIDE was expected, these ANOVAs were conducted with the factors HEMISPHERE and ELECTRODE separately for left-sided TMS and right-sided TMS.

The two-way ANOVA for TMS applied to the left DLPFC yielded a main effect for BRAIN REGION [ $F(1,23) = 39.09$ ;  $p < 0.001$ ;  $\eta_p^2 = 0.63$ ]; no other main effects or interaction effects were found. TEP amplitudes were higher at frontal electrodes than at temporo-occipital electrodes. The descriptively highest N100 amplitude was found over the DLPFC ipsilateral to TMS (Table 3 and Figure 3); however, lateralization was not significant in this condition.

The two-way ANOVA for TMS applied to the right DLPFC showed a main effect for HEMISPHERE [ $F(1,23) = 13.86$ ;  $p = 0.001$ ;  $\eta_p^2 = 0.38$ ], a main effect for BRAIN REGION [ $F(1,23) = 42.57$ ;  $p < 0.001$ ;  $\eta_p^2 = 0.65$ ], and a HEMISPHERE × BRAIN REGION interaction [ $F(1,23) = 9.48$ ;  $p = 0.005$ ;  $\eta_p^2 = 0.29$ ]. In order to further elucidate this interaction effect, we performed univariate repeated-measures ANOVAs with the factor HEMISPHERE separately for frontal and temporo-occipital electrodes.

In the univariate ANOVA with the factor HEMISPHERE for frontal electrodes, there was a main effect [ $F(1,23) = 15.96$ ;  $p = 0.001$ ;  $\eta_p^2 = 0.41$ ] explained by higher amplitudes over the stimulated hemisphere compared to the contralateral hemisphere (Table 3). In the univariate ANOVA with the factor HEMISPHERE for temporo-occipital electrodes, no main effect was

found [ $F(1,23) = 2.84$ ;  $p = 0.60$ ;  $\eta_p^2 = 0.01$ ]. The highest N100 amplitude was found at the site of stimulation (ipsilateral frontal electrode; [Table 3](#) and [Figure 3](#)).

#### *Comparison of the N100 Between the Locus of Stimulation and Cz*

In a repeated-measures ANOVA with the factors TMS SIDE and ELECTRODE LOCALIZATION (factor levels: “electrode at the site of stimulation” and “electrode Cz”), there was a main effect for the factor ELECTRODE LOCALIZATION [ $F(1,23) = 14.60$ ;  $p = 0.001$ ;  $\eta_p^2 = 0.39$ ]. N100 amplitudes were higher at the site of stimulation compared to at Cz ([Table 3](#)). No other main effects or interaction effects were found.

#### *Comparison of the LatTEP N100 Peak Across Brain Regions*

In a univariate repeated-measures ANOVA with the dependent variable LatTEP N100 amplitude, we found a significant main effect of BRAIN REGION [levels: LatTEP F5/F6 and LatTEP P9/P10;  $F(1,23) = 6.70$ ;  $p = 0.016$ ;  $\eta_p^2 = 0.23$ ], with higher LatTEP N100 amplitudes at frontal electrodes.

### 2.1.4 Discussion

The major findings of the study were that TEPs evoked by TMS to the TOC and the DLPFC contained systematically lateralized negative long-latency components over the stimulated brain region that most likely reflect transcranial TMS effects on the targeted cortex area. It was possible to isolate lateralized activity at the stimulation site in LatTEPs by stimulating homologous sites in both hemispheres and subtracting invariable evoked activity, an approach that can improve TEP methodology in future studies aiming to assess local cortical functions.

#### 2.1.4.1 LatTEP Components at the Stimulation Site

We specifically searched for evoked components with long-latency ranges and a lateralized ipsilateral topography because components with lateralized topography confined to the site of stimulation are most likely not a correlate of unspecific processes (Conde et al., 2019). Our hypothesis predicted that TEP amplitudes in the stimulated brain region would be systematically higher ipsilateral to TMS than contralateral to TMS. In all stimulation conditions, the highest amplitudes were systematically found over the stimulation site. TEP peak amplitudes in the stimulated brain region were lateralized with higher amplitudes over the stimulated hemisphere in three of four conditions. For TMS over the left DLPFC, the N100 amplitude was also descriptively higher in ipsilateral compared to that in contralateral

electrodes, but the difference did not surpass the threshold of statistical significance possibly due to low sample size and measurement error. In agreement with our hypothesis, no systematic lateralization toward the side of stimulation was found in electrodes outside the stimulated brain region (e.g., frontal electrodes for TOC TMS).

#### 2.1.4.2 Isolating Lateralized Activity in LatTEPs

To eliminate evoked activity, which was not systematically lateralized to the side of TMS, we adopted the methodology of the LRP (Coles, 1989), which, to our knowledge, has not been applied to TEPs before. Lateralized negativity at the site of stimulation that may be masked by symmetrical processes in conventional maps can be unmasked in LatTEP topoplots (e.g., [Figure 1B](#) in time window 120–140 ms). In TOC stimulation, a prominent lateralized negativity was found with a topographic maximum around electrode LatTEP P9/P10 ([Figure 1B](#)); in DLPFC stimulation, there was a negative maximum located over the targeted brain region around electrode LatTEP F5/F6 ([Figure 4B](#)). The statistical comparison of LatTEP peaks across the two brain regions corroborated the results found for conventional TEPs that higher LatTEP amplitudes can be found in the stimulated compared to the non-stimulated brain region for both TOC and DLPFC stimulation. It is noteworthy that LatTEP negativity can result from ipsilateral negative voltages and contralateral positive voltages. Therefore, the interpretation of LatTEPs needs to take into account the original time course and topography of TEPs of both sides. As there was no prominent positivity contralateral as a potential cause of the negative LatTEP maxima, they are caused by a negativity in ipsilateral electrodes surrounding the target site.

#### 2.1.4.3 Do Lateralized Site-Specific Components Represent Transcranially Evoked Activity?

Although lateralized components specific to the stimulation site likely reflect direct transcranial effects of TMS (Conde et al., 2019), potential alternative explanations include decay artifacts, which are commonly observed close to the site of stimulation. These artifacts result from an initial quick polarization of the electrode contact by the TMS pulse and a subsequent continuous discharge. The time course of decay artifacts is highly consistent across trials and individuals with a peak within the first 10–50 ms followed by an exponential decay of the voltage (Ilmoniemi et al., 2015; Rogasch et al., 2014). Thus, the time course of the lateralized components observed in our study with a slow deflection beginning at approximately 100 ms is not compatible with a decay artifact.

A second alternative explanation may be artifacts related to muscle twitches, which can be mostly observed when stimulating in the vicinity of cranial muscles. These artifacts present with very high amplitudes (10–1,000  $\mu\text{V}$ ) have a biphasic course with a positive and a negative peak occurring within the first 20 ms and last up to a maximum of 60 ms. The topography is reminiscent of a tangential dipole with adjacent positive and negative poles (Mutanen et al., 2013; Rogasch et al., 2014). In this case, not only the time course but also the amplitude and topography are incompatible with muscle twitches. Thus, we consider transcranially evoked activity in the targeted cortex area to be the most likely origin of the lateralized late components.

While to our knowledge previous studies have not assessed the extent of lateralization of TEPs in an approach similar to ours, our results are nevertheless compatible with the results of some previous TMS-EEG studies. TEP topographies with maxima located over the stimulated hemisphere in the vicinity of the stimulation site can often be found in studies targeting M1 (Bonato et al., 2006; Bruckmann et al., 2012; Jarczok et al., 2016; Paus et al., 2001; Yamanaka et al., 2013). However, in TMS-EEG investigations targeting other brain areas, such topographies were found at short latencies but not at long latencies (Du et al., 2017; Herring et al., 2015; Noda et al., 2016; Rogasch et al., 2014). Because of smaller amplitudes of transcranially evoked components in DLPFC stimulation, lateralized components may be overshadowed by central unspecific activity more easily than in M1 stimulation. Calculation of LatTEPs may be useful to uncover LatTEP components masked by more prominent non-lateralized components.

#### 2.1.4.4 Non-specific Evoked Components Overlap With Transcranially Evoked Components

In all four stimulation conditions, invariable components overlapping with site-specific components were observed. Topographies across all stimulation conditions display a symmetrical negativity with a maximum at the vertex (time range from 80 to 120 ms; [Figures 1B, 4B](#)), and a symmetrical positivity with a maximum at the vertex co-occurring with a bilateral temporo-occipital negativity is (140–180 ms; [Figures 1B, 4B](#)). A uniform time course in electrode Cz was found with a negative peak at approximately 100 ms and a positive peak at approximately 180 ms ([Figure 3](#)) for all conditions. Because of the shorter latency and the significantly lower peak amplitude compared to the lateralized site-specific negative peaks, lateralized components cannot be explained by volume conduction from the process observed at Cz.

As we intended to identify local activity specific to the stimulated cortical site in the presence of sensory-evoked potentials, no masking procedure was applied. The spatiotemporal pattern of the non-specific component is compatible with an auditory evoked potential (AEP), which is characterized by a N100-P180 complex with a frontocentral, mostly symmetrical topography (Hine & Debener, 2007; Lightfoot, 2016; Mahajan & McArthur, 2012). Additionally, somatosensory-evoked potentials (SSEPs) present with deflections with similar latencies (N140, P190) and contralateral or bilateral maxima over somatosensory areas (Allison et al., 1992; Genna et al., 2016; Goff et al., 1977) that likely contribute to the overall topography of TEPs. However, given their known topography, AEPs and SSEPs cannot be the underlying causes of ipsilateral LatTEP components. AEPs are mostly symmetrical in binaural stimulation or can present with lateralized late negative AEP components (N1) with higher amplitudes over the contralateral hemisphere (Hine & Debener, 2007; McCallum & Curry, 1980). Late negative SSEP components also present with higher contralateral amplitudes (Genna et al., 2016; Hashimoto, 1988). Additionally, sensory-evoked potentials are generated in cortical areas specific to the respective sensory modality. A shift of the topographic maximum to the stimulated brain region when the target site changes are not compatible with AEPs or SSEPs. Our results are in agreement with the findings of a comparison of TMS with a sensory stimulation, in which the most prominent difference between the two stimulation conditions at long latencies was observed in electrodes close to the stimulation site. A principal component analysis revealed a component consistent with lateralized activity over the stimulated cortex area that explained approximately 59% of the variance only in the real TMS condition. In both conditions, there were components compatible with a non-lateralized central N100-P180 complex (Biabani et al., 2019). Together with our findings, this is consistent with the notion that transcranially evoked components can be found over the site of stimulation, whereas potentials at other sites are substantially confounded by sensory input. Understanding the composition of TEPs is particularly relevant, as it may not be possible to eliminate sensory confounders completely with current procedures (Biabani et al., 2019; Siebner et al., 2019; ter Braack et al., 2015).

#### 2.1.4.5 Latencies in TOC and DLPFC Stimulation

Latencies of the late negative peaks at the site of stimulation varied substantially across brain regions but were consistent across hemispheres within one brain region. A systematic evaluation of DLPFC latencies at electrodes close to the locus of stimulation reported mean

latencies of approximately 110 to 115 ms (Lioumis, Kicić, et al., 2009) well compatible with our results (approximately 115 ms). Posterior cortex areas are less well characterized, and we are not aware of studies that systematically investigated the variance of latencies and amplitudes of TEPs in the temporal or occipital cortex. However, the data of several previous studies are compatible with markedly longer latencies in posterior cortex areas (Belardinelli et al., 2019; Herring et al., 2015; Rosanova et al., 2009; Samaha et al., 2017), although some reported conflicting results (Kerwin et al., 2018). Our findings suggest that the second prominent negative TEP peak in TOC TMS has a latency of approximately 170–180 ms.

A direct statistical comparison of DLPFC and TOC stimulation latencies in our study is not possible because of methodological differences. However, the difference between groups of approximately 4 standard deviations of the mean DLPFC latency most likely reflects that TEPs differ substantially across different stimulated cortical areas (Casarotto et al., 2010; Kähkönen et al., 2005; Lioumis, Kicić, et al., 2009).

#### 2.1.4.6 Neurobiological Processes Associated With the Generation of TEPs

Transcranial magnetic stimulation causes synchronized depolarization in pyramidal cells and interneurons (Di Lazzaro & Ziemann, 2013) and consequentially fluctuations of excitatory postsynaptic potentials in the targeted cortex. Therefore, local TMS-evoked activity generated by the targeted population of neurons can be expected to be found at the stimulated cortex site. However, after the initial activation of local neurons, secondary activation of other (potentially remote) cortical and subcortical structures occurs that is not fully understood. Our results add evidence that not only short latency but also long-latency transcranially evoked components generated by the stimulated cortical region can be found in the compound TEP. Based mostly on experiments targeting M1 the N100 component has been linked to inhibitory activity (Bender et al., 2005; Bruckmann et al., 2012; Nikulin et al., 2003). Pharmacological interventions point to an involvement of GABA-B-ergic neurotransmission (Premoli, Castellanos, et al., 2014). In agreement with our findings, pharmacological effects of GABA-B agonist baclofen were found close to the stimulation site but not at remote electrodes. Despite the differences in latencies between TOC and DLPFC, late components may reflect GABA-ergic neurotransmission as the latency of GABA-B-associated inhibitory postsynaptic potentials varies, substantially depending on properties of the local neurons (Thomson & Destexhe, 1999). However, experiments such as pharmacological challenges (Premoli, Castellanos, et al., 2014) would be necessary to further elucidate the underlying neurobiology

of TEPs outside M1. Our results suggest that researchers should also specifically consider TEP components located over the targeted brain area and lateralized toward the stimulated hemisphere when further investigating TEPs.

#### 2.1.4.7 Limitations

Temporo-occipital cortex and dorsolateral prefrontal cortex stimulations were applied to separate groups of subjects. Thus, a direct comparison of absolute values or within-subject comparisons of variables across the two stimulation sites is not possible. However, the different samples and methodological differences cannot account for the effects of hemispheric lateralization and the stimulation site-specific topographies of evoked activity found across all conditions. We argue that the finding of evoked activity at the site of stimulation despite these differences supports the generalizability and robustness of the results.

#### 2.1.4.8 Conclusion

The results of the present study show that TEPs contain long-latency negative components that are lateralized toward the stimulated hemisphere and have their topographic maxima at the respective stimulation sites. Removing not systematically lateralized evoked activity by calculating LatTEPs reduced overshadowing by unspecific components and revealed negative maxima located around the target sites. The systematic lateralization and the localization at the stimulation site suggest that these components are correlates of cortical activity evoked directly by local effects of the magnetic field. Clinical and research applications of TEPs can benefit from specifically focusing on LatTEP components at the stimulation site.

## 2.2 Study 2: Topography and lateralization of long-latency trigeminal somatosensory evoked potentials

Since we know that co-evoked sensory input can confound TEPs and that AEPs have already been studied, we have embedded a study that aimed at gaining insights into the topography and lateralization of trigeminal SSEPs in time windows around 100 ms that are relevant for the TMS-evoked N100. In this study, we electrically stimulated the trigeminal nerve and analyzed the resulting potentials according to their lateralization and topography. The knowledge about trigeminal SSEPs that we gained with our results could then be applied to the interpretation of our clinical TMS-evoked N100 research.

### 2.2.1 Introduction

The aim of this study was to examine the topographic distribution, time-course, and lateralization of long-latency trigeminal somatosensory evoked potentials (SSEPs).

SSEPs are potentials generated by electrical or mechanical stimulation of a nerve (Nevalainen et al., 2006). It is common to divide SSEPs into short- and long-latency potentials, with long latencies defined as >100 ms (Wu et al., 2012). SSEPs have been discussed in the context of neurological disorders (Horn & Tjepkema-Cloostermans, 2017; Lachance et al., 2020). However, beyond their clinical use (Bennett et al., 1987), trigeminal SSEPs play a role in other contexts as well.

There is an ongoing debate in the literature about how transcranial magnetic stimulation (TMS) combined with electroencephalogram (EEG) studies and sham conditions should be designed to best assess the extent to which trigeminal SSEPs contribute to evoked activity after TMS (Belardinelli et al., 2019; Conde et al., 2019). TMS-EEG offers an opportunity to study cortical functions in neurological and psychiatric conditions and thus for the development of biomarkers for disorders such as depression or anxiety disorders (Croarkin et al., 2011; Teng et al., 2017). However, with commonly used TMS-EEG designs that do not use a proper sensory masking, TMS-evoked potentials (TEPs) represent both transcranially evoked neuronal activity and peripherally evoked potentials such as auditory evoked potentials (AEPs) and SSEPs (Biabani et al., 2019; Lioumis, Kicić, et al., 2009). An understanding of the topography and lateralisation of peripherally evoked potentials in TEPs is relevant as masking procedures may be imperfect in suppressing them (Jarczok et al., 2021) AEPs result from the clicking sound of the TMS coil (Nikouline et al., 1999; Rogasch et al., 2014; ter Braack et al., 2015). AEPs have

been suggested to consist of a biphasic N100-P180 complex with fronto-central and temporal peaks (Rogasch et al., 2014; ter Braack et al., 2015), but also show a contralateral asymmetry when stimulating monaurally (Hine & Debener, 2007; Langers et al., 2005). Furthermore, TMS of especially the dorsolateral prefrontal cortex (DLPFC) activates the supraorbital branch of the trigeminal nerve that evokes trigeminal SSEPs. Long-latency SSEPs may confound commonly investigated TEPs such as the N100 (Bender et al., 2005; Biabani et al., 2019) which is one of the most commonly investigated TEP components in TMS to the motor cortex (M1) and the DLPFC (Kerwin et al., 2018; Premoli et al., 2018; Roos et al., 2021). The topography of SSEP during stimulation of peripheral nerves in the limbs has been examined previously with conflicting results (Allison et al., 1992; Genna et al., 2016). Some studies indicated a long-latency somatosensory component, which appears as a negativity at central electrodes contralateral to stimulation approximately 140 ms after the stimulus onset, called N140 (Genna et al., 2016; Kida et al., 2004; Nakata et al., 2011). Other studies found the N140 to be more bilateral, but with an asymmetry to the contralateral hemisphere (Desmedt & Robertson, 1977; Hämäläinen et al., 1990). There is a lack of current studies systematically investigating the topography of trigeminal nerve stimulation. Results of Bennett and Jannetta (1980) indicated that there is a negative deflection in central-contralateral electrodes at approximately 140 ms also after trigeminal but not peripheral nerve stimulation. Still other studies described the N140 to be a vertex component (Allison et al., 1992; Goff et al., 1977). However, the assumption of a contralateral distribution of trigeminal SSEPs is supported by the fact that trigeminal afferents cross to the contralateral side and ascend to thalamic structures. From here, afferent signals continue to the primary and secondary somatosensory cortex (Trepel, 2017). There is still little research on trigeminal SSEPs with longer latencies and possible differences between SSEP to peripheral nerve and SSEP to trigeminal nerve stimulation remain unclear. We investigated whether trigeminal SSEPs present with a negative, contralateral maximum at approximately 140 ms (Genna et al., 2016). Thus, we electrically stimulated the supraorbital branch of the trigeminal nerve on the forehead. Due to the importance of long-latency trigeminal SSEPs for TMS-EEG designs, we additionally compared contralateral components of the TEP during TMS of the DLPFC to those during electrical stimulation of the trigeminal nerve. Both procedures produced a clicking sound, which is why we compared the contralateral potentials in TMS with those of electrical nerve stimulation with and without auditory masking. This comparison with/without auditory

masking allowed us to assess potential influences of auditory evoked potentials and their overlaps with SSEPs.

## 2.2.2 Methods and Material

### 2.2.2.1 Subjects

A total of 15 healthy subjects (11 females, 4 males) aged 20-25 years participated, one subject had to be excluded from data analysis due to electrical noise that could not be removed. Further information and stimulation parameters of the sample are found in Table A1 in the supplementary material. Only subjects with no TMS exclusion criteria (Rossi et al., 2009) were included. Subjects were instructed to fixate a cross on the computer located approximately 1 m in front of them. The different conditions of the electrical nerve stimulation and TMS were in a counterbalanced order.

### 2.2.2.2 Electroencephalography

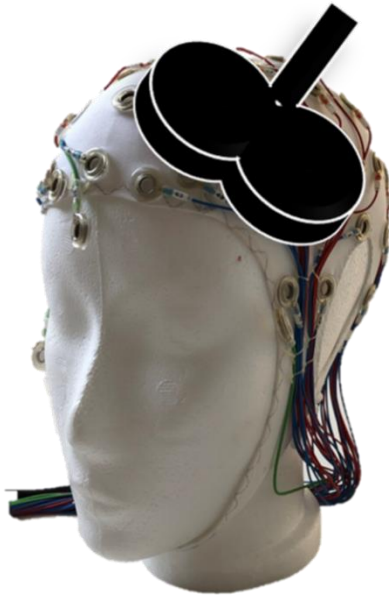
A TMS compatible custom made 64-channel BrainCap (Easycap GmbH, Herrsching, Germany) with sintered Ag/Ag-Cl electrodes was used for recordings. Electrodes were positioned in an equidistant montage with electrodes arranged on five concentric rings around electrode Cz. Electrodes on the horizontal and vertical central line corresponded to the 10-20 system and other electrodes close to the 10-20 system locations (Chatrian et al., 1985). Accordingly, all electrodes were named after the nearest electrodes in the 10-10 system. Additional electrooculogram electrodes were placed on the nasion and under the right and left eye. The ground electrode was located near Pz while Cz served as recording reference electrode. Impedances were kept  $< 5 \text{ k}\Omega$ . DC-EEG was recorded with a sampling rate of 5000 Hz by BrainVision Recorder (v1.20.0801, Brain Products GmbH, Gilching, Germany) and was amplified by a BrainAmp DC amplifier (Brain Product GmbH).

### 2.2.2.3 Electrical Nerve Stimulation

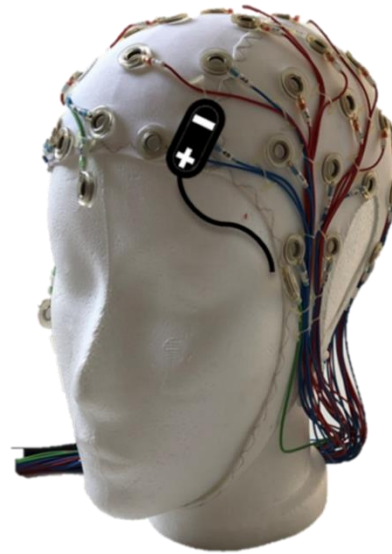
For the electrical nerve stimulation, the neuro stimulator TWISTER (Dr. Langer GmbH, Germany; Software: TWISTER V1.19) was used. A bipolar electrode was fixed on the forehead under the EEG cap above the exit point of the supraorbital branch of the trigeminal nerve, approximately at the position of Fp2 in 10-20 system on the right side and SO1 on the left side (Fig. 1). The positive pole of the bipolar electrode was oriented towards the nose. The

intensities of the electrical nerve stimulation were determined individually by all subjects themselves by a direct comparison to the intensity of the subjective skin sensation of TMS applied at 120 % of the subjects resting motor threshold (RMT). By adjusting the intensity of the electrical nerve stimulations to be similar to the skin sensation during TMS within each subject, we aimed at achieving comparability of SSEPs between the two types of stimulation. The mean intensity of the electrical nerve stimulation was  $4.4 \pm 2.7$  mA (Table 1). A total of 130 electrical stimuli with inter-trial intervals varying evenly between 5 and 8 s (mean 6.5 s) and a trial duration of 1.5 s were applied to each side. 65 of them were presented with masking of auditory potentials and the other 65 without auditory masking. AEPs were masked by white noise presented through in-ear headphones with active noise cancellation (N20nc, AKG Acoustics GmbH). The mean volume of the white noise was  $91.7 \pm 4.3$  dB to mask the mean sound volume of approximately 75 dB of the electrical nerve stimulator. Inserted headphones are better compatible with scalp electrodes and were found to be as efficient in noise masking as external headphones (ter Braack et al., 2015). We did not eliminate the clicking sound of the stimulator placed behind the subjects to keep it similar to the coil-click during TMS, in order to assess possible confounding effects of AEPs and as there are still TMS-EEG studies that do not perform masking or participants report hearing the TMS click despite noise masking (Belardinelli et al., 2019; Siebner et al., 2019). While minimization of artefacts is appropriate in studies using TMS-EEG as a biomarker for psychopathology research, we believe that studies addressing potential confounders should well describe all sources of potential artefacts (in order to recognize these confounders in the data).

A) TMS left



B) Electrical nerve stimulation left



*Study 2 Figure 1.* Stimulation positions of the transcranial magnetic stimulation (TMS) coil over the left dorsolateral prefrontal cortex (DLPFC) (A) and of the electrode of the electrical nerve stimulation over the supraorbital branch of the trigeminal nerve (B). Note that the electrode in (B) was placed at the depicted location but below the cap in the actual measurement in order to assure direct contact of the electrode with the subject's skin.

Study 2 Table 1. Mean peak latencies, amplitudes, and test values of deviations from the baseline over all stimulation conditions.

	peak latency (ms) $\bar{x} \pm SD$	peak amplitude $\bar{x} \pm SD$ ( $\mu V$ )	t-values (df)	p-values
<b>N140 mean peak amplitudes</b>				
ENS <sup>1</sup> with auditory masking				
Left-sided stimulation (C6)	137.6 $\pm$ 13.0	-1.5 $\pm$ 1.7	-3.41 (13)	.005**
Right-sided stimulation (C5)	136.4 $\pm$ 13.0	-1.5 $\pm$ 1.2	-4.73 (13)	<.001**
Lateralized activity (C5/C6)	127.1 $\pm$ 12.2	1.0 $\pm$ 0.9	4.17 (13)	.001**
ENS without auditory masking				
Left-sided stimulation (C6)	143.1 $\pm$ 6.2	-1.5 $\pm$ 1.1	-5.28 (13)	<.001**
Right-sided stimulation (C5)	133.4 $\pm$ 9.8	-1.4 $\pm$ 1.6	-3.38 (13)	.005**
Lateralized activity (C5/C6)	125.9 $\pm$ 11.4	0.9 $\pm$ 1.3	2.71 (13)	.02*
TMS				
Left-sided stimulation (C6) 100-120 ms	- <sup>2</sup>	-0.9 $\pm$ 1.4	-2.48(13)	.03*
Left-sided stimulation (C6) 120-140 ms	132.0 $\pm$ 8.3	-1.7 $\pm$ 1.1	-6.14 (13)	<.001**
Right-sided stimulation (C5) 100-120 ms	118.6 $\pm$ 11.0	-1.2 $\pm$ 1.6	-2.8 (13)	.015*
Right-sided stimulation (C5) 120-140 ms	129.9 $\pm$ 12.8	-0.6 $\pm$ 1.9	-1.08 (13)	.30
Lateralized activity (C5/C6) 100-120 ms	116.3 $\pm$ 17.8	0.9 $\pm$ 1.2	2.88 (13)	.01*
Lateralized activity (C5/C6) 120-140 ms	135.7 $\pm$ 16.6	0.4 $\pm$ 1.5	1.07 (13)	.30

Note. <sup>1</sup> = electrical nerve stimulation; \* = significant; \*\* = highly significant; <sup>2</sup> = mean amplitude exported

It should be noted that electrical nerve stimulation causes an electrical artifact at the stimulation site that must be distinguished from evoked activity.

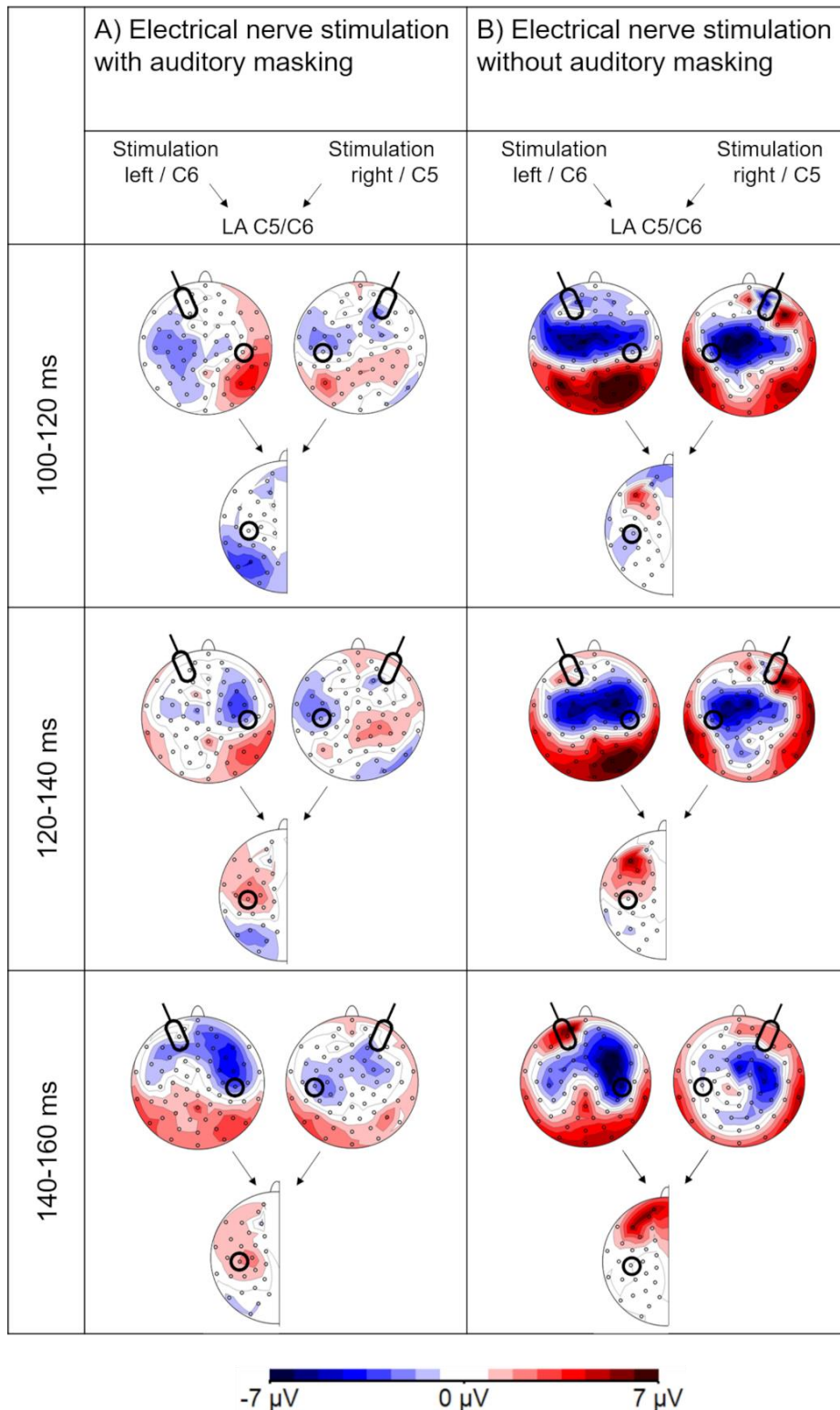
An additional single-subject measurement was performed to determine technical stimulation artifacts close to the stimulation site. During the investigation of this subject, the electrode of the electrical nerve stimulation was turned 180 degrees after the first half of the trials of each stimulation protocol, with the goal to reduce the artifact through a reversal of the polarity in half of the trials (reversed after 33 trials). Due to the reversed polarity, the electrical artifact

was strongly reduced, on average (Fig. 2). However, positioning the electrode in the other direction was described by the subject as painful as the cable attached one end of the electrode pressed against the head under the EEG cap which is why the electrode was not reversed in the whole experiment.

#### 2.2.2.4 Transcranial Magnetic Stimulation

TMS was applied using a figure-eight coil (MCF-B65, outer diameter 75 mm) connected to a MagPro X100 with MagOption stimulator (MagVenture, Farum, Denmark). According to Rusjan et al. (2010), the coil was positioned over electrodes F5 and F6 (Fig. 1), as this is an often used method of stimulating the left and right DLPFC in TMS-EEG research without individual structural magnetic resonance imaging (MRI) data. We are aware that the position of TMS thus differed slightly from that of the electrical nerve stimulation. The electrode was positioned more anterior on the forehead than the TMS coil over the DLPFC (Fig. 1). This was necessary as the electrode was placed beneath the electrode cap and a positioning at more posterior locations would have detached a larger number of electrodes of interest from the scalp. However, it can be assumed that despite this difference in localization, V1 of the trigeminal nerve was activated in both cases (Kemp et al., 2011).

The coil was held manually by a trained examiner throughout the experiment. The handle was pointing sideways-backwards approximately 45° to the midsagittal line. The TMS protocol was triggered by the Presentation software 18.1 (NeuroBehavioral Systems, Berkley, USA). A biphasic single-pulse TMS protocol with a total of 90 stimuli and an inter-stimulus interval varying evenly between 5 and 8 s (mean 6.5 s) was applied over the left and right DLPFC. Stimulation intensities were determined by stimulating the left motor cortex. To measure motor evoked potentials (MEPs) an electromyogram (EMG) was recorded. EMG was recorded from the contralateral (right) hand with the active electrode over the first dorsal interosseus muscle. The reference electrode was placed over the basic phalanx of digit III, a ground electrode was placed on the inside of the right forearm. The location where MEPs were maximal was defined as the motor hotspot. The RMT was determined according to the maximum likelihood method (Awiszus, 2003) using the software TMS Motor Threshold Assessment Tool (MTAT 2.0; available online at <https://www.clinicalresearcher.org/software.htm>). The stimulation intensity for TMS single-pulse protocol was set to 120% of the individual RMT.



*Study 2 Figure 2.* Single-subject measurement with (A) electrical nerve stimulation with and (B) without auditory masking. Illustrated polarity of the electrical nerve stimulation was reversed after half number of trials. For stimulation of the left side, the electrode of interest over contralateral (right) somatosensory area (C6) is marked by a black circle. For stimulation of the right side, the electrode of interest over contralateral (left) somatosensory area is also marked by the black circle. Lateralized activity (LA) is depicted with electrodes shown on the left side of the head; C5/C6 is marked by a black circle (LA C5/C6).

### 2.2.2.5 EEG data analysis

#### *Pre-processing*

EEG was pre-processed by BrainVision Analyzer (v2.1.2.327, Brain Products GmbH, Gilching, Germany). We intended to perform the analysis as identical as possible for the electrical nerve stimulation and TMS. The data was reduced to a sampling rate of 500 Hz. The electrical and TMS artifacts were removed by linear interpolation (Thut et al., 2011). Because of the difference in the duration of electrical and TMS artifacts, there was a difference in the interpolation period between the two stimulation types. Due to the duration of the electrical artifact, a time window of -10-100 ms was interpolated. As we intended to analyse long-latency potentials with latencies longer than 100 ms, the artifact, which ended at approximately at 90 ms, did not impede the measurements of the components of interest. As TMS produced a shorter artifact, a time window from -10-20 ms was interpolated. Afterwards, the data were re-referenced to an average reference and then segmented to epochs of  $\pm 500$  ms around the onset of the respective stimulus separately for each stimulation condition and side. Muscle artifacts, movements, electrode artifacts and eye blinks were removed by artifact rejection and a following independent component analysis. To reduce electrical 50 Hz noise and very low frequencies, a 50 Hz notch filter and a 0.5 low cut-off filter were applied to the data. The period of -100-10ms served as baseline. Finally, segments were averaged over all trials for each condition and stimulation side separately.

#### *Analysis of evoked potential components*

Due to the literature on SSEPs that postulated a somatosensory N140 to have a contralateral maximum around C5/C6, we specifically investigated our data around this time window and localization. In addition, we checked for other prominent peaks or topographic maxima with latencies longer than 100 ms.

*N140.* For the analysis of the somatosensory N140 during the electrical nerve stimulation and TMS, a peak detection was performed at the respective electrodes C5 or C6 contralateral to the side of stimulation for the time interval 120-160 ms, based on previous SSEP studies (Genna et al., 2016; Kida et al., 2004; Nakata et al., 2011). Electrodes C5 and C6 were chosen, because they are likely to lie over the somatosensory cortex (Hashimoto, 1988; Kaiser, 2010), which is said to be responsible for processing input of trigeminal fibers (Djuric et al., 1977; Genna et al., 2016). Furthermore, our topographies of electrical stimulation with auditory

masking showed their negative maximum around these electrodes. Mean amplitudes  $\pm 10$  ms around the detected peaks and mean peak latencies were exported for both hemispheres of the electrical nerve stimulation conditions and TMS and were used for statistical analyses.

*Lateralized activity.* Lateralized activity was calculated by subtracting the potential amplitude on the contralateral hemisphere from the potential amplitude on the ipsilateral hemisphere for both stimulation sides (see Fig. B1 in the supplementary material). Afterwards, the mean value of lateralization for left and right sided stimulation was calculated. The formula was analogous to the calculation of lateralized readiness potentials (Coles, 1989).

The following is an example calculation:

$$\text{lateralized activity C5/C6} = \frac{C5(\text{TMS left}) - C6(\text{TMS left}) + C6(\text{TMS right}) - C5(\text{TMS right})}{2}$$

Each electrode pair of homologous electrodes was calculated according to this principle. Thus, in figures 2,3,4,5, and 7 the information from both hemispheres and both stimulation sides were mapped on one (here left) hemisphere.

The calculation of lateralized activity is a method to represent lateralized components such as the trigeminal SSEP or the TMS-evoked N100. Symmetrical activity such as AEPs are eliminated by the subtraction procedure.

The calculation according to ipsilateral activity is more conventional and thus improves the applicability of our topographies to future investigations. This means that components with an ipsilateral lateralization appear with their original polarity when the lateralized activity is calculated (i.e. ipsilateral negative potentials lead to negative deflections in the lateralized activity). Contralateral negativities such as trigeminal SSEPs, in contrast, lead to positive deflections in the lateralized activity due to the subtraction of ipsilateral minus contralateral potentials.

In conclusion, lateralized activity results are well suited to isolate potential components which systematically depend on the stimulation site. However, they always need to be analyzed together with the “original data” maps for left- and right-sided stimulation. This is necessary to determine whether lateralized activity reflects ipsi- or contralateral activity as both, ipsilateral negativity and contralateral positivity can result in negative lateralized activity. For lateralized activity, a peak detection was performed for somatosensory N140 in the time interval 120-160 ms at the calculated electrode C5/C6. Mean amplitudes  $\pm 10$ ms around the peaks and peak latencies were exported.

*Explorative TMS-evoked N100 analysis.* To exploratively analyze the N100 at the left and right DLPFC after TMS, peaks were detected at ipsilateral F5 (for left TMS) and F6 (for right TMS) in the time window 80-140 ms (Lioumis, Kičić, Savolainen, Mäkelä, & Kähkönen, 2009; Loheswaran et al., 2018; Rusjan et al., 2010). Mean amplitudes  $\pm 10$  ms around the N100 peak and peak latencies were exported for TMS. A N100 was expected ipsilaterally to the stimulation side at F5 and F6 after TMS, but not after electrical nerve stimulation. Due to the missing N100 peak no individual peak detection could be performed for the electrical nerve stimulation conditions. Therefore, the mean peak latency for the N100 for TMS was applied to each subject in the electrical nerve stimulation conditions in order to examine whether somatosensory stimulation would evoke confounding potentials at the site and during the time-interval of the N100. We exported mean amplitudes  $\pm 10$  ms for all conditions.

#### 2.2.2.6 Statistics

Statistics were performed with IBM SPSS Statistics 25 software (IBM Corp., Armonk, NY, USA; Version 25).

- (1) SSEP components: Potential components as well as their lateralization were tested for significant deviations from the baseline by one paired *t*-tests.
- (2) SSEP components versus AEP: Regarding the somatosensory N140 evoked by trigeminal stimulation, amplitudes of ipsi- and contralateral C5 and C6 were examined by a 2x2x2 ANOVA for repeated measurements with the within-subject factors STIMULATION TYPE, STIMULATION SIDE and HEMISPHERE. The factor STIMULATION TYPE included the two electrical nerve stimulation conditions (1) with auditory masking and (2) without auditory masking. The SIDE discriminated between (1) left- and (2) right-sided stimulation. The factor HEMISPHERE included the amplitudes on the (1) left and on the (2) right hemisphere. Significant interactions were tracked by post-hoc ANOVAs with repeated measurements and *t*-tests with Bonferroni-Holm correction.
- (3) SSEP components versus TEPs (including AEP): For the comparison of TMS and the electrical nerve stimulation conditions with and without auditory masking, amplitudes of ipsi- and contralateral C5 and C6 were examined in a repeated measurement 3x2x2 ANOVA with the factors STIMULATION TYPE, STIMULATION SIDE and HEMISPHERE. Significant interactions were again tracked by ANOVAs with repeated measurements and post-hoc *t*-tests with Bonferroni-Holm correction.

(4) Explorative analysis TMS-evoked N100 vs electrical nerve stimulation (with and without auditory masking): We exploratively compared the TMS-evoked N100 at the stimulation site with the electrical nerve stimulation condition via a repeated measurement 3x2x2 ANOVA with the factors STIMULATION TYPE, STIMULATION SIDE and HEMISPHERE.

In all tests, a  $p$ -value  $< .05$  indicated a significant difference between conditions. One-sided tests were used to assess previously made directed hypotheses (e.g. larger amplitudes on the contralateral hemisphere). As effect size, partial eta-squared (partial  $\eta^2$ ) and Cohen's  $d$  ( $d$ ) were used. If necessary, the values were given in Greenhouse-Geisser corrected form.

### 2.2.3 Results

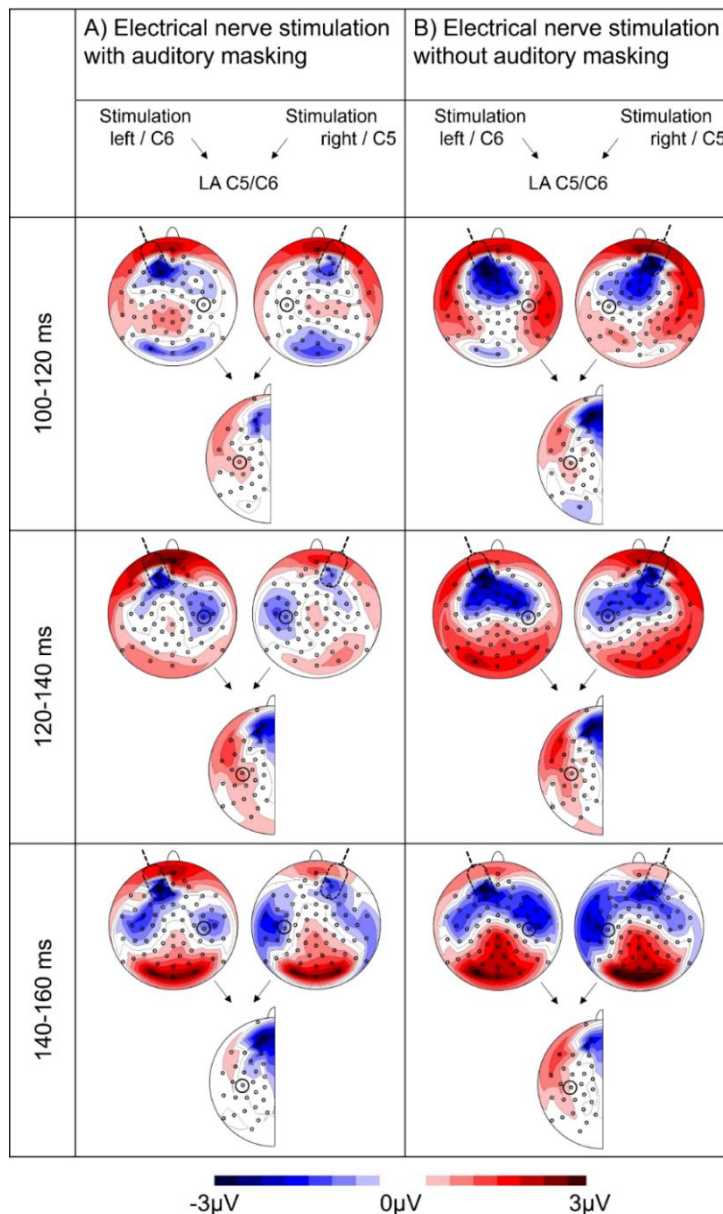
We found contralateral negativities at approximately 140 ms after electrical stimulation of the trigeminal nerve on the left and on the right side that are described in detail below. After TMS of the DLPFC, there was a contralateral negativity in a comparable time window when stimulating the left side. There was no corresponding potential over the contralateral hemisphere around 140 ms when TMS was applied on the right DLPFC. However, lateralized activity of TMS showed a contralateral negativity that occurred around 120 ms.

#### 2.2.3.1 Trigeminal SSEP N140 at C5/C6: topographies (120-140ms) and time courses

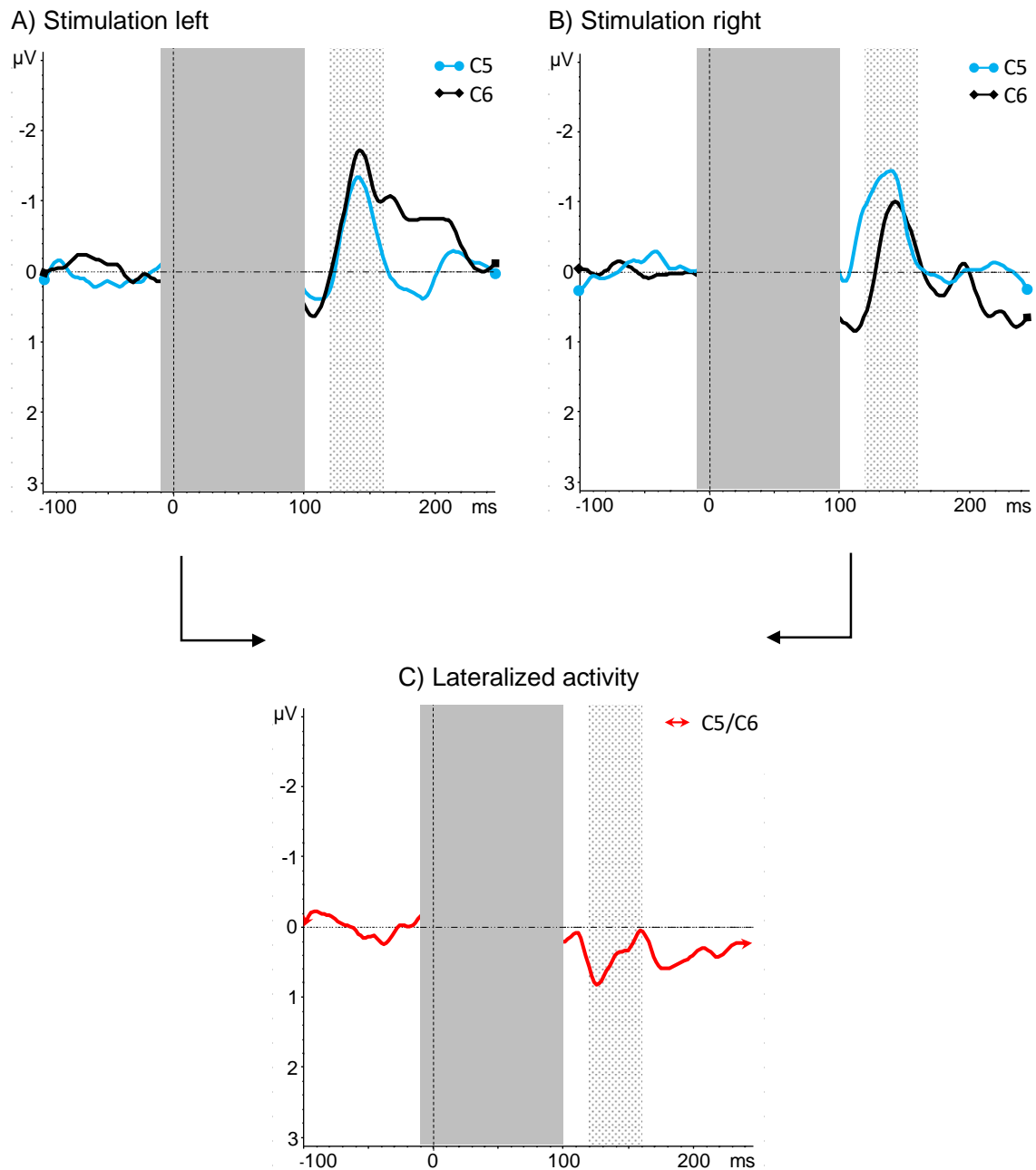
##### *Electrical nerve stimulation with auditory masking*

*Stimulation left.* The topographies between 120-140 ms for electrical nerve stimulation on the left side with auditory masking indicated a contralateral negativity at centroparietal electrodes around C6 (Fig. 3). The negative peak at C6 occurred with a mean peak latency of  $137.6 \pm 13.0$  ms (mean  $\pm$  SD) (mean peak amplitude C6 =  $-1.5 \pm 1.7$   $\mu$ V; Fig. 4A; significant difference to baseline, Table 1). There was no ipsilateral positive peak around electrode C5 between 120-140 ms that could confound contralateral cortical activation when analyzing lateralized activity (Fig. 4A).

Next to the stimulation site around Fp1 and AF3, there was a high-amplitude electrical artifact that could not be removed by data pre-processing. In an additional single-subject measurement, the polarity of the stimulating electrode was reversed after half of the trials. The artifact at the stimulation site was thereby strongly reduced in the average, showing that the more anterior negative deflection in electric nerves stimulation represents an electrical artifact (Fig. 2).



*Study 2 Figure 3.* Topographic distribution after electrical stimulation of the trigeminal nerve on the forehead in different time windows. (A) shows the condition with auditory masking and (B) without auditory masking. For stimulation of the left side, the electrode of interest over contralateral (right) somatosensory areas (C6) is marked by a black circle. For stimulation of the right side, the electrode of interest over contralateral (left) somatosensory areas is marked by the black circle. Lateralized activity (LA) is depicted with electrodes shown on the left side of the head; C5/C6 is marked by a black circle (LA C5/C6).



Study 2 Figure 4. Electrical nerve stimulation with auditory masking (A) on the left side at electrode of interest over the contralateral (right) somatosensory areas C6 (black  $\blacklozenge$ ) and ipsilateral C5 (light blue  $\bullet$ ), (B) stimulation on the right side at electrode of interest over the contralateral (left) somatosensory areas C5 (light blue  $\bullet$ ) and ipsilateral C6 (black  $\blacklozenge$ ) and (C) lateralized activity at C5/C6 (red  $\blacktriangleright$ ). Interpolated time window to remove the electrical artifact is marked in gray. Time window for peak detection of the trigeminal somatosensory evoked potential (SSEP) N140 is marked by the dotted area.

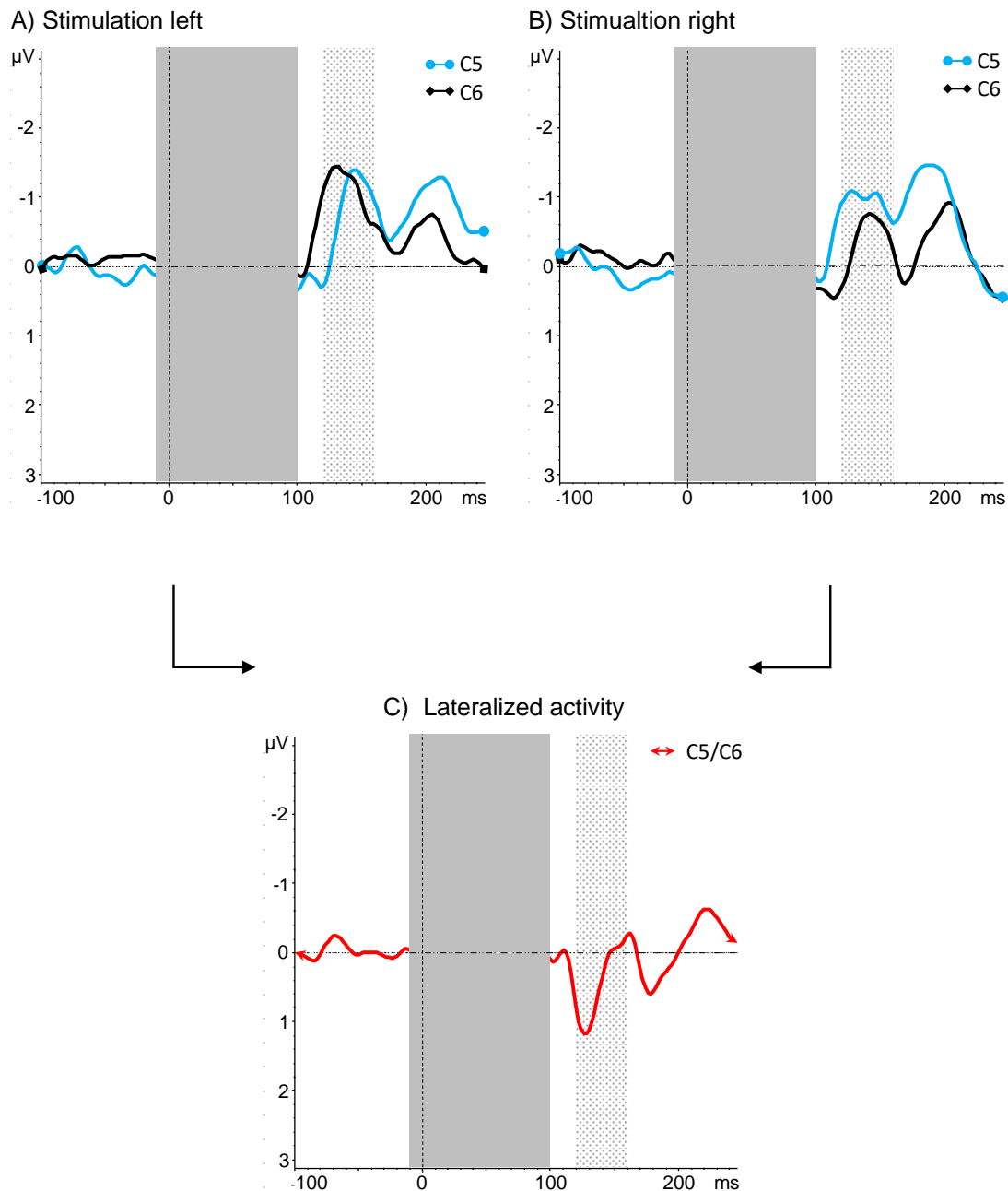
*Stimulation right.* The topography of right-sided stimulation also showed a significant contralateral negativity at centroparietal electrodes around electrode C5 (Table 1) with a latency of  $136.4 \pm 13.0$  ms (mean peak amplitude C5 =  $-1.5 \pm 1.2$   $\mu$ V; Fig. 4B). There was no ipsilateral positive peak around electrode C6 between 120-140 ms that could confound contralateral nerve activation when analyzing lateralized activity (Fig. 4B). The electrical artifact seen at the stimulation site was strongly reduced by electrode reversal during half of the trials in a single subject (Fig. 2).

*Lateralized activity.* When analyzing lateralized activity, electrical nerve stimulation with auditory masking topographically showed a systematically lateralized positive peak in C5/C6 with a latency of  $127.1 \pm 12.2$  ms and a mean peak amplitude of  $1.0 \pm 0.9$   $\mu$ V (Fig. 4C, Table 1). This peak was the only lateralized peak at electrode C5/C6 between 120-140 ms and was generated by the two negative peaks on the contralateral hemisphere. Ipsilateral positive peaks did not confound the lateralized potential. Note that we subtracted contralateral from ipsilateral potentials, so that a contralateral negativity produces positive amplitudes in this measure of lateralized activity.

Another lateralized positivity between 120-140 ms occurred around electrode FT9/10, however we did not further analyze this part, as it was produced by a positivity ipsilateral to stimulation and was also strongly reduced by electrode reversal during half of the trials in the single subject (Fig. 2).

#### *Electrical nerve stimulation without auditory masking*

*Stimulation left.* For electrical nerve stimulation on the left side without auditory masking, the contralateral negativity at C6 between 120-140 ms occurred with a latency of  $143.1 \pm 6.2$  ms and a mean peak amplitude of  $-1.5 \pm 1.1$   $\mu$ V (Fig. 5A) (significant difference to baseline, Table 1). There was no ipsilateral positive peak between 120-140 ms that could confound contralateral nerve activation when analyzing lateralized activity (Fig. 5A). An electrical artifact at the stimulation site was confirmed which was strongly reduced by electrode reversal during half of the trials in a single subject (Fig. 2). Additionally, there was an auditory evoked negativity in frontocentral and central electrodes (Fig. 3) caused by the absence of auditory masking.



*Study 2 Figure 5.* Electrical trigeminal nerve stimulation without acoustic masking (A) on the left side at electrode of interest over the contralateral (right) somatosensory areas C6 (black  $\blacklozenge$ ) and ipsilateral C5 (light blue  $\bullet$ ), (B) on the right side at electrode of interest over the contralateral (left) somatosensory areas C5 (light blue  $\bullet$ ) and ipsilateral C6 (black  $\blacklozenge$ ) and (C) lateralized activity at C5/C6 (red  $\blacktriangleright$ ). Interpolated time window to remove the electrical artifact is marked in gray. Time window for peak detection of the trigeminal somatosensory evoked potential (SSEP) N140 is marked by the dotted area.

*Stimulation right.* Stimulation on the right without auditory masking also resulted in a significant negativity at centroparietal C5 on the contralateral hemisphere between 120 and 140 ms (Table 1) with a latency of  $133.4 \pm 9.8$  ms (mean peak amplitude C5 =  $-1.4 \pm 1.6$   $\mu$ V ; Fig. 5B). There was no ipsilateral positive peak between 120-140 ms that could confound contralateral nerve activation when analyzing lateralized activity (Fig. 5B).

The frontal electrical artifact, which was strongly reduced by electrode reversal during half of the trials in a single subject, was confirmed as well (Fig. 2). Additionally, there was again an auditory evoked negativity in frontocentral and central electrodes (Fig. 3) caused by the absence of auditory masking.

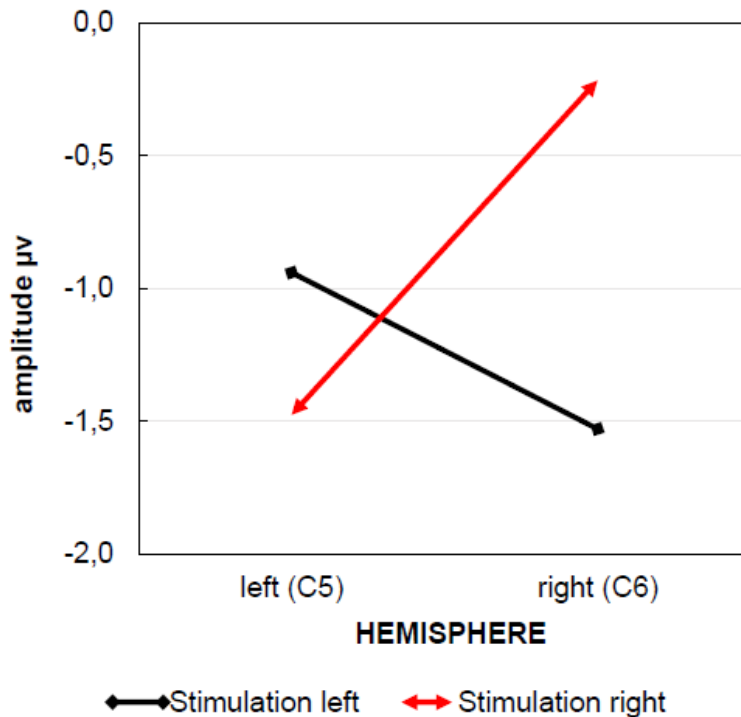
*Lateralized activity.* In the lateralized activity the positivity in C5/C6 was confirmed between 120-140 ms as well with a latency of  $125.9 \pm 11.4$  ms, and a mean peak amplitude of  $0.9 \pm 1.3$   $\mu$ V (Fig. 5C) (significant difference to baseline, Table 1). This peak was the only lateralized positive peak at electrode C5/C6 between 120-140 ms and was generated by the two negative peaks on the contralateral hemisphere. Furthermore, ipsilateral positive peaks did not confound this effect (Fig. 5C). Note again that we subtracted contralateral from ipsilateral potentials, so that a contralateral negativity produced positive amplitudes in this measure of lateralized activity.

Another lateralized positivity between 120-140 ms occurred again around electrode FT9/10 (Fig. 3), however we did not further analyze this part, as it was produced by a positivity ipsilateral to stimulation and strongly reduced by electrode reversal during half of the trials in the single subject (Fig. 2).

*Statistical analysis: trigeminal SSEP N140 at C5/C6 after electrical nerve stimulation with and without auditory masking*

*2x2x2 ANOVA N140 (C5, C6).* Regarding the contralateral N140 of trigeminal SSEPs at C5 and C6, there was no significant three-way interaction STIMULATION TYPE, STIMULATION SIDE and HEMISPHERE ( $F(1,13) = 1.05, p = .32, \text{partial } \eta^2 = .08$ ). However, there was a significant interaction STIMULATION SIDE x HEMISPHERE ( $F(1,13) = 17.86, p = .001^{**}, \text{partial } \eta^2 = .58$ , Fig. 6). When tracking this interaction by *t*-tests, for right side stimulation, significantly larger amplitudes over the contralateral (left) hemisphere were found ( $t(13) = 5.74, p < .001^{**}, d = 1.53$ ). Stimulation on the left side showed a trend towards larger amplitudes on the contralateral hemisphere ( $t(13) = 1.42, p = .09, d = .38$ ). Overall, the data pointed towards

larger negative amplitudes on the contralateral hemisphere that changed their lateralization according to the stimulation side (Fig. 6).



*Study 2 Figure 6.* Two-way interaction STIMULATION SIDE x HEMISPHERE over both electrical nerve stimulation conditions. Stimulation of the left side (black line ◆) is shown at the electrode of interest over the contralateral (right) somatosensory areas C6 and at ipsilateral C5. Stimulation of the right side (red line ►) is shown at the electrode of interest over the contralateral (left) somatosensory areas C5 and at ipsilateral C6.

### 2.2.3.2 Comparison of electrical nerve stimulation with and without auditory masking and TMS of the DLPFC

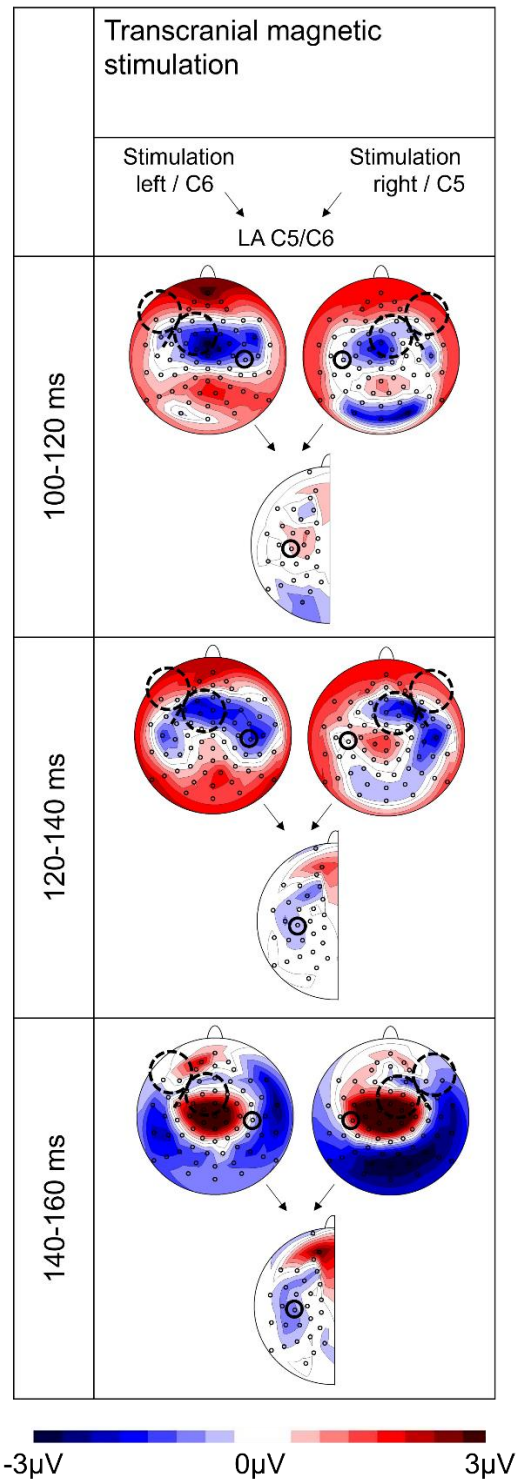
*Contralateral activation 120-140 ms after TMS of DLPFC (is there comparable brain activation after TMS of the DLPFC which resembled electrical trigeminal stimulation?)*

*Left DLPFC TMS.* Corresponding to electrical nerve stimulation of the trigeminal, left-sided TMS showed a significant negativity at C6 (Table 1 & Fig. 7) between 120-140 ms with a mean peak latency of  $132.0 \pm 8.3$  ms (mean peak amplitude C6 =  $-1.7 \pm 1.1$  µV; Fig. 8A). This contralateral peak in centroparietal electrodes already between 100-120 ms with an amplitude of  $-0.9 \pm 1.4$  µV (significant difference to baseline ( $p = .03$ ), Table 1). There was no

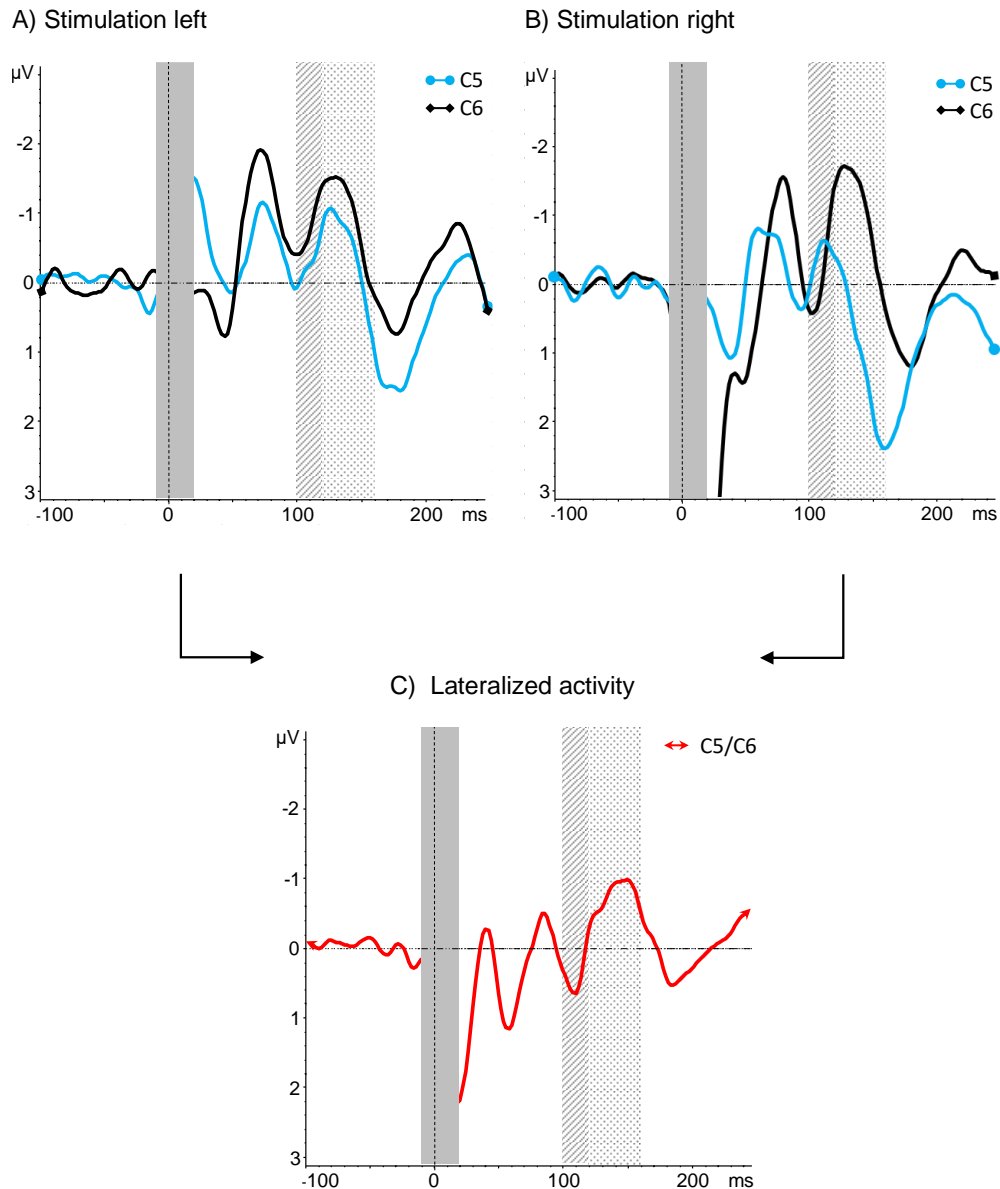
ipsilateral positive peak that could confound contralateral activation of the brain by TMS when analyzing lateralized brain activity (Fig. 8A).

Additionally, a negativity in central electrodes, topographically similar to the AEP in the electrical nerve stimulation condition without auditory masking was visible between 120-140 ms.

As an obvious difference to electrical nerve stimulation, there was no electrical artifact at the stimulation site used for trigeminal stimulation.



*Study 2 Figure 7.* Topographic distribution of transcranial magnetic stimulation (TMS). TMS of the left dorsolateral prefrontal cortex (DLPFC) is shown in the left column (Stimulation left / C6) and the electrode of interest over contralateral (right) somatosensory areas (C6) is marked by a red circle. TMS of the right DLPFC is shown in the right column (Stimulation right / C5) and the electrode of interest over contralateral (left) somatosensory areas (C5) is marked by a red circle. Lateralized activity (LA) is also depicted with electrodes shown on the left side of the head; C5/C6 is marked by a red circle (LA C5/C6).



*Study 2 Figure 5.* Transcranial Magnetic Stimulation (TMS) of the dorsolateral prefrontal cortex (DLPFC) (A) on the left side at electrode of interest over the contralateral (right) somatosensory areas C6 (black  $\blacklozenge$ ) and ipsilateral C5 (light blue  $\bullet$ ), (B) on the right side at electrode of interest over the contralateral (left) somatosensory areas C5 (light blue  $\bullet$ ) and ipsilateral C6 (black  $\blacklozenge$ ) and (C) lateralized brain activity at C5/C6 (red  $\blacktriangleright$ ). Interpolated time window to remove the electrical artifact is marked in gray. Time window for the peak detection of the trigeminal SSEP N140 is marked by the dotted area. The alternative earlier time window in which comparable potentials to those of trigeminal somatosensory evoked potential (SSEP) were found is marked by the hatched area.

*Right DLPFC TMS.* TMS on the right side did not lead to a significant contralateral negativity at C5 between 120-140 ms (mean peak latency =  $129.9 \pm 12.8$  ms; mean peak amplitude =  $-0.6 \pm 1.9$   $\mu\text{V}$ ; Fig. 8B) (no significant difference to baseline with  $p = .30$ , Table 1). A contralateral

negativity in centroparietal electrodes was significant in an earlier time window of 100-120 ms with a latency of  $118.6 \pm 11.0$  ms and an amplitude of  $-1.2 \pm 1.6$   $\mu$ V (Table 1 & Fig. 7). The potential topography in this time window 100-120 ms was similar to the topography in the condition electrical stimulation without auditory masking. There was no ipsilateral positive peak that could confound contralateral activation of the brain by TMS when analyzing lateralized brain activity (Fig. 8B).

A negativity in central electrodes, topographically similar to the AEP in the electrical nerve stimulation condition without auditory masking was visible.

Again, different to electrical nerve stimulation, there was no electrical artifact at the stimulation site.

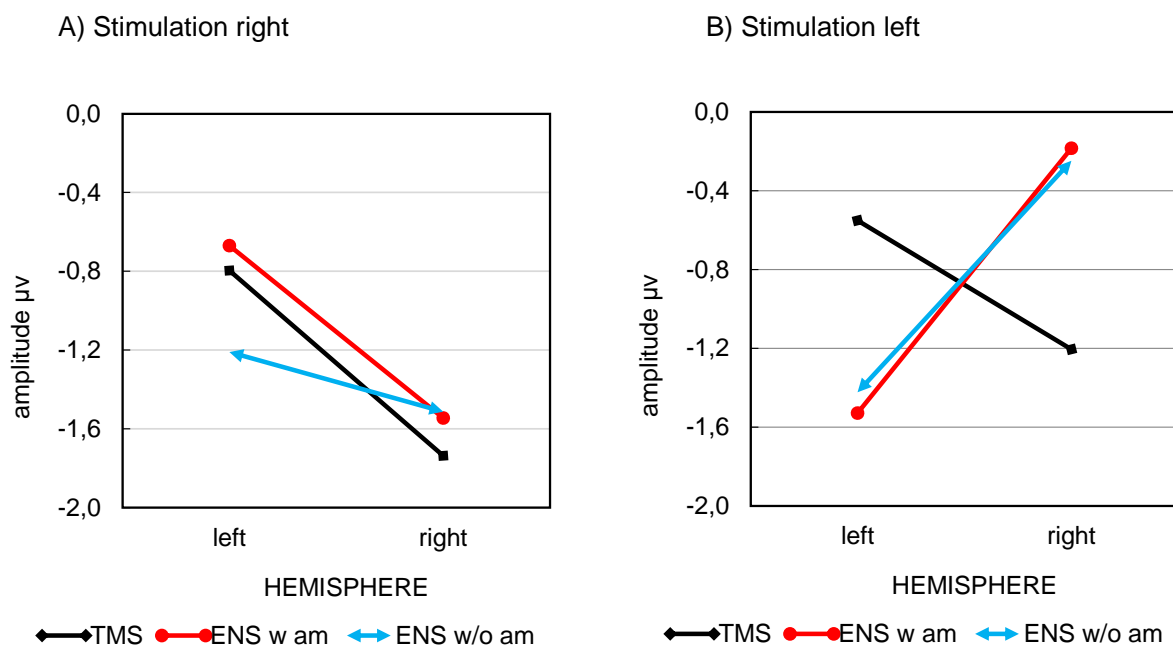
*Lateralized activity DLPFC TMS.* In the lateralized activity in response to TMS no comparable positive peak at C5/C6 was found between 120-140 ms (mean peak latency =  $135.7 \pm 16.6$  ms, mean peak amplitude =  $0.4 \pm 1.5$ ; no significant difference to baseline ( $p = .30$ ), Table 1). A lateralized positivity at C5/C6 was significant in the earlier time window of 100-120 ms with a mean latency of  $116.3 \pm 17.8$  ms and a mean peak amplitude of  $0.9 \pm 1.2$   $\mu$ V (Fig. 8C) ( $p = .01$ , Table 1). Its topography was similar to lateralized positivity following electrical trigeminal stimulation, however, it was located slightly more frontally and closer to the midline. Note again that we subtracted contralateral from ipsilateral potentials as described previously. This peak was the only lateralized positive peak at electrode C5/C6 between 100-120 ms and was generated by the two negative peaks on the contralateral hemisphere. Ipsilateral positive peaks (Fig. 8) did not confound this effect.

#### *Trigeminal SSEP N140 at C5/C6: statistical comparison across stimulation conditions*

*3x2x2 ANOVA N140 (C5, C6).* A trend towards a three-way interaction between the factors STIMULATION TYPE, STIMULATION SIDE and HEMISPHERE ( $F(2,26) = 3.0$ ,  $p = .07$ , partial  $\eta^2 = .19$ ; Fig. 9) was observed in the contralateral N140 at C5 and C6. When the trend was followed by a 3x2 ANOVA for right side stimulation, the interaction STIMULATION TYPE x HEMISPHERE was significant ( $F(2,26) = 4.72$ ,  $p = .02^*$ , partial  $\eta^2 = .27$ ). An one-way ANOVA for each STIMULATION TYPE for the right SIDE showed significantly higher negative amplitudes over the contralateral (left) HEMISPHERE for the two electrical nerve stimulation conditions (with auditory masking:  $t(13) = -3.76$ ,  $p = .003^{**}$ ,  $d = -1.00$ ; without auditory masking:  $t(13) = -2.87$ ,  $p = .01^*$ ,  $d = 3.74$ ). For TMS there were no significant differences between the hemispheres

(TMS:  $t(13) = 0.91$ ,  $p = .19$ ,  $d = .24$ ). Thus, TMS on the right side did not lead to a comparable contralateral negativity as we found in both electrical stimulation conditions.

For the left side, there was no significant two-way interaction STIMULATION TYPE x HEMISPHERE ( $F(2,26) = 0.62$ ,  $p = .55$ , partial  $\eta^2 = .05$ ). However, there was a significant main effect HEMISPHERE on the left SIDE with higher negative amplitudes on the contralateral (right) hemisphere ( $F(1,13) = 4.71$ ,  $p = .049^*$ , partial  $\eta^2 = .27$ ). All stimulation conditions thus led to a comparable contralateral negativity when the left side was stimulated.



*Study 2 Figure 9.* Three-way interaction between STIMULATION TYPE\*STIMULATION SIDE\*HEMISPHERE divided by factor SIDE. All stimulation types are shown for stimulation of the left side (A) at electrode of interest over the contralateral (right) somatosensory areas C6 and at ipsilateral C5. Stimulation types for stimulation of the right (B) side are shown at electrode of interest over the contralateral (left) somatosensory areas C5 and ipsilateral C6. TMS (black  $\blacklozenge$ ) = transcranial magnetic stimulation, ENS w am (red  $\blacktriangleright$ ) = Electrical nerve stimulation with auditory masking, ENS w/o am (light blue  $\bullet$ ) = Electrical nerve stimulation without auditory masking.

### 2.2.3.3 Explorative analysis of the TMS-evoked N100 in the DLPFC at F5 and F6

*Ipsilateral activation 100-120 ms after TMS of DLPFC at F5/F6 (is there an ipsilateral N100 in the TMS condition?)*

*Left DLPFC TMS.* TMS on the left side led to a significant negativity at F5 (Table 1) ipsilateral to stimulation side with a mean peak latency of  $107.9 \pm 16.6$  ms and a mean peak amplitude of  $-3.5 \pm 4.3 \mu\text{V}$ .

*Right DLPFC TMS.* With right-sided TMS of the DLPFC, an ipsilateral negativity at F6 with a mean peak latency of  $110.3 \pm 15.3$  ms and a mean peak amplitude of  $-2.5 \pm 3.6$   $\mu$ V (Table 1) occurred.

*Lateralized activity DLPFC TMS.* The lateralized activity of TMS showed a negative N100 peak with a latency of  $109.3 \pm 20.0$  ms at F5/F6 between 100-120 ms (mean peak amplitude =  $-2.2 \pm 3.3$   $\mu$ V, Table 1).

*Possible confounding effects of both electrical stimulation conditions during the TMS-evoked N100 component at the respective recording sites F5 / F6*

*Electrical nerve stimulation left.* In left-sided stimulation, neither electrical nerve stimulation with (mean amplitude:  $-0.5 \pm 3.1$   $\mu$ V; no significant difference to baseline with  $p = 1.0$ , Table 1) nor without auditory masking (mean amplitude:  $-1.2 \pm 1.6$   $\mu$ V; no significant difference to baseline with  $p = .10$ , Table 1) resulted in a significant negativity at the stimulation site at F5.

*Electrical nerve stimulation right.* Even with right-sided stimulation, neither electrical nerve stimulation with (mean amplitude:  $-0.4 \pm 1.8$   $\mu$ V; no significant difference to baseline with  $p = 1.0$ , Table 1) nor without auditory masking (mean amplitude:  $-0.1 \pm 3.1$   $\mu$ V; no significant difference to baseline with  $p = 1.0$ , Table 1) resulted in a significant negativity at the stimulation site at F6.

*Lateralized activity electrical nerve stimulation.* In the lateralized activity of the electrical nerve stimulation conditions, no significant negativity could be found at F6/F6 (with masking:  $-0.7 \pm 1.3$   $\mu$ V, no significant difference to baseline with  $p = .34$ ; without masking:  $-0.6 \pm 2.6$   $\mu$ V, no significant difference to baseline with  $p = 1.0$ , Table 1).

*Ipsilateral TMS-evoked N100: Statistical comparison TMS-evoked N100 of the DLPFC and electrical nerve stimulation*

*3x2x2 ANOVA N100 (F5, F6).* The 3x2x2 ANOVA showed a significant three-way interaction STIMULATION TYPE x SIDE x HEMISPHERE ( $F(2,26) = 3.65$ ,  $p = .04^*$ , partial  $\eta^2 = .22$ ).

The three-way interaction was tracked with two 3x2 ANOVAs, separately for stimulation on the left and on the right SIDE.

On the right STIMULATION SIDE, there was a significant interaction (STIMULATION TYPE x HEMISPHERE:  $F(2,26) = 6.02$ ,  $p = .007$ , partial  $\eta^2 = .32$ ). A one-way ANOVA for each STIMULATION TYPE for the right SIDE showed a significant main effect in HEMISPHERE for TMS

( $F(1,13) = 5.30, p = .04, \text{partial } \eta^2 = .29$ ). TMS exhibited higher negative amplitudes on the right HEMISPHERE ipsilateral to stimulation. For both electrical nerve stimulation conditions with and without auditory masking there was no significant difference between the left and right HEMISPHERE while stimulating on the right SIDE (with auditory masking:  $F(1,13) = .09, p = .77, \text{partial } \eta^2 = .01$ ; without auditory masking:  $F(1,13) = 1.18, p = .30, \text{partial } \eta^2 = .08$ ) On the left SIDE, the interaction STIMULATION TYPE x HEMISPHERE was not significant (STIMULATION TYPE x HEMISPHERE:  $F(2,26) = 1.22, p = .31, \text{partial } \eta^2 = .09$ ). However, there were significant main effect STIMULATION TYPE ( $F(2,26) = 6.29, p = .01^*, \text{partial } \eta^2 = .33$ ). TMS showed higher negative amplitudes compared to both electrical nerve stimulation conditions. Furthermore, there was a significant main effect HEMISPHERE with higher negative amplitudes on the left HEMISPHERE in TMS and both electrical nerve stimulations ( $F(1,13) = 6.77, p = .02^*, \text{partial } \eta^2 = .34$ ).

#### 2.2.4 Discussion

The aim of this study was to analyze trigeminal SSEPs after 100 ms with respect to latency, amplitude, and topography after electrical nerve stimulation of the trigeminus. In addition, we wanted to investigate whether contralateral components comparable to trigeminal SSEPs occur after TMS. For this purpose, we compared electrical and magnetic stimulation.

A main finding was the detection of trigeminal SSEPs in central electrodes around C5 and C6 with asymmetry to the contralateral hemisphere at approximately 140 ms after electrical stimulation of the trigeminus. A comparable potential on the contralateral hemisphere with a similar topography (a negative maximum around C6) was found after TMS to the left DLPFC. TMS of the right DLPFC also showed a right-sided negative maximum around C6 but without pronounced contralateral negativity in this time window. In another recently published study, in a different sample, we found a comparable contralateral negative maximum at C5/C6 for both right and left DLPFC TMS in the time window 120-140 ms. However, also in that sample, the topographies showed a clear lateralization towards C6 only for left-sided TMS, for right-sided TMS the negative potentials around C5/C6 were quite symmetrical, indicating a consistently stronger processing on the right hemisphere (Jarczok et al., 2021).

In an earlier time-window 100-120 ms, the analysis of lateralization revealed contralateral negativity after TMS. However, we cannot exclude that lateralized AEPs contribute to the negative activity in this time window. Maps between 100-120 ms showed a frontocentral and

contralaterally lateralized negativity which resembled the topography of electrical nerve stimulation without auditory masking, but not electrical nerve stimulation when auditory masking was used. Therefore, these potentials most likely represent an AEP and lateralized components of the AEP (Bender et al., 2006; Conde et al., 2019).

#### 2.2.4.1 Trigeminal SSEPs

We found trigeminal SSEPs after electrical nerve stimulation to have their maximum on the contralateral hemisphere at centroparietal electrodes (Fig. 3, 120-140 ms) representing most likely a somatosensory N140 (Desmedt & Robertson, 1977; Genna et al., 2016; Hämäläinen et al., 1990). Regarding lateralized activity, the trigeminal SSEPs occurred in both electrical nerve stimulation conditions at C5/C6. However, electrical stimulation of the left side only showed a trend towards a contralateral maximum, as ipsilateral activity was also present. Taking this trend together with the topographies (Fig. 3, 120-140 ms and 140-160 ms), it appears that trigeminal SSEPs initially peaked on the contralateral hemisphere (120-140 ms) and then became more bilateral (140-160 ms). This is consistent with studies on peripheral nerve stimulation that reported bilateral SSEPs to have an asymmetry to the contralateral hemisphere (T. L. Chen et al., 2008; Desmedt & Robertson, 1977; Hämäläinen et al., 1990). Trigeminal SSEPs with longer latencies are likely to be generated in bilateral secondary somatosensory cortex (SII) (Allison et al., 1992; Conde et al., 2019). Bilateral SII receives unilateral input of the primary somatosensory cortex (SI) and purportedly plays a major role in higher sensory processing and the integration of tactile information (Bradley et al., 2016; Eickhoff et al., 2006). There is evidence for an asymmetric activation of bilateral SII after electrical stimulation of peripheral nerves with higher amplitudes over the contralateral hemisphere (Jung et al., 2009; Yu et al., 2018). Activation of SII is considered to occur as surface activity at central electrodes around C5/C6 and CP5/6 (Bradley et al., 2016; Kaiser, 2010). An asymmetry in SII activation after electrical stimulation of the trigeminal nerve could thus be an underlying reason for our results of a bilateral SSEP with contralateral maximum around C5/C6.

While searching for comparable potentials in TMS of the DLPFC, we found a similar bilateral topography with contralateral maximum around 140 ms only in TMS on the left side (Fig.7, 120-140 ms). There was no contralateral negative maximum around C5 when TMS was applied

to the right DLPFC. Taking our TMS topographies and the results of another recently published study (Jarczok et al., 2021), we believe that parts of an SSEP possibly contribute to the TEP topography to varying extents, especially on the right hemisphere. There is some evidence for a hemispheric difference with right lateralized somatosensory processing in the inferior parietal cortex (BA 40) and dorsolateral prefrontal cortex after thermal somatosensory stimulation of the right and left arm (Coghill et al., 2001). Activation in the left hemisphere only occurred after right-sided stimulation, whereas the right hemisphere was activated by both right- and left-sided stimulation (Coghill et al., 2001). However, most SSEP research did not report such a preponderance of right-hemispheric somatosensory processing, but describe bilateral activation with a contralateral maximum when stimulating the right side (i.e. Chen et al., 2008; Genna et al., 2016). This is consistent with our trigeminal SSEP data with auditory masking, in which we also found no evidence of a general predominance of the right hemisphere.

Furthermore, it must be considered that SSEPs could overlap with lateralized AEP components. AEPs can be divided into the N1a, N1b and N1c (Alain et al., 1997; Knight et al., 1988). The frontocentral negativity that we found in electrical stimulation without auditory masking and TMS can most likely be attributed to the auditory N1b (Bender et al., 2006). Moreover, the N1b around 100 ms was found to exhibit contralateral asymmetry with monaural stimulation (Hine & Debener, 2007; Langers et al., 2005). This is to a limited extent the case with TMS (coil click closer to the ipsilateral ear), but not with electrical nerve stimulation, as the clicking neurostimulator was positioned in the midline behind the subjects. In addition, there is evidence for the auditory N1c to occur around 120 ms with a contralateral temporal maximum (Bender et al., 2006; Tonnquist-Uhlen et al., 2003). Hence, we cannot exclude that the contralateral negative activity in our TEPs also contained lateralized components of an auditory N1b / N1c.

In summary, it appears that contralateral potentials between 100-120 ms are more likely due to lateralized AEP components and later activity between 120-140 ms to SSEPs. The topographies of electrical nerve stimulation with auditory masking (Fig. 3) reinforce this conclusion by showing contralateral negativities between 120-140 ms but not 100-120 ms.

Our results on SSEPs and their topography are not only relevant for TEPs over the DLPFC, but also for studies that stimulate, for example, the motor cortex as a region of interest. The V1 of the trigeminal nerve extends over the motor cortex (Fillmore & Seifert, 2015) and can thus

lead to SSEPs even with TMS-EEG of M1. Thus, our results can also be applied to other stimulation sites where the trigeminal nerve is innervated.

Future studies including TMS with proper auditory masking and/or an anesthesia of the corresponding skin nerves will have to resolve the issue of the amount to which trigeminal SSEP contribute to TEPs, since we cannot fully exclude that lateralized parts of the AEP projecting to temporal and frontocentral areas account for the topographies of the peripherally evoked part of TEPs. Furthermore, future studies should continue to work on ways to reduce trigeminal artefacts directly during recording of TMS-EEG by checking TEP amplitudes online, as has been suggested by Belardinelli et al. (2019). In addition, AEP masking techniques that combine white noise with coil click frequencies should be used in future TMS-EEG designs to best eliminate AEPs already during recording (see supplementary material of Massimini et al., 2005; Rocchi et al., 2021). This is important in view of the fact that the TMS click cannot always be completely masked with white noise alone (Biabani et al., 2019). In this context, an understanding of the topography of SSEP contribution to TEPs can inform studies aiming at minimizing the effects of peripherally evoked components on TEPs and may also be useful in settings in which adequate masking cannot be achieved (e.g. when children do not tolerate masking).

#### 2.2.4.2 TMS-evoked N100

We exploratively analyzed the TMS-evoked N100 as an often examined TEP component (Bender et al., 2005; Kerwin et al., 2018; Loheswaran et al., 2018; Premoli, Rivolta, et al., 2014; Rogasch et al., 2015). We found a TMS-evoked N100 after TMS of the DLPFC as ipsilateral negativity at F5 and F6 around 100 ms (Lioumis, Kičić, et al., 2009; Tallus et al., 2013) which was significantly larger than any possible confounding potentials by SSEP in the corresponding time interval. None of the electrical nerve stimulation conditions led to a comparable significant negativity at F5 and F6 with a similar topography or amplitude. However, it must be considered that latencies <100 ms could not be analyzed in the electrical nerve stimulation conditions due to the interpolation period of 100 ms. These results can therefore only serve as an indication that the ipsilateral N100 tended to occur only in TMS. Due to the ipsilateral lateralization of the N100, it could be cautiously assumed that the trigeminal SSEP is distinguishable from the TMS-evoked N100 because of its contralateral topography and latency of about 140 ms. However, we would like to emphasize that no claims can be made

about the comparison of the two conditions are before 100 ms, as no data for this time range is available for the electrical nerve stimulation.

#### 2.2.4.3 Limitations

Despite the attempt to keep the conditions of electrical and magnetic stimulation equal, there were slight differences regarding the sensation, sound, and exact location of the stimulations. However, the comparability of the two types was reinforced by aligning the intensities of sensation between electrical nerve stimulation and TMS. Moreover, the supraorbital branch of the trigeminal nerve innervates both the forehead and the front part of the scalp (Kemp et al., 2011) and was thus stimulated in both TMS and electric nerve stimulation, although there was a slight difference in sensation and localization. Furthermore, the large electrical artifact led to a long interpolation time window and made it impossible to examine shorter-latency somatosensory potentials. This restriction had little impact on our results, since we focused in this study on SSEPs with longer latencies >100 ms. The limitations due to the interpolation period therefore refer solely to the exploratory analysis of the N100. It should also be mentioned that there have been suggestions for a general alternative for interpolating a period of time to remove artifacts. Lioumis et al. (2018) and Rogasch et al. (2020) have suggested methods for the removal of artifacts should be removed in future TMS-EEG designs. However, interpolating the TMS or electrical artifact is a common method often used in TMS-EEG studies so that we stuck to this procedure (Bergmann et al., 2012; Premoli et al., 2018). Additionally, the ground electrode was located near Pz and Cz was the reference electrode. However, this study aimed to examine mainly trigeminal SSEPs and not AEPs. Lateralized SSEPs were not affected by the ground and reference electrode on the midline.

#### 2.2.4.4 Conclusion

Overall, we found long-latency trigeminal SSEPs after electrical stimulation with masking of auditory potentials bilaterally, but with a contralateral maximum between 120 and 140 ms. There was contralateral activity after TMS of the DLPFC, which could be partly due to trigeminal SSEPs. However, future studies will have to resolve the issue of the extent to which trigeminal SSEP contribute to TEPs, since we cannot fully exclude that lateralized parts of an AEP contribute to the topographies of the peripherally evoked part of TEPs.

In conclusion, we suggest that SSEPs are capable, in principle, of inducing contralateral negative components in the TEP if they occur in spite of proper auditory masking.

### 2.3 Study 3: Fearful facial expressions reduce inhibition levels in the dorsolateral prefrontal cortex in subjects with specific phobia

From the two previous studies, we know that the TMS-evoked N100 most likely occurs ipsilaterally as a negativity over the DLPFC and that trigeminal SSEPs can probably be distinguished from the N100 by their contralateral topography. The TMS-evoked N100 is next used as a measure of cortical inhibition in a clinical context. Due to the high prevalence of specific phobias, possible cortical dysfunctions of this group of anxiety disorders will be investigated using the N100. A sample of young adults with specific phobias was compared to a control group regarding their N100 amplitudes.

#### 2.3.1 Introduction

Anxiety disorders are the most frequently diagnosed neuropsychiatric disorders, with specific phobias having the highest prevalence among anxiety disorders (Beesdo-Baum & Knappe, 2012; Beesdo et al., 2010). In spite of their high prevalence, the neuronal mechanisms of the pathophysiology of specific phobias have not yet been fully elucidated (Linares et al., 2012). The dorsolateral prefrontal cortex (DLPFC) is responsible for cognitive control via top-down regulation of associative and attentional processes (Cohen et al., 1997; MacDonald et al., 2000). There is evidence for cognitive control deficits in specific phobias, e.g. an impaired ability of the DLPFC to inhibit interfering information (Bishop et al., 2007; Del Casale et al., 2012). Meanwhile, limbic system activation increases in response to threatening stimuli, but decreases with higher inhibitory influences from prefrontal cortex areas (Hariri et al., 2000, 2003). Thus, the pathophysiology of specific phobias is thought to involve mutual interactions between limbic and prefrontal regions (Del Casale et al., 2012; Linares et al., 2012). In specific phobias, an adaptive balance between both systems might be shifted towards a hyperactive amygdala and a relatively hypoactive DLPFC, resulting in insufficient top-down control of attention especially in the presence of fear-related stimuli. In order to accomplish an efficient top-down emotion regulation, and to focus attention to be able to accomplish a task in spite of fearful stimuli, it is necessary to shield goal-directed activation in the DLPFC against bottom-

up unspecific arousal increases (e.g. by input from limbic and/or subcortical areas). Inhibitory interneurons are thought to be crucial in maintaining a specific network activation pattern in the DLPFC in order to shield the behavioural goal encoded by this activation pattern against influences of interfering stimuli (Grace & Rosenkranz, 2002). Thus, such an inhibitory deficit in the DLPFC could contribute as a risk factor to ineffective top-down control and thus to less efficient shielding. This could impair the ability to organize goal-directed behavior in dealing with fear-related stimuli.

Previous functional neuroimaging studies failed to reflect the mechanism responsible for this deficient top-down control and provide inconsistent data. While some authors associate anxiety disorders with a reduced DLPFC activation (Bishop, 2009), others describe an increase (Basten et al., 2011; Eysenck et al., 2007). To our knowledge, there is no study investigating the mechanism of cortical inhibition directly in the DLPFC in specific phobias.

Using transcranial magnetic stimulation (TMS) with simultaneous electroencephalography (EEG), functional processes of cortical networks can be investigated (Massimini et al., 2005; Rogasch & Fitzgerald, 2013). Time-locked responses to TMS in the EEG signal are called TMS-evoked potentials (TEP). A commonly studied TEP component is the N100 (Bender et al., 2005; Bruckmann et al., 2012; Rogasch et al., 2015). TMS-EEG-studies suggest that the N100 reflects cortical inhibition (Bender et al., 2005; Bonnard et al., 2009) mediated by metabotropic gamma-aminobutyric acid (GABA) B-receptors (Premoli, Rivolta, et al., 2014; Rogasch & Fitzgerald, 2013). GABA-B-receptors are of special interest as they seem to be crucial in the pathophysiology of anxiety disorders (Cryan & Kaupmann, 2005; Möhler, 2012; Mombereau et al., 2004). Hence, monitoring TMS-evoked N100 allows a non-invasive investigation of cortical inhibition in specific phobias.

We hypothesized that young adults with specific phobia would show an inhibitory deficit in the DLPFC which is increased by the processing of fear-related stimuli like fearful facial expressions, compared to controls (Del Casale et al., 2012; Phelps, 2006; Straube et al., 2004). According to our hypothesis, we expected a smaller amplitude of the TMS-evoked N100 over the DLPFC as a parameter of intracortical inhibition (electrodes F5/F6). Furthermore, there is evidence that emotional processing can modulate cortical activity (Bishop et al., 2007). However, it remains unclear whether emotional processing affects intracortical inhibition in the DLPFC. Therefore, we sought to examine the N100 during emotional processing, where a

reduced N100 in specific phobia compared to control subjects would support the notion that a disinhibition of the DLPFC contributes to (over-)activation by emotional processing.

## 2.3.2 Methods and Material

### 2.3.2.1 Subjects

A total of 48 subjects between 18-25 years participated in the study. 22 of them were subjects with specific phobia and 26 subjects without any psychiatric disorder formed the control group. Two subjects of the control group were excluded from data analysis due to unremovable prolonged TMS (“decay”) artefacts (Veniero et al., 2009). Two more subjects, one of each group, were excluded from the 1-back task analysis due to technical problem with the presentation software.

The diagnosis and type of specific phobia was based on the research criteria of the Diagnostic and Statistical Manual of Mental Disorders, Fifth Edition (DSM-5). Therefore, we applied the Structured Clinical Interview for DSM-5 disorders (SCID) (First et al., 2019). 15 subjects had a specific phobia of an animal type, 1 subject of blood-injection-injury, 3 subjects of natural environment and 3 subjects of situational type. The specific phobia group exhibited no other anxiety, psychiatric, or neurological disorder. The criteria for control subjects were the absence of abnormalities in the DSM-5 criteria. The severity of comorbid depressive symptoms as a potential confounding factor was assessed with the Hamilton depression rating scale (Hamilton, 1960) according to the structured interview by Williams (Williams, 1988). Detailed characteristics of samples can be found in Table 1.

None of the subjects took any psychotropic drugs. Subjects were screened for TMS exclusion criteria according to (Rossi et al., 2009).

Study 3 Table 1. *Characteristics of the analysed study samples.*

Diagnostic group	Specific phobia	Control group
Sample size ( <i>N</i> )	22	24
Gender ( <i>N</i> )	21 females, 1 male	21 females, 3 males
Age (mean $\pm$ SD, in years)	22.5 $\pm$ 2.2	22.7 $\pm$ 1.8
Age range (in years $\pm$ SD)	18.1-25.7	18.4-25.9
IQ (CFT 20-R, mean $\pm$ SD)	112 $\pm$ 10.2	115 $\pm$ 11.6
IQ range	97-138	95-143
Hamilton depression rating scale	1.7 $\pm$ 2.0	1.5 $\pm$ 1.4
Handedness ( <i>N</i> )	20 right, 2 left	24 right
1-mV-threshold (mean $\pm$ SD)	62 $\pm$ 11.5 %	60 $\pm$ 10.9 %
Resting motor threshold (mean $\pm$ SD)	53 $\pm$ 9.1 %	52 $\pm$ 9.8 %

*Note.* SD, standard deviation.

### 2.3.2.2 Transcranial magnetic stimulation (TMS)

Biphasic single-pulse TMS was applied using a MagPro X100 with MagOption stimulator and a 75 mm outer diameter figure-of-eight coil (MCF-B65, Magventure, Farum, Denmark). Electrodes positions F5/F6 were used for TMS as this has been found a clinically useful method to localize the DLPFC in the absence of individual structural MRI data (De Witte et al., 2018; Rusjan et al., 2010). The coil was held by a trained examiner. The TMS pulses were triggered by the Presentation software 18.1 (NeuroBehavioral Systems, Berkley, USA).

Motor evoked potentials (MEPs) were measured from the right hand at the first dorsal interosseal muscle. The reference electrode was attached at the proximal phalanx of the index finger. Resting motor threshold (RMT) was determined by threshold hunting ((Awiszus, 2003); MTAT 2.0; available online at <https://www.clinicalresearcher.org/software.htm>). 120% of the individual RMT was used as stimulation intensity for TMS. In the rest condition, a TMS protocol with a total of 90 stimuli with an inter-stimulus interval of 5 to 8s (mean 6.5s) was applied to the left and right DLPFC (45 pulses left, 45 pulses right).

### 2.3.2.3 1-back-task

In our 1-back paradigm, 195 standardized and evaluated emotional expressions of different actors were presented in a pseudorandomized order with the Presentation software 18.1. Subjects had to remember the emotional expression (fearful, angry, neutral) and had to decide via mouse click whether the presented emotion was equal to the emotion previously

presented by a different actor (1-back task). An emotional 1-back task with low working memory-related load was sufficient and appropriate for our investigation of the interference of emotional processing and everyday cognitive control, assuring that the emotional expression was processed. Each trial lasted 2.5 s, the emotional expression was shown for 1s followed by 1.5s of blank screen/fixation cross and the possibility to give a response as well as the need to maintain the emotion in working memory for the next trial. The trials were divided into three blocks to avoid exhaustion. The right DLPFC was targeted because processing of visual n-back tasks takes place predominantly in the right hemisphere (Owen et al., 2005). Concurrently with the 1-back task, on average, 20 TMS stimuli were applied to the right DLPFC following fearful, 20 following angry, and 20 following neutral emotional expression stimuli. Unfortunately, one pulse from a varying stimulus category was not presented in each protocol, resulting in a total of 59 instead of 60 TMS stimuli. TMS stimuli were applied 250ms after emotional expression stimulus offset, on average every 3.4 trials. A short training session always preceded the actual test phase.

The order of the 1-back task and TMS at rest was counterbalanced across subjects.

#### 2.3.2.4 Electroencephalographic recordings

We used equidistant 64-channel BrainCaps with sintered Ag/Ag-Cl electrodes (Easycap GmbH, Herrsching, Germany). Impedances were kept  $<5$  k $\Omega$ . Cz served as reference electrode during recording. EEG channels were named according to the closest corresponding channel in the 10-20 system (Chatrian et al., 1985). Two infraorbital electrodes were placed 1 cm below both the right and the left eye. Continuous direct current EEG with a sampling rate of 5000 Hz was recorded by the BrainVision Recorder (Brain Products GmbH, Gilching, Germany).

#### 2.3.2.5 EEG Data analysis

##### *Signal processing*

EEG-data were processed offline via BrainVision Analyzer (BrainProducts GmbH, Gilching, Germany). Data were reduced to a 500 Hz sampling rate and then re-referenced to an average reference. For the investigation of TMS-evoked N100 at rest and during 1-back task, the EEG data were segmented based on TTL triggers used to synchronize EEG and TMS indicating the occurrence of a TMS pulse into intervals of 1s (0.5s before the TMS pulse and 0.5s thereafter). The time window between -10ms to 20ms around the TMS pulse was interpolated to avoid a

contamination of the EEG segments by the TMS pulse artefact. Trials with muscle artefacts, movements and electrode artefacts were removed (1.74% of trials removed). The time window from -110ms to -10ms before the TMS stimulus was chosen as baseline to prevent contamination of the baseline by a potential broadening of the TMS pulse artefact through the downsampling procedure. Independent component analysis was applied to remove artefacts such as eye blinks and movements. A DC-trend correction was applied to correct for any drifts (Hennighausen et al., 1993), although data inspection showed no systematic influences of DC detrending. Then, all trials for each condition and stimulation side were averaged.

#### *N100 DLPFC analysis*

The TMS-evoked N100 was determined as the highest negative peak at ipsilateral F5 or F6 in the interval 80-140ms after left and right TMS. This time window as well as F5 and F6 as electrodes of interest were chosen based on previous other TMS-EEG studies (Lioumis, Kičić, et al., 2009; Loheswaran et al., 2018). Mean amplitudes from -10 to 10ms around the peak were exported.

#### 2.3.2.6 Statistics

Statistics were performed with IBM SPSS Statistics 25 software (IBM Corp., Armonk, NY, USA; Version 25). The Kolmogorov-Smirnov test did not indicate a significant deviation from normal distribution.

To compare N100 amplitudes evoked by DLPFC TMS at rest between the two groups, a 2x2 ANOVA was performed with the within-subject factor STIMULATION SIDE (left, right DLPFC stimulation) and the between-subject factor GROUP (specific phobia, control group). Significant interactions were followed-up by one-way ANOVAs and Bonferroni corrected *post-hoc* tests.

The 1-back task effect on N100 amplitude was analyzed by a 2x2 ANOVA with the within-subject factor CONDITION (rest vs. 1-back task) and the between-subject factor GROUP (specific phobia, control group). The error rate was compared between the two groups by a *t*-test.

The effect of the emotional expressions on TMS-evoked N100 amplitude were tested by a 3x2 ANOVA with the within-subject factor EMOTION (fearful, angry, and neutral faces) and the between-subject factor GROUP (specific phobia, control group).

Reaction times were examined by a 3x2 ANOVA with the within-subject factor RT EMOTION (reaction time after fearful, angry, neutral faces) and the between-group factor GROUP. Significant interactions were followed up by one-way ANOVAs and Bonferroni-corrected *post-hoc* tests.

To investigate possible influences of different subtypes of specific phobias, an analogous analysis was conducted comparing subjects with animal phobia as largest subgroup in our sample with controls. Furthermore, possible differences between animal phobia and other phobias were compared. For more information on the statistics and results see supplementary material B1.

A  $p$ -value  $< .05$  indicated a significant effect. If necessary, the values were given in Greenhouse-Geisser or Bonferroni corrected form.

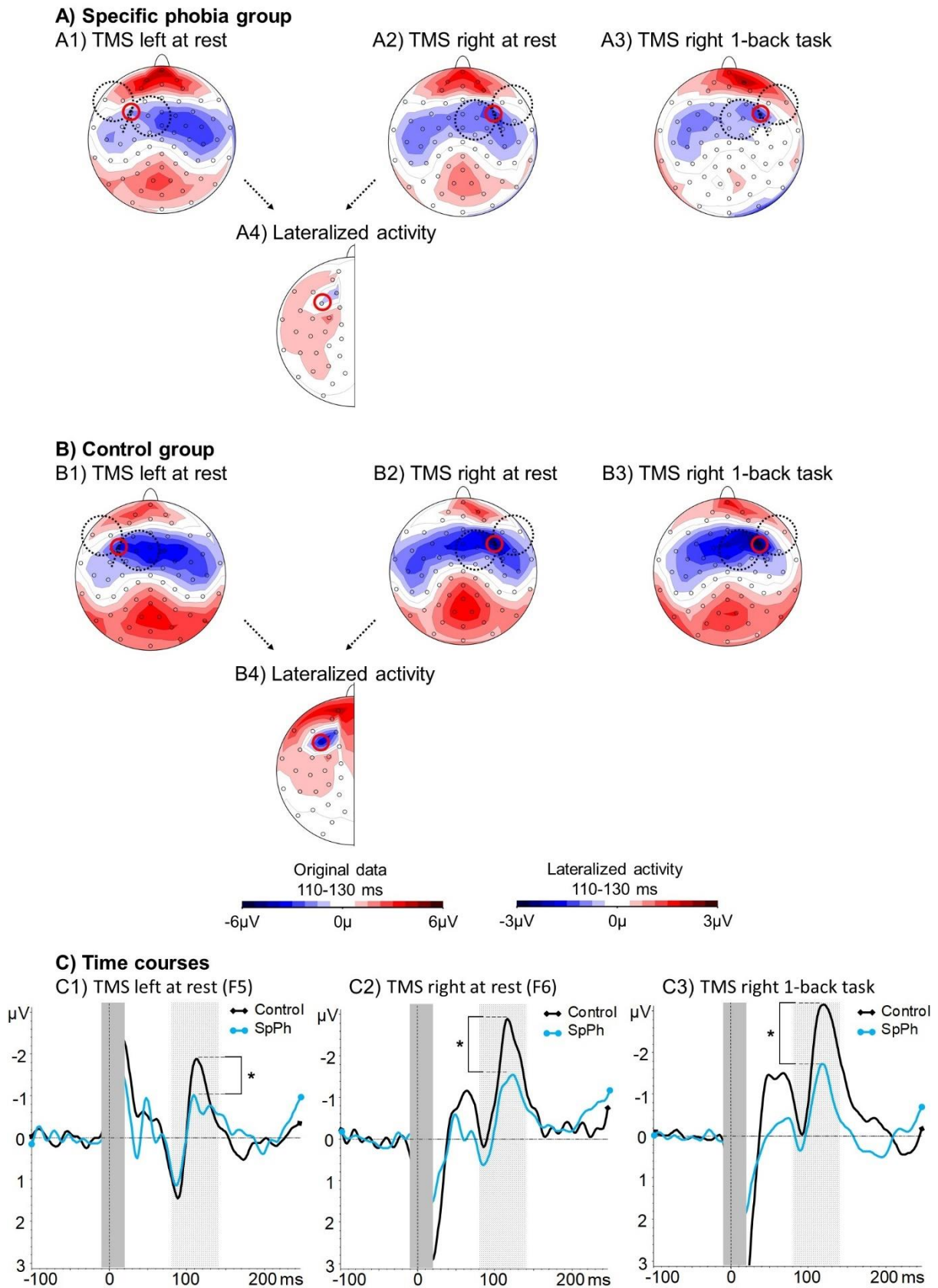
### 2.3.3 Results

#### 2.3.3.1 TMS-evoked N100 at rest

The specific phobia group showed smaller N100 amplitudes at the stimulation site than the control group (GROUP:  $F(1,44)=4.39$ ,  $p=.04^*$ , partial  $\eta^2=.09$ ; Figure 1). This was true for both right (specific phobia:  $-3.3\pm 3.1\mu V$ , control group:  $-5.5\pm 4.1\mu V$ ; Table 2; Figure 1) and left sided stimulation (specific phobia:  $-2.3\pm 3.7\mu V$ , control group:  $-3.8\pm 4.3\mu V$ ). Right sided stimulation tended to evoke larger N100 amplitudes irrespective of group (main effect SIDE:  $F(1,44)=3.97$ ,  $p=.053$ , partial  $\eta^2=.08$ ).

STIMULATION SIDE and GROUP did not interact ( $F(1,44)=.22$ ,  $p=.65$ , partial  $\eta^2=.01$ ).

All effect sizes and their corresponding confidence intervals are given in Table 1 in the supplementary material.



*Study 3 Figure 6.* (a) Topographic distribution of N100 in the specific phobia and (b) control group when stimulating the left (a1 and b1) and right (a2 and b2) side at rest and during an emotional 1-back task condition (a3 and b3). The electrodes of interest underlying the site of stimulation are circled in red (stimulation left = F5, stimulation right = F6). Original data maps are plotted on 6  $\mu\text{V}$  scale. Lateralized activity (a4 and b4) was extracted to illustrate TMS-evoked brain activation by subtracting symmetrical activity to visualize activation at the stimulation site which exceeded contralateral potentials. The calculation results in one channel (depicted arbitrarily on the left side of the head) encompassing signals from both stimulation sides (right and left) and both hemispheres of the rest condition. The calculation is shown in Supplementary Material (B. lateralized activity: description and calculation). TMS, transcranial magnetic stimulation

*Study 3 Table 2. Mean peak latencies and amplitudes over all stimulation conditions ipsilateral to the stimulation side at F5 and F6.*

	N100 latency (ms) $\bar{x} \pm \text{SD}$	N100 amplitude $\bar{x} \pm \text{SD}$ ( $\mu\text{V}$ )
<b>N100 DLPFC rest condition</b>		
TMS left F5: specific phobia group	113.6 $\pm$ 16.6	-2.3 $\pm$ 3.7
TMS left F5: control group	115.8 $\pm$ 15.2	-3.8 $\pm$ 4.3
TMS right F6: specific phobia group	115.6 $\pm$ 9.1	-3.3 $\pm$ 3.1
TMS right F6: control group	113.8 $\pm$ 16.1	-5.5 $\pm$ 4.1
<b>N100 DLPFC 1-back task condition</b>		
TMS right F6 task: specific phobia group	110.6 $\pm$ 16.6	-3.8 $\pm$ 3.1
TMS right F6 task: control group	123.6 $\pm$ 11.4	-6.4 $\pm$ 3.7
<b>N100 DLPFC emotional expressions</b>		
<b>Specific phobia group</b>		
TMS right F6 fear	114.8 $\pm$ 16.1	-1.9 $\pm$ 3.7
TMS right F6 anger	113.7 $\pm$ 14.1	-3.7 $\pm$ 7.6
TMS right F6 neutral	111.1 $\pm$ 14.8	-4.2 $\pm$ 4.4
<b>Control group</b>		
TMS right F6 fear	113.0 $\pm$ 17.2	-5.6 $\pm$ 3.7
TMS right F6 anger	117.4 $\pm$ 15.5	-6.0 $\pm$ 4.5
TMS right F6 neutral	118.9 $\pm$ 15.5	-6.1 $\pm$ 4.4

*Note.* DLPFC, dorsolateral prefrontal cortex; TMS, transcranial magnetic stimulation.

### 2.3.3.2 TMS-evoked N100: 1-back task

N100 amplitudes during the 1-back task were not significantly changed by working memory-related processes (CONDITION:  $F(1,42)=1.81, p=.19$ , partial  $\eta^2=.04$ ; Table 2; Figure 1). There was no significant interaction between the 1-back task and the diagnostic groups (CONDITION x GROUP  $F(1,42)=.18, p=.67$ , partial  $\eta^2=.004$ ). The main effect of GROUP ( $F(1,42)=6.12, p=.02^*$ , partial  $\eta^2=.13$ ) was confirmed during the 1-back task with the specific phobia group showing smaller N100 amplitudes at the stimulation site (F6) than the control group (Figure 1).

The specific phobia group made significantly more errors during the 1-back task compared to the control group (specific phobia:  $22.05\pm 7.49$  errors, controls:  $16.33\pm 8.60$  errors;  $t(38.7)=-2.27, p=.03^*$ ,  $d=-.71$ ; Table 3)

Study 3 Table 3. *Reaction times and error rates for the specific phobia and the control group.*

	Reaction time (ms $\pm$ SD)			Number of errors (N $\pm$ SD)			Correct rate (% $\pm$ SD)	
	Neutral faces	Angry faces	Fearful faces	Overall errors	Neutral faces	Angry faces		Fearful faces
Specific phobia group	1035,71 (187,94)	1123,76 (218,40)	1072,94 (202,95)	22,05 (7,49)	5,95 (3,24)	9,4 (4,54)	6,20 (2,75)	88,69 (3,84)
Control group	1068,59 (261,15)	1163,50 (281,97)	1129,56 (263,71)	15,73 (8,87)	4,27 (2,64)	6,95 (5,37)	4,50 (3,00)	91,93 (4,55)

*Note.* SD, standard deviation.

### 2.3.3.3 TMS-evoked N100: effect of emotional facial expression

We found a significant main effect of EMOTION ( $F(1.68,70.69)=4.02, p=.03^*$ , partial  $\eta^2=.09$ ; Figure 2). Fearful facial expressions led to significantly smaller amplitudes compared to neutral ones, but not compared to angry facial expressions over both groups (fear vs. neutral:  $t(43)=-3.08, p=.01^*$ ,  $d=.46$ ; fear vs. anger:  $t(43)=1.63, p=.33, d=.25$ ; anger vs. neutral:  $t(43)=.79, p=1.00, d=.12$ ; Figure 2).

The emotion effect remained significant when considering the specific phobia group alone ( $F(1.54,30.88)=4.90, p=.02^*$ , partial  $\eta^2=.20$ ). This was not the case for the control group alone ( $F(2,44)=.34, p=.73$ , partial  $\eta^2=.02$ ). However, despite a descriptively larger mean difference

(see Figure 2), a larger emotion effect for the specific phobia than for the control group could not be shown statistically (EMOTION x GROUP:  $F(1.68,70.69)=1.48$ ,  $p=.24$ , partial  $\eta^2=.03$ ).

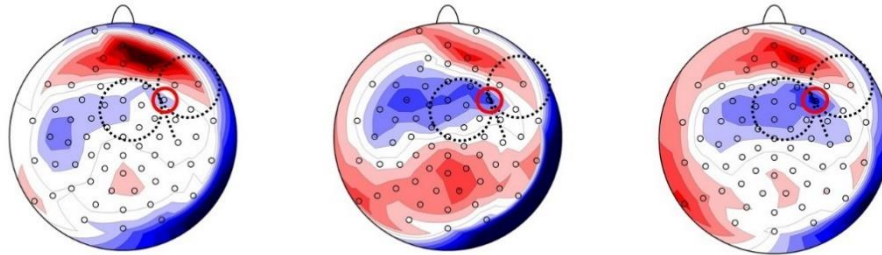
A 3x2 ANOVA on reaction times with the factors RT EMOTION and GROUP examining changes in reaction times according to the emotional expressions showed a significant main effect of RT EMOTION ( $F(2,78)=29.48$ ,  $p<.001^{**}$ , partial  $\eta^2=.43$ ). In both groups, reaction times were significantly longer when memorizing fearful compared to neutral facial expressions ( $t(40)=-4.57$ ,  $p<.001^{**}$ ,  $d=-.71$ ; Table 3). However, longer reaction times were found when memorizing angry facial expressions, compared to both neutral ( $t(40)=-6.98$ ,  $p<.001^{**}$ ,  $d=-1.1$ ; Table 3) as well as fearful facial expressions ( $t(40)=3.73$ ,  $p=.002^{**}$ ,  $d=.58$ ; Table 3). There was no difference between the specific phobia and the control group in reaction times (GROUP:  $F(1,39)=.05$ ,  $p=.83$ , partial  $\eta^2<.001$ ) and no interaction between GROUP and EMOTION ( $F(2,78)=.46$ ,  $p=.64$ , partial  $\eta^2=.01$ ).

**A) Specific phobia group**

A1) Fearful expressions

A2) Angry expressions

A3) Neutral expressions

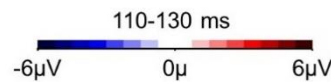
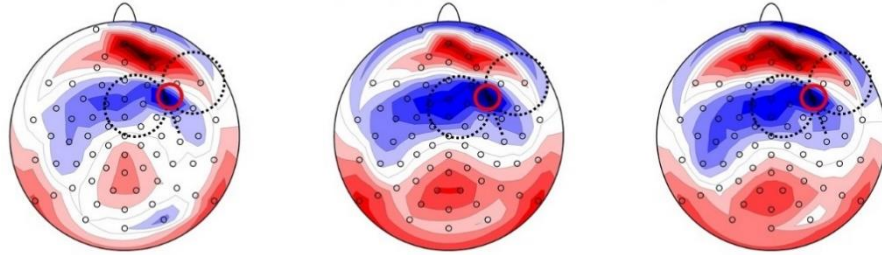


**B) Control group**

B1) Fearful expressions

B2) Angry expressions

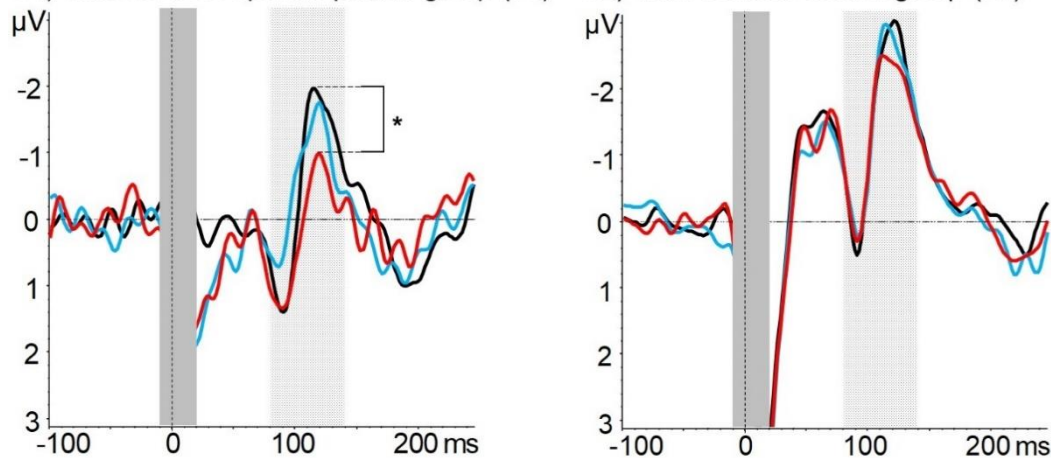
B3) Neutral expressions



**C) Time courses**

C1) Time courses specific phobia group (F6)

C2) Time courses control group (F6)



■ Fearful expressions  
■ Angry expressions  
■ Neutral expressions

*Study 3 Figure 2.* (a) Topographic distributions of the TMS evoked N100 responses to the emotional face stimuli (fear, anger, and neutral), shown separately for the specific phobia and (b) control group. The electrode of interest at the site of stimulation (F6) is circled in red. (c) Time courses during right side TMS at F6 in the 1-back task condition for the emotional stimuli, illustrated separately for the specific phobia and the control group. The interpolation period is overlaid by a gray bar. The dotted areas mark the time window for N100 peak detection. TMS, transcranial magnetic stimulation

#### 2.3.3.4 Analyses of subtypes of specific phobia

The 2x2 ANOVA comparing subjects with animal phobias and the control group (15 animal phobias vs. 24 controls) showed a trend towards a main effect of GROUP ( $F(1,37)=3.62$ ,  $p=.07$ , partial  $\eta^2=.09$ ) with animal phobias showing smaller N100 amplitudes compared to controls (Table 1).

Within the group of specific phobias, comparing 15 animal phobias vs. 7 subjects with other specific phobia subtypes, there was no difference in the N100 amplitude between the groups of subtypes (SUBTYPE ( $F(1,20)<.001$ ,  $p=1.0$ , partial  $\eta^2<.001$ ).

In the emotional 1-back task, the 3x2 ANOVA comparing subjects with animal phobias and the control group showed smallest N100 amplitudes for fearful expressions (EMOTION ( $F(1.70, 59.50)=4.19$ ,  $p=.03^*$ , partial  $\eta^2=.11$ ).

#### 2.3.4 Discussion

To our knowledge, this study examined, for the first time, a marker of intracortical inhibition in the DLPFC in specific phobias. We found reduced TMS-evoked N100 amplitudes in the DLPFC in the specific phobia compared to the control group at rest.

Furthermore, emotional processing when memorizing fearful compared to neutral facial expressions led to a reduction in intracortical inhibition in the DLPFC in the specific phobia group as reflected by the N100.

In contrast, there was no significant change in the N100 amplitude of the DLPFC during working memory-related processing in the 1-back task with a low working memory load compared to a rest condition.

##### 2.3.4.1 TMS-evoked N100 in the DLPFC

The N100 in the DLPFC as part of the TEP has been discussed to occur as lateralized negative deflection at the stimulation site (Jarczok et al., 2021; Rocchi et al., 2021). We found an ipsilateral N100 at the stimulation site at electrodes F5 and F6 with significantly smaller amplitudes in the specific phobia compared to the control group. The N100 as a parameter for intracortical inhibition is likely to reflect GABA-B reactivity in the DLPFC (Premoli, Rivolta, et al., 2014). A reduced N100 could thus indicate a lower GABA-B-mediated inhibition in the DLPFC in specific phobias. Interestingly, there was a general group-specific reduction in the

N100 in the absence of phobic stimuli. Both groups were free of any psychotropic drugs at the time of participation. Hence, medication can be excluded as a cause for the N100 reduction. Additionally, there were no comorbid anxiety disorders, major depression, or any other psychiatric disorder in both groups.

There is evidence for anxiety disorders, and thus specific phobias, to be characterized by higher levels of trait anxiety (Raymond et al., 2017). This implies that trait anxiety as a relatively stable predisposition over time (Vagg et al., 1980) may be associated with a general impairment of intracortical inhibition in specific phobias.

The finding of a reduced N100 in anxious subjects contributes to the literature on how trait anxiety modulates DLPFC activation (Bishop, 2009; Eysenck et al., 2007). Neuroimaging studies have found a threat-independent deficit of the DLPFC inhibiting interfering information in highly anxious subjects (Basten et al., 2011; Bishop et al., 2007; Derakshan & Eysenck, 2009). Furthermore, insufficient recruitment of the DLPFC, which is required for inhibitory control and was measured by a distractor inhibition task, has been suggested in high trait anxiety (Bishop, 2009). However, these studies examined general activation levels in the DLPFC and did not elucidate the exact mechanisms of how cortical processing is altered with respect to changes in excitability and/or inhibition. Our results indicate a dysfunctional top-down control of the DLPFC in specific phobias by showing reduced GABA-B-mediated intracortical inhibition in the left and right DLPFC at rest.

Another important finding of this study was a reduced N100 amplitude in specific phobias in response to fearful facial expressions compared to neutral ones. Thus, processing of fearful stimuli modulated intracortical inhibition levels in the DLPFC. We would like to point out that we cannot exclude that this is true to a similar extent for the control group, as the interaction CONDITION x GROUP did not reach statistical significance. We presented emotional facial expressions in our 1-back task paradigm as this has been described as an adequate method to activate the amygdala especially in anxious subjects (Breiter et al., 1996; Yang et al., 2002). Fearful facial expressions are a relevant biological stimulus indicating potential threat (Whalen, 1998).

A reduced inhibition in specific phobias could be related to a more active mirror system in anxious subjects viewing fearful compared to e.g. happy expressions (Rahko et al., 2010). Behavioral and neuroimaging data of previous studies suggest an impaired attentional control

of the DLPFC during the confrontation with fearful facial expressions (Bishop et al., 2004). It was shown that this trait also modulates neural activity in addition to state anxiety when processing fearful compared to neutral facial expressions (Bishop, 2009; Bishop et al., 2007). Higher state anxiety induced by fearful facial expressions was found to be associated with lower activity in the DLPFC and higher amygdala response (Bishop et al., 2004). Our results show a modulation of intracortical inhibition in the DLPFC, possibly due to an unspecific bottom-up arousal increase in the limbic system during the processing of fearful face expressions.

Moreover, we found the longest reaction times and highest error rates when memorizing angry facial expressions, but no significant N100 reduction. Therefore, longer processing time and effectiveness cannot be used to explain impaired DLPFC inhibition. The latter was specifically related to emotional processing of fearful facial expressions.

In addition, we found no significant N100 reduction in working memory-related processing at low load (1-back) in either group, highlighting that DLPFC inhibition in specific phobias was modulated by emotional processing of fear-relevant stimuli in the DLPFC and not by a low load 1-back task. However, it remains unclear whether a modulation effect would only become apparent at higher load. Studies comparing low with high perceptual load in anxiety found that anxiety did not affect DLPFC activity at high perceptual load (Bishop et al., 2007). Moreover, the lack of a modulating working memory effect could be due to the short time interval between stimulus offset and TMS pulse, as maintenance processes become more important after approximately 500ms (Figueira et al., 2018). However, longer maintenance intervals could make the memory-related aspects of the task more difficult.

In our sample, we included different subtypes of specific phobias, with animal phobias being the largest sub-group. Since the emotion effect was even more pronounced when considering the animal phobia subgroup alone, we can conclude that our results of reduced N100 amplitudes in response to fearful expressions are valid for subjects with animal phobia.

Other subtypes were mixed and underrepresented with  $n=7$ . Therefore, we cannot say with certainty that our results also apply to other non-animal phobias. However, there was no significant difference in the N100 amplitude between the subtypes in any condition.

Accordingly, we found no evidence for significant differences between different specific phobia subtypes. Further studies are needed to confirm the effect of an impaired inhibition in the DLPFC that we found for animal phobias is also valid for other subtypes of specific phobia

(Lueken et al., 2011). For further details on the analysis of different subtypes see supplementary material B.

Since we had a moderate sample size ( $n=46$ ), we added confidence intervals for our calculated effect sizes (see Table A1 in the supplementary material) to allow the reader to compare our effects with those of other related studies and to facilitate the reproducibility of our results in future studies. A more detailed discussion on the power of our results can be found in the supplementary material C.

Taken together, we found impaired intracortical inhibition in the DLPFC in the specific phobia group at rest, which was additionally modulated by the confrontation with fearful facial expressions. Thus, a generally impaired inhibitory function in the DLPFC was associated with specific phobias. In this respect, the existence of a categorical psychiatric diagnosis (independent of the subject's actual state) can be compared to a persistent anxiety trait in a dimensional model. Moreover, inhibition in specific phobias was modulated by processing of fearful facial expressions. This is possibly due to nonspecific bottom-up increases in limbic system activation during emotional processing of fearful faces, comparable to mild acute state anxiety.

#### 2.3.4.2 Limitations

A limitation results from TMS, which was performed without neuronavigation. However, TMS was aligned to the localization described by Rusjan and colleagues (Rusjan et al., 2010), often used in TMS-EEG studies (Fitzgerald et al., 2009; Jarczok et al., 2021; Rogasch et al., 2015). Furthermore, TMS was performed without auditory masking, thus auditory-evoked potential (AEPs) may have contributed to the TEP. AEPs are divided into three components: N1a, N1b and N1c (Alain et al., 1997; Bender et al., 2006; Knight et al., 1988). However, AEPs do not occur at the stimulation site since lateralized parts like the N1c appear to have a contralateral topography with monaural stimulation as is to a limited extent the case with TMS (Hine & Debener, 2007; Langers et al., 2005). Thus, AEPs do not mimic a transcranial N100.

#### 2.3.4.3 Conclusion

In summary, we found reduced intracortical inhibition reflected by a reduced N100 amplitude in the DLPFC in the specific phobia compared with the control group. This suggests that

specific phobias and an impaired inhibitory function of the DLPFC are associated. Moreover, we found that intracortical inhibition in the DLPFC in specific phobias was additionally modulated by memorizing fearful facial expressions. To our knowledge, this study presents, for a first time, a parameter for the dysfunction of prefrontal inhibition in specific phobias.

### 3 Overarching conclusion and Outlook

This dissertation represents a combination of clinical and fundamental research. The gained knowledge of the applied methodology formed the foundation for the interpretation of the clinical results. The aim of this dissertation was the investigation of the neuropathological mechanisms of specific phobias. The study of anxiety disorders has become even more important in the wake of the covid pandemic, with an increase in depression and anxiety disorders (Taquet et al., 2021)

A combination of TMS and EEG provides a non-invasive method for the investigation of the neuropathological mechanisms and the research of biomarkers of mental disorders. Over the last decade, TMS-EEG has become increasingly important in various contexts (Croarkin et al., 2011; Teng et al., 2017). The TMS-evoked N100, a negative deflection around 100 ms after TMS, has often been used as a parameter for GABAB-mediated inhibition. The N100 also represented the target parameter in the study on the neuropathological mechanisms of specific phobias conducted within the framework of this dissertation. Furthermore, a correct interpretation of the TEP topography was important for this study in order to prevent misconceptions that could negatively impact clinical decision-making. Therefore, we aimed to fill knowledge gaps in the TMS-EEG methodology.

**Study 1 (methodological: N100 in the DLPFC and TOC).** In study 1, we addressed the question of whether the N100 occurred systematically lateralized and varied with the stimulation site. For this purpose, the evoked activity after TMS at two different stimulation sites was examined with regard to lateralized components. We **found systematically lateralized potentials in the TEP that varied dependent on the stimulated brain area and hemisphere.** The latency of this lateralized activity differed between the stimulation sites DLPFC and TOC, with approximately 60 ms **longer latencies occurring in TOC.** However, a direct comparison of the two stimulation effects was not possible due to two different samples having been used. Nevertheless, the ipsilateral lateralization and localization at the stimulation site indicated that the activity in the DLPFC and TOC, respectively, most likely represented true transcranially evoked activity.

**Study 2 (methodological: trigeminal SSEPs).** Study 2 addressed the question of which parts of the TEP represented sensory evoked potentials and which represented true transcranially evoked activity so that the TEP could be interpreted correctly. In order to achieve this goal, it is important to know the topographies of sensory potentials and with what latency they occur.

The least data is available on trigeminal SSEPs in time windows <100ms, which are relevant for the TMS-evoked N100. For this reason, we electrically stimulated the trigeminal nerve and compared the electrically and TMS-evoked topography. We found that **trigeminal SSEPs first occurred contralaterally and then became bilateral around centroparietal electrodes between 140-160 ms**. Due to the methodology used, the topography of the trigeminal SSEPs could only be examined from 100 ms onwards. Consequently, no causal conclusions could be drawn with regard to the proportion of SSEPs in the TMS-evoked N100. However, the results indicate that **trigeminal SSEPs can probably be distinguished from the N100 in the DLPFC by their contralateral topography and longer latency**.

It is important to emphasize that this assumption only refers to the N100 in the DLPFC. The influence of trigeminal SSEPs at more posterior stimulation sites such as the TOC remains to be investigated, as we found different latencies for transcranially evoked activity after TMS of the DLPFC and the TOC (see study 1). In addition, a contribution of SSEPs at the ipsilateral parts of the TEP at more posterior stimulation sites cannot be excluded, as we found that SSEPs become bilateral in later time windows. Caution should thus be exercised when interpreting the TEP at stimulation sites like the TOC. Suitable sensory masking will be important for this in future studies, which are currently being done (Rocchi et al., 2021; Russo et al., 2022).

The results of the two methodological studies (study 1 & 2) were applied to the interpretation of the TEP topographies from the clinical study (study 3). Since we examined the N100 in the DLPFC for this study, we focused on ipsilateral activity and did not interpret contralateral potentials as transcranially evoked activity.

**Study 3 (clinical: specific phobias vs. controls)**. In the third study, a group of young adults diagnosed with a specific phobia was compared to a control group regarding their N100 amplitudes in response to transcranial magnetic stimulation. We found an **impaired inhibitory top-down control of the DLPFC in subjects with a specific phobia compared to the control group, which was reflected in a smaller N100 amplitude**. In the **group with specific phobias**, the **inhibition deficit seemed to be additionally modulated by the confrontation with fearful facial expressions compared to neutral ones**. This could be due to bottom-up arousal increases in the limbic system that occur during emotional processing. However, it should be added that we did not find a significant interaction between the emotional facial expressions and the groups. Further analysis of the emotional facial expressions within the individual

groups should therefore be regarded as exploratory. Furthermore, it cannot be excluded that this modulation effect could also be found in control subjects.

Moreover, the results suggest that a **reduced inhibition might also be transferable to the subtype of animal phobia alone**. However, a group difference could not be found in all conditions, so it should be verified in further studies. Furthermore, no conclusion could be drawn regarding other subtypes of specific phobia, as they were underrepresented in the sample. Therefore, other subtypes should also be the subject of future studies.

Building on the results of this dissertation on the TMS-EEG methodology and specific phobias, further clinical research will be conducted.

The first step is to investigate whether an inhibitory deficit in DLPFC top-down control occurs only in specific phobias or also in other groups of anxiety disorders such as social or generalized anxiety disorder. Therefore, we will evaluate and analyze the other samples collected in the study “Cortical Excitability and Anxiety Disorders” (Table 1). If a similar effect occurs in other groups of anxiety disorders, this could indicate that a reduced TMS-evoked N100 may reflect a biological marker for a pathological mechanism in various groups of anxiety disorders.

To further support this hypothesis, another study will be prospectively conducted with patients diagnosed with an anxiety disorder to investigate the effects of repetitive TMS (rTMS) on anxiety disorders. There is already evidence for the clinical use of rTMS in the treatment of anxiety symptoms. After right-sided low-frequency rTMS of the DLPFC, subjects with major depression showed a significant reduction in anxiety symptoms (L. Chen et al., 2019). Furthermore, in patients with social and generalized anxiety disorders, symptom improvement was noted in some cases after a single prefrontal 1 Hz-rTMS session (Bystritsky et al., 2009; Paes et al., 2013).

Investigating the N100 in the DLPFC after rTMS in patients with anxiety disorders would provide an advance in understanding the mechanism of action of the anxiolytic effects of rTMS in anxiety disorders. If the amplitude of the N100 increases in patients with anxiety disorders after rTMS, this could indicate that rTMS improves anxiety symptoms by increasing GABAB-mediated inhibition in the DLPFC.

Furthermore, it would be important to investigate whether the deficient inhibitory ability that we found in young adults with specific phobia is already prevalent in childhood and

adolescence. For this reason, it is important to know which maturation processes cortical excitability and inhibition undergo in unaffected children and adolescents and how cortical excitability develops over time. A study on cortical maturation in unaffected children and adolescents is currently being initiated by our research group. We plan to transfer the knowledge gained about functional cortical excitability to the investigation of children and adolescents with anxiety disorders to draw conclusions about a possible impairment of DLPFC inhibition by anxiety disorders already in childhood and adolescence.

Since not only anxiety disorders are associated with altered cortical excitability, the question arises whether an impaired prefrontal inhibition reflected in a reduced N100 amplitude in the DLPFC is also present in other mental disorders. There is some evidence for patients with anorexia nervosa, for example, to show reduced inhibition levels in motor areas possibly due to affected GABA-ergic inhibition (Khedr et al., 2014). Furthermore, McClelland et al. (2016) found modest evidence for high-frequency rTMS of the left DLPFC having symptom-reducing effects in patients with anorexia nervosa. Further studies on anorexia nervosa showed decreasing activity in the prefrontal cortex with increasing inhibitory demand in tasks requiring prefrontal inhibition (Oberndorfer et al., 2011). It was concluded that individuals with anorexia nervosa needed fewer inhibitory resources in the form of lower prefrontal activity to maintain a behavior (Oberndorfer et al., 2011). Furthermore, patients with anorexia nervosa were found to have an attentional bias towards emotional, i.e. body or food-related stimuli (Smeets et al., 2008). This attentional bias has been found to lead to a shift of attention towards body shape, image, and weight (Aspen et al., 2013; Hartmann et al., 2020). The DLPFC is crucial for directing attention from a disturbance-relevant stimulus towards an alternative stimulus. Accordingly, the question arises as to the role of the DLPFC in the pathophysiology of anorexia nervosa and whether there is also an impaired top-down inhibition in patients with anorexia nervosa. However, it has to be emphasized that this is only a hypothesis at this stage, as the data on anorexia nervosa is limited. Therefore, a fundamental study is currently being planned to investigate whether patients with anorexia nervosa show altered N100 amplitudes in the DLPFC. Therefore, we want to investigate the N100 in the DLPFC during acute anorexia symptoms, compared to the time after weight gain in a longitudinal study.

In conclusion, TMS-EEG is a promising method for investigating neuropathological mechanisms of different mental disorders. Although TMS-EEG has methodological difficulties,

researchers worldwide are working on how TMS-EEG studies should be designed to minimize the risk of misinterpretation. However, even with today's knowledge, TMS-EEG can be used well for clinical studies if it is known what to look out for in application and analysis. In this context, this dissertation represents the first steps for further research into pathophysiological mechanisms of mental disorders using TMS-EEG and rTMS.

#### 4 Declaration of contributions to the publications

##### **Study 1: Co-authorship**

Lena Pokorny was involved in data collection, supported in data analysis, revision, and proof reading of the manuscript.

Jarczok, T. A., Roebruck, F., Pokorny, L., Biermann, L., Roessner, V., Klein, C., & Bender, S. (2021). Single-Pulse TMS to the Temporo-Occipital and Dorsolateral Prefrontal Cortex Evokes Lateralized Long Latency EEG Responses at the Stimulation Site. *Frontiers in Neuroscience*, 15. <https://doi.org/10.3389/fnins.2021.616667>

##### **Study 2: First authorship**

Lena Pokorny (first and corresponding author) was responsible for the acquisition, analysis, visualization, and interpretation of the data. She also contributed to the design of the study and wrote the original manuscript.

Pokorny, L., Jarczok, T. A., & Bender, S. (2022). Topography and lateralization of long-latency trigeminal somatosensory evoked potentials. *Clinical Neurophysiology*, 135, 37–50. <https://doi.org/10.1016/J.CLINPH.2021.11.073>

##### **Study 3: Shared first authorship**

Lena Pokorny (first and corresponding author) was responsible for the acquisition of data and supervision of the data analysis. She was responsible for the interpretation and visualization of data and contributed to the design of the study. She wrote the statistics, results and discussion of the original-manuscript and was involved in editing and critical writing-revision of the introduction and methods.

Pokorny, L., Besting, L., Roebruck, F., Jarczok, T. A., & Bender, S. (2021). Fearful facial expressions reduce inhibition levels in the dorsolateral prefrontal cortex in subjects with specific phobia. *Depression and Anxiety*. <https://doi.org/10.1002/DA.23217>

## 5 References

- Adams, T. G., Sawchuk, C. N., Cisler, J. M., Lohr, J. M., & Olatunji, B. O. (2014). Specific Phobias. In P. Emmelkamp & T. Ehring (Eds.), *The Wiley Handbook of Anxiety Disorders* (1st ed., pp. 295–320). John Wiley & Sons, Ltd. <https://doi.org/10.1002/9781118775349.CH18>
- Alain, C., L. Woods, D., & Covarrubias, D. (1997). Activation of duration-sensitive auditory cortical fields in humans. *Electroencephalography and Clinical Neurophysiology - Evoked Potentials*, *104*(6), 531–539. [https://doi.org/10.1016/S0168-5597\(97\)00057-9](https://doi.org/10.1016/S0168-5597(97)00057-9)
- Allison, T., McCarthy, G., & Wood, C. C. (1992). The relationship between human long-latency somatosensory evoked potentials recorded from the cortical surface and from the scalp. *Electroencephalography and Clinical Neurophysiology/ Evoked Potentials*, *84*(4), 301–314. [https://doi.org/10.1016/0168-5597\(92\)90082-M](https://doi.org/10.1016/0168-5597(92)90082-M)
- Alpers, G., Abelson, J., Wilhelm, F., & Roth, W. (2003). Salivary cortisol response during exposure treatment in driving phobics. *Psychosomatic Medicine*, *65*(4), 679–687. <https://doi.org/10.1097/01.PSY.0000073872.85623.0C>
- Alyagon, U., Shahar, H., Hadar, A., Barnea-Ygael, N., Lazarovits, A., Shalev, H., & Zangen, A. (2020). Alleviation of ADHD symptoms by non-invasive right prefrontal stimulation is correlated with EEG activity. *NeuroImage: Clinical*, *26*, 102206. <https://doi.org/10.1016/J.NICL.2020.102206>
- American Psychiatric Association. (2022). *Diagnostic and statistical manual of mental disorders (5th ed., text rev.)*. American Psychiatric Pub. <https://doi.org/https://doi.org/10.1176/appi.books.9780890425596>
- Aspen, V., Darcy, A. M., & Lock, J. (2013). A Review of Attention Biases in Women with Eating Disorders. *Cognition & Emotion*, *27*(5), 820. <https://doi.org/10.1080/02699931.2012.749777>
- Awiszus, F. (2003). TMS and threshold hunting. *Supplements to Clinical Neurophysiology*, *56*(C), 13–23. [https://doi.org/10.1016/S1567-424X\(09\)70205-3](https://doi.org/10.1016/S1567-424X(09)70205-3)
- Bandelow, B., Aden, I., Alpers, G. W., Benecke, A., Benecke, C., Beutel, M. E., Deckert, J., Domschke, K., Eckhardt-Henn, A., Geiser, F., Gerlach, A. L., Harfst, T., Hau, S., S., H., Hoyer, J., Hunger-Schoppe, C., Kellner, M., Köllner, V., Kopp, I. B., ... Beutel, M. E. (2021). *S3 -Leitlinie Behandlung von Angststörungen, Version 2*. <https://www.awmf.org/leitlinien.html>
- Bandelow, B., Baldwin, D., Abelli, M., Bolea-Alamanac, B., Bourin, M., Chamberlain, S. R., Cinosi, E., Davies, S., Domschke, K., Fineberg, N., Grünblatt, E., Jarema, M., Kim, Y.-K., Maron, E., Masdrakis, V., Mikova, O., Nutt, D., Pallanti, S., Pini, S., ... Riederer, P. (2017). Biological markers for anxiety disorders, OCD and PTSD: A consensus statement. Part II: Neurochemistry, neurophysiology and neurocognition. *The World Journal of Biological Psychiatry : The Official Journal of the World Federation of Societies of Biological Psychiatry*, *18*(3), 162. <https://doi.org/10.1080/15622975.2016.1190867>
- Barker, A. T., Jalinous, R., & Freeston, I. L. (1985). Non-invasive magnetic stimulation of human motor cortex. *Lancet*, *1*(8437), 1106–1107. [https://doi.org/10.1016/s0140-6736\(85\)92413-4](https://doi.org/10.1016/s0140-6736(85)92413-4)
- Basten, U., Stelzel, C., & Fiebach, C. J. (2011). Trait Anxiety Modulates the Neural Efficiency of Inhibitory Control. *J Cogn Neurosci* .., *23*(10), 3132–3145. [https://doi.org/10.1162/jocn\\_a\\_00003](https://doi.org/10.1162/jocn_a_00003)
- Becker, E. S., Rinck, M., Turke, V., Kause, P., Goodwin, R., Neumer, S., & Margraf, J. (2007). Epidemiology of specific phobia subtypes: findings from the Dresden Mental Health Study. *Eur Psychiatry*, *22*(2), 69–74. <https://doi.org/10.1016/j.eurpsy.2006.09.006>

- Beesdo-Baum, K., & Knappe, S. (2012). Developmental epidemiology of anxiety disorders. *Child and Adolescent Psychiatric Clinics*, 21(3), 457–478.  
<https://doi.org/https://doi.org/10.1016/j.chc.2012.05.001>
- Beesdo, K., Pine, D. S., Lieb, R., & Wittchen, H.-U. (2010). Incidence and risk patterns of anxiety and depressive disorders and categorization of generalized anxiety disorder. *Arch Gen Psychiatry*, 67(1), 47–57. <https://doi.org/10.1001/archgenpsychiatry.2009.177>
- Belardinelli, P., Biabani, M., Blumberger, D. M., Bortoletto, M., Casarotto, S., David, O., Desideri, D., Etkin, A., Ferrarelli, F., Fitzgerald, P. B., Fornito, A., Gordon, P. C., Gosseries, O., Harquel, S., Julkunen, P., Keller, C. J., Kimiskidis, V. K., Lioumis, P., Miniussi, C., ... Ilmoniemi, R. J. (2019). Reproducibility in TMS–EEG studies: A call for data sharing, standard procedures and effective experimental control. *Brain Stimulation*, 12(3), 787–790.  
<https://doi.org/10.1016/j.brs.2019.01.010>
- Bender, S., Basseler, K., Sebastian, I., Resch, F., Kammer, T., Oelkers-Ax, R., & Weisbrod, M. (2005). Transcranial magnetic stimulation evokes giant inhibitory potentials in children. *Annals of Neurology*, 58(1), 58–67. <https://doi.org/10.1002/ana.20521>
- Bender, S., Oelkers-Ax, R., Hellwig, S., Resch, F., & Weisbrod, M. (2008). The topography of the scalp-recorded visual N700. *Clinical Neurophysiology*, 119(3), 587–604.  
<https://doi.org/10.1016/J.CLINPH.2007.11.008>
- Bender, S., Oelkers-Ax, R., Resch, F., & Weisbrod, M. (2006). Frontal lobe involvement in the processing of meaningful auditory stimuli develops during childhood and adolescence. *NeuroImage*, 33(2), 759–773. <https://doi.org/10.1016/j.neuroimage.2006.07.003>
- Bennett, A. J., Wastell, D. G., Barker, G. R., Blackburn, C. W., & Rood, J. P. (1987). Trigeminal somatosensory evoked potentials. A review of the literature as applicable to oral dysaesthesias. *International Journal of Oral and Maxillofacial Surgery*, 16(4), 408–415.  
[https://doi.org/10.1016/S0901-5027\(87\)80076-0](https://doi.org/10.1016/S0901-5027(87)80076-0)
- Bennett, M., & Jannetta, P. J. (1980). Trigeminal evoked potentials in humans. *Electroencephalography and Clinical Neurophysiology*, 48(5), 517–526.  
[https://doi.org/10.1016/0013-4694\(80\)90287-4](https://doi.org/10.1016/0013-4694(80)90287-4)
- Bergmann, T. O., Mölle, M., Schmidt, M. A., Lindner, C., Marshall, L., Born, J., & Siebner, H. R. (2012). EEG-guided transcranial magnetic stimulation reveals rapid shifts in motor cortical excitability during the human sleep slow oscillation. *Journal of Neuroscience*, 32(1), 243–253.  
<https://doi.org/10.1523/JNEUROSCI.4792-11.2012>
- Bhagwagar, Z., Wylezinska, M., Taylor, M., Jezzard, P., Matthews, P. M., & Cowen, P. J. (2004). Increased Brain GABA Concentrations Following Acute Administration of a Selective Serotonin Reuptake Inhibitor. <https://doi.org/10.1176/Appi.Ajp.161.2.368>, 161(2), 368–370.  
<https://doi.org/10.1176/APPI.AJP.161.2.368>
- Biabani, M., Fornito, A., Mutanen, T. P., Morrow, J., & Rogasch, N. C. (2019). Characterizing and minimizing the contribution of sensory inputs to TMS-evoked potentials. *Brain Stimulation*, 12(6), 1537–1552. <https://doi.org/10.1016/j.brs.2019.07.009>
- Bishop, S. J. (2009). Trait anxiety and impoverished prefrontal control of attention. *Nat Neurosci*, 12(1), 92–98. <https://doi.org/10.1038/nn.2242>
- Bishop, S. J., Duncan, J., Brett, M., & Lawrence, A. D. (2004). Prefrontal cortical function and anxiety: Controlling attention to threat-related stimuli. *Nature Neuroscience*, 7(2), 184–188.  
<https://doi.org/10.1038/nn1173>
- Bishop, S. J., Jenkins, R., & Lawrence, A. D. (2007). Neural processing of fearful faces: Effects of

- anxiety are gated by perceptual capacity limitations. *Cerebral Cortex*, *17*(7), 1595–1603. <https://doi.org/10.1093/cercor/bhl070>
- Böhnlein, J., Altegoer, L., Muck, N. K., Roesmann, K., Redlich, R., Dannlowski, U., & Lehr, E. J. (2020). Factors influencing the success of exposure therapy for specific phobia: A systematic review. *Neuroscience and Biobehavioral Reviews*, *108*, 796–820. <https://doi.org/10.1016/J.NEUBIOREV.2019.12.009>
- Bonato, C., Miniussi, C., & Rossini, P. M. (2006). Transcranial magnetic stimulation and cortical evoked potentials: a TMS/EEG co-registration study. *Clin Neurophysiol*, *117*(8), 1699–1707. <https://doi.org/10.1016/j.clinph.2006.05.006>
- Bonnard, M., Spieser, L., Meziane, H. B., de Graaf, J. B., & Pailhous, J. (2009). Prior intention can locally tune inhibitory processes in the primary motor cortex: direct evidence from combined TMS-EEG. *Eur J Neurosci*, *30*(5), 913–923. <https://doi.org/10.1111/j.1460-9568.2009.06864.x>
- Bradley, C., Joyce, N., & Garcia-Larrea, L. (2016). Adaptation in human somatosensory cortex as a model of sensory memory construction: a study using high-density EEG. *Brain Structure and Function*, *221*(1), 421–431. <https://doi.org/10.1007/s00429-014-0915-5>
- Breiter, H. C., Etcoff, N. L., Whalen, P. J., Kennedy, W. A., Rauch, S. L., Buckner, R. L., Strauss, M. M., Hyman, S. E., & Rosen, B. R. (1996). Response and habituation of the human amygdala during visual processing of facial expression. *Neuron*, *17*(5), 875–887. [https://doi.org/10.1016/s0896-6273\(00\)80219-6](https://doi.org/10.1016/s0896-6273(00)80219-6)
- Bruckmann, S., Hauk, D., Roessner, V., Resch, F., Freitag, C. M., Kammer, T., Ziemann, U., Rothenberger, A., Weisbrod, M., & Bender, S. (2012). Cortical inhibition in attention deficit hyperactivity disorder: new insights from the electroencephalographic response to transcranial magnetic stimulation. *Brain*, *135*(Pt 7), 2215–2230. <https://doi.org/10.1093/brain/aws071>
- Bystritsky, A., Kerwin, L. E., & Feusner, J. D. (2009). A preliminary study of fMRI-guided rTMS in the treatment of generalized anxiety disorder: 6-Month follow-up. *Journal of Clinical Psychiatry*, *70*(3), 431–432. <https://doi.org/10.4088/JCP.08l04641>
- Carr, J. A. (2015). I'll take the low road: the evolutionary underpinnings of visually triggered fear. *Frontiers in Neuroscience*, *9*(414). <https://doi.org/10.3389/FNINS.2015.00414>
- Casarotto, S., Romero Lauro, L. J., Bellina, V., Casali, A. G., Rosanova, M., Pigorini, A., Defendi, S., Mariotti, M., & Massimini, M. (2010). EEG responses to TMS are sensitive to changes in the perturbation parameters and repeatable over time. *PLoS One*, *5*(4), e10281. <https://doi.org/10.1371/journal.pone.0010281>
- Chatrian, G. E., Lettich, E., & Nelson, P. L. (1985). Ten percent electrode system for topographic studies of spontaneous and evoked EEG activities. *American Journal of EEG Technology*, *25*(2), 83–92. <https://doi.org/10.1080/00029238.1985.11080163>
- Chen, L., Hudaib, A.-R., Hoy, K. E., & Fitzgerald, P. B. (2019). Is rTMS effective for anxiety symptoms in major depressive disorder? An efficacy analysis comparing left-sided high-frequency, right-sided low-frequency, and sequential bilateral rTMS protocols. *Depression and Anxiety*, *36*(8), 723–731. <https://doi.org/10.1002/da.22894>
- Chen, T. L., Babiloni, C., Ferretti, A., Perrucci, M. G., Romani, G. L., Rossini, P. M., Tartaro, A., Del Gratta, C., San, H., Cassino, R., San, I., & Pisana, R. (2008). Human secondary somatosensory cortex is involved in the processing of somatosensory rare stimuli: An fMRI study. *NeuroImage*, *40*(4), 1765–1771. <https://doi.org/10.1016/j.neuroimage.2008.01.020>
- Cicchetti, D. V. (1994). Guidelines, Criteria, and Rules of Thumb for Evaluating Normed and Standardized Assessment Instruments in Psychology. *Undefined*, *6*(4), 284–290.

<https://doi.org/10.1037/1040-3590.6.4.284>

- Clark, D. L., Boutros, N. N., & Mendez, M. F. (2010). *The Brain and Behavior - An Introduction to Behavioral Neuroanatomy* (3rd ed.). Cambridge University Press.  
<https://doi.org/10.1152/jn.2001.85.6.2602>
- Coelho, C. M., & Purkis, H. (2009). The Origins of Specific Phobias: Influential Theories and Current Perspectives: <https://doi.org/10.1037/A0017759>, 13(4), 335–348.  
<https://doi.org/10.1037/A0017759>
- Coghill, R. C., Gilron, I., & Iadarola, M. J. (2001). Hemispheric Lateralization of Somatosensory Processing. *J Neurophysiol*, 85(6), 2602–2612. <https://doi.org/10.1152/jn.2001.85.6.2602>
- Cohen, J. D., Perlstein, W. M., Braver, T. S., Nystrom, L. E., Noll, D. C., Jonides, J., & Smith, E. E. (1997). Temporal dynamics of brain activation during a working memory task. *Nature*, 386(6625), 604–608. <https://doi.org/10.1038/386604a0>
- Coles, M. G. H. (1989). Modern Mind-Brain Reading: Psychophysiology, Physiology, and Cognition. *Psychophysiology*, 26(3), 251–269. <https://doi.org/10.1111/J.1469-8986.1989.TB01916.X>
- Conde, V., Tomasevic, L., Akopian, I., Stanek, K., Saturnino, G. B., Thielscher, A., Ole, T., & Roman, H. (2019). The non-transcranial TMS-evoked potential is an inherent source of ambiguity in TMS-EEG studies. *NeuroImage*, 185(October 2018), 300–312.  
<https://doi.org/10.1016/j.neuroimage.2018.10.052>
- Cook, M., & Mineka, S. (1990). Selective Associations in the Observational Conditioning of Fear in Rhesus Monkeys. *Journal of Experimental Psychology: Animal Behavior Processes*, 16(4), 372–389. <https://doi.org/10.1037/0097-7403.16.4.372>
- Cracco, R. Q., Amassian, V. E., Maccabee, P. J., & Cracco, J. B. (1989). Comparison of human transcallosal responses evoked by magnetic coil and electrical stimulation. *Electroencephalography and Clinical Neurophysiology/Evoked Potentials Section*, 74(6), 417–424. [https://doi.org/10.1016/0168-5597\(89\)90030-0](https://doi.org/10.1016/0168-5597(89)90030-0)
- Craske, M. G., Treanor, M., Conway, C., Zbozinek, T., & Vervliet, B. (2014). Maximizing Exposure Therapy: An Inhibitory Learning Approach. *Behaviour Research and Therapy*, 58, 10.  
<https://doi.org/10.1016/j.BRAT.2014.04.006>
- Croarkin, P. E., Wall, C. A., King, J. D., Kozel, A., & Daskalakis, Z. J. (2011). Pain During Transcranial Magnetic Stimulation in Youth. *Innovations in Clinical Neuroscience*, 8(12), 18–23.  
<https://doi.org/10.1016/j.inclin.2011.12.001>
- Cryan, J. F., & Kaupmann, K. (2005). Don't worry 'B'happy!: a role for GABAB receptors in anxiety and depression. *Trends in Pharmacological Sciences*, 26(1), 36–43.  
<https://doi.org/10.1016/j.tips.2004.11.004>
- de Lijster, J. M., Dierckx, B., Utens, E. M. W. J., Verhulst, F. C., Zieldorff, C., Dieleman, G. C., & Legerstee, J. S. (2017). The Age of Onset of Anxiety Disorders: A Meta-analysis. *Canadian Journal of Psychiatry. Revue Canadienne de Psychiatrie*, 62(4), 237.  
<https://doi.org/10.1177/0706743716640757>
- De Witte, S., Klooster, D., Dedoncker, J., Duprat, R., Remue, J., & Baeken, C. (2018). Left prefrontal neuronavigated electrode localization in tDCS: 10–20 EEG system versus MRI-guided neuronavigation. *Psychiatry Research - Neuroimaging*, 274, 1–6.  
<https://doi.org/10.1016/j.pscychresns.2018.02.001>
- Del Casale, A., Ferracuti, S., Rapinesi, C., Serata, D., Piccirilli, M., Savoia, V., Kotzalidis, G. D., Manfredi, G., Angeletti, G., Tatarelli, R., & Girardi, P. (2012). Functional neuroimaging in specific phobia.

- Psychiatry Research - Neuroimaging*, 202(3), 181–197.  
<https://doi.org/10.1016/j.psychresns.2011.10.009>
- Derakshan, N., & Eysenck, M. W. (2009). Anxiety, processing efficiency, and cognitive performance: New developments from attentional control theory. *European Psychologist*, 14(2), 168–176.  
<https://doi.org/10.1027/1016-9040.14.2.168>
- Desmedt, J. E., & Robertson, D. (1977). Differential enhancement of early and late components of the cerebral somatosensory evoked potentials during forced-paced cognitive tasks in man. *The Journal of Physiology*, 271(3), 761–782. <https://doi.org/10.1113/jphysiol.1977.sp012025>
- Di Lazzaro, V., & Ziemann, U. (2013). The contribution of transcranial magnetic stimulation in the functional evaluation of microcircuits in human motor cortex. *Frontiers in Neural Circuits*, 7(18), 1–9. <https://doi.org/10.3389/FNCIR.2013.00018/BIBTEX>
- Djuric, S., Milenkovic, Z. J., Karabasevic, P., Jolic, M., & Stamenovic, J. (1977). Middle Latency Somatosensory Evoked Potentials of the Trigeminal Nerve in Normal Subjects and Clinical Correlation. *Medicine and Biology*, 4(1), 44–47.
- Du, X., Sen, F., Ann, C., Laura, S., Chiappelli, J., Kochunov, P., & Hong, L. E. (2017). N100 as a generic cortical electrophysiological marker based on decomposition of TMS - evoked potentials across five anatomic locations. *Experimental Brain Research*, 235(1), 69–81.  
<https://doi.org/10.1007/s00221-016-4773-7>
- Eickhoff, S. B., Schleicher, A., Zilles, K., & Amunts, K. (2006). The Human Parietal Operculum. I. Cytoarchitectonic Mapping of Subdivisions. *Cerebral Cortex*, 16(2), 245–267.  
<https://doi.org/10.1093/cercor/bhi105>
- Eimer, M. (1998). The lateralized readiness potential as an on-line measure of central response activation processes. *Behavior Research Methods, Instruments, & Computers*, 30(1), 146–156.  
<https://doi.org/10.3758/BF03209424>
- Enz, R., & Cutting, G. R. (1998). Molecular composition of GABAC receptors. *Vision Research*, 38(10), 1431–1441. [https://doi.org/10.1016/S0042-6989\(97\)00277-0](https://doi.org/10.1016/S0042-6989(97)00277-0)
- Eysenck, M. W., Derakshan, N., Santos, R., & Calvo, M. G. (2007). Anxiety and Cognitive Performance: Attentional Control Theory. *Emotion*, 7(2), 336–353. <https://doi.org/10.1037/1528-3542.7.2.336>
- Fales, C. L., Barch, D. M., Burgess, G. C., Schaefer, A., Mennin, D. S., Gray, J. R., & Braver, T. S. (2008). Anxiety and cognitive efficiency: Differential modulation of transient and sustained neural activity during a working memory task. *Cognitive, Affective and Behavioral Neuroscience*, 8(3), 239–253. <https://doi.org/10.3758/CABN.8.3.239>
- Figueira, J. S. B., Pacheco, L. B., Lobo, I., Volchan, E., Pereira, M. G., de Oliveira, L., & David, I. A. (2018). “Keep that in mind!” The role of Positive Affect in working memory for maintaining goal-relevant information. *Frontiers in Psychology*, 9(1228).  
<https://doi.org/10.3389/fpsyg.2018.01228>
- Fillmore, E. P., & Seifert, M. F. (2015). Anatomy of the Trigeminal Nerve. In R. S. Tubbs, E. Rizk, M. Shoja, M. Loukas, N. Barbaro, & R. Spinner (Eds.), *Nerves and Nerve Injuries* (Vol. 1, pp. 319–350). Academic Press. <https://doi.org/10.1016/B978-0-12-410390-0.00023-8>
- First, M. B., Williams, J. B. W., Karg, R. S., Spitzer, R. L., Beesdo-Baum, K., Zaudig, M., & Wittchen, H.-U. (2019). *SCID-5-CV: Strukturiertes Klinisches Interview für DSM-5-Störungen - Klinische Version*. Hogrefe.
- Fitzgerald, P. B., Maller, J. J., Hoy, K. E., Thomson, R., & Daskalakis, Z. J. (2009). Exploring the optimal

- site for the localization of dorsolateral prefrontal cortex in brain stimulation experiments. *Brain Stimulation*, 2(4), 234–237. <https://doi.org/10.1016/j.brs.2009.03.002>
- Fredrikson, M., Sundin, O., & Frankenhaeuser, M. (1985). Cortisol excretion during the defense reaction in humans. *Psychosomatic Medicine*, 47(4), 313–319. <https://doi.org/10.1097/00006842-198507000-00001>
- Freedberg, M., Reeves, J. A., Hussain, S. J., Zaghoul, K. A., & Wassermann, E. M. (2020). Identifying site- and stimulation-specific TMS-evoked EEG potentials using a quantitative cosine similarity metric. *PLOS ONE*, 15(1), e0216185. <https://doi.org/10.1371/JOURNAL.PONE.0216185>
- Freund, T. F., Gulyás, A. I., Acsády, L., Görcs, T., & Tóth, K. (1990). Serotonergic control of the hippocampus via local inhibitory interneurons. *Proceedings of the National Academy of Sciences of the United States of America*, 87(21), 8501–8505. <https://doi.org/10.1073/PNAS.87.21.8501>
- Galili, I., Kaplan, D., & Lehavi, Y. (2006). Teaching Faraday's law of electromagnetic induction in an introductory physics course. *American Journal of Physics*, 74(4), 337–343. <https://doi.org/10.1119/1.2180283>
- Ganella, D. E., Barendse, M. E. A., Kim, J. H., & Whittle, S. (2017). Prefrontal-Amygdala Connectivity and State Anxiety during Fear Extinction Recall in Adolescents. *Frontiers in Human Neuroscience*, 11, 587. <https://doi.org/10.3389/FNHUM.2017.00587>
- Garcia, R. (2017). Neurobiology of fear and specific phobias. *Learning & Memory*, 24(9), 462–471. <https://doi.org/10.1101/LM.044115.116>
- Genna, C., Artoni, F., Fanciullacci, C., Chisari, C., Oddo, C. M., & Micera, S. (2016). Long-latency components of somatosensory evoked potentials during passive tactile perception of gratings. *Annu Int Conf IEEE Eng Med Biol*, 1648–1651. <https://doi.org/10.1109/EMBC.2016.7591030>
- George, M. S. (2019). Whither TMS: A One-Trick Pony or the Beginning of a Neuroscientific Revolution? *Am J Psychiatry*, 176(11), 904–910. <https://doi.org/10.1176/APPI.AJP.2019.19090957>
- Goff, G. D., Matsumiya, Y., Allison, T., & Goff, W. R. (1977). The scalp topography of human somatosensory and auditory evoked potentials. *Electroencephalography and Clinical Neurophysiology*, 42(1), 57–76. [https://doi.org/10.1016/0013-4694\(77\)90151-1](https://doi.org/10.1016/0013-4694(77)90151-1)
- Gordon, P. C., Desideri, D., Belardinelli, P., Zrenner, C., & Ziemann, U. (2018). Comparison of cortical EEG responses to realistic sham versus real TMS of human motor cortex. *Brain Stimulation*, 11(6), 1322–1330. <https://doi.org/10.1016/j.brs.2018.08.003>
- Grace, A. A., & Rosenkranz, J. A. (2002). Regulation of conditioned responses of basolateral amygdala neurons. *Physiology & Behavior*, 77(4–5), 489–493. [https://doi.org/doi:10.1016/s0031-9384\(02\)00909-5](https://doi.org/doi:10.1016/s0031-9384(02)00909-5)
- Gray, J. (1990). *Psychobiological Aspects of Relationships Between Emotion and Cognition: A Special Issue of Cognition and Emotion (Special Issues of Cognition and Emotion)*. Psychology Press Ltd.
- Hallett, M. (2000). Transcranial magnetic stimulation and the human brain. *Nature*, 406, 147–150. <https://doi.org/10.1038/35018000>
- Hallett, M. (2007). Transcranial Magnetic Stimulation: A Primer. *Neuron*, 55(2), 187–199. <https://doi.org/10.1016/J.NEURON.2007.06.026>
- Hämäläinen, H., Kekoni, J., Sams, M., Reinikainen, K., & Näätänen, R. (1990). Human somatosensory evoked potentials to mechanical pulses and vibration: contributions of SI and SII somatosensory cortices to P50 and P100 components. *Electroencephalography and Clinical Neurophysiology*,

- 75(1–2), 13–21. [https://doi.org/10.1016/0013-4694\(90\)90148-D](https://doi.org/10.1016/0013-4694(90)90148-D)
- Hamilton, M. (1960). A rating scale for depression. *Journal of Neurology, Neurosurgery, and Psychiatry*, 23(1), 56–62. <https://doi.org/10.1136/jnnp.23.1.56>
- Hariri, A. R., Bookheimer, S. Y., & Mazziotta, J. C. (2000). Modulating emotional responses: effects of a neocortical network on the limbic system. *Neuroreport*, 11(1), 43–48. <https://doi.org/10.1097/00001756-200001170-00009>
- Hariri, A. R., Mattay, V. S., Tessitore, A., Fera, F., & Weinberger, D. R. (2003). Neocortical modulation of the amygdala response to fearful stimuli. *Biological Psychiatry*, 53(6), 494–501.
- Hartmann, A. S., Borgers, T., Thomas, J. J., Giabbiconi, C. M., & Vocks, S. (2020). Faced with one's fear: Attentional bias in anorexia nervosa and healthy individuals upon confrontation with an obese body stimulus in an eye-tracking paradigm. *Brain and Behavior*, 10(11), e01834. <https://doi.org/10.1002/BRB3.1834>
- Hashimoto, I. (1988). Trigeminal evoked potentials following brief air puff: Enhanced signal-to-noise ratio. *Annals of Neurology*, 23(4), 332–338. <https://doi.org/10.1002/ana.410230404>
- Helfrich, C., Pierau, S. S., Freitag, C. M., Roeper, J., Ziemann, U., & Bender, S. (2012). Monitoring Cortical Excitability during Repetitive Transcranial Magnetic Stimulation in Children with ADHD: A Single-Blind, Sham-Controlled TMS-EEG Study. *PLoS ONE*, 7(11), e50073. <https://doi.org/10.1371/journal.pone.0050073>
- Hennighausen, E., Heil, M., & Roesler, F. (1993). A correction method for DC drift artifacts. *Electroencephalography and Clinical Neurophysiology*, 86, 199–204. [https://doi.org/10.1016/0013-4694\(93\)90008-j](https://doi.org/10.1016/0013-4694(93)90008-j)
- Herring, J. D., Thut, G., Jensen, O., & Bergmann, T. O. (2015). Attention Modulates TMS-Locked Alpha Oscillations in the Visual Cortex. *Journal of Neuroscience*, 35(43), 14435–14447. <https://doi.org/10.1523/JNEUROSCI.1833-15.2015>
- Hettema, J. M., Neale, M. C., & Kendler, K. S. (2001). A review and meta-analysis of the genetic epidemiology of anxiety disorders. *American Journal of Psychiatry*, 158(10), 1568–1578. <https://doi.org/10.1176/appi.ajp.158.10.1568>
- Hill, A. T., Rogasch, N. C., Fitzgerald, P. B., & Hoy, K. E. (2016). TMS-EEG: A window into the neurophysiological effects of transcranial electrical stimulation in non-motor brain regions. *Neuroscience & Biobehavioral Reviews*, 64, 175–184. <https://doi.org/10.1016/J.NEUBIOREV.2016.03.006>
- Hine, J., & Debener, S. (2007). Late auditory evoked potentials asymmetry revisited. *Clinical Neurophysiology*, 118(6), 1274–1285. <https://doi.org/10.1016/j.clinph.2007.03.012>
- Horn, J., & Tjepkema-Cloostermans, M. C. (2017). Somatosensory evoked potentials in patients with hypoxic-ischemic brain injury. *Seminars in Neurology*, 37(1), 60–65. <https://doi.org/10.1055/s-0036-1594252>
- Ilmoniemi, R. J., Hernandez-Pavon, J. C., Makela, N. N., Metsomaa, J., Mutanen, T. P., Stenroos, M., & Sarvas, J. (2015). Dealing with artifacts in TMS-evoked EEG. *Proceedings of the Annual International Conference of the IEEE Engineering in Medicine and Biology Society, EMBS, 2015-November*, 230–233. <https://doi.org/10.1109/EMBC.2015.7318342>
- Ilmoniemi, R. J., & Kičić, D. (2010). Methodology for Combined TMS and EEG. *Brain Topography*, 22(4), 233–248. <https://doi.org/10.1007/s10548-009-0123-4>
- Ilmoniemi, R. J., Virtanen, J., Ruohonen, J., Karhu, J., Aronen, H. J., Näätänen, R., & Katila, T. (1997).

- Neuronal responses to magnetic stimulation reveal cortical reactivity and connectivity. *NeuroReport*, 8(16), 3537–3540. <https://doi.org/10.1097/00001756-199711100-00024>
- Jarczok, T. A., Fritsch, M., Kröger, A., Schneider, A. L., Althen, H., Siniatchkin, M., Freitag, C. M., & Bender, S. (2016). Maturation of interhemispheric signal propagation in autism spectrum disorder and typically developing controls: a TMS-EEG study. *Journal of Neural Transmission (Vienna, Austria : 1996)*, 123(8), 925–935. <https://doi.org/10.1007/S00702-016-1550-5>
- Jarczok, T. A., Roebruck, F., Pokorny, L., Biermann, L., Roessner, V., Klein, C., & Bender, S. (2021). Single pulse TMS to the temporo-occipital and dorsolateral prefrontal cortex evokes lateralized long latency EEG responses at the stimulation site. *Frontiers in Neuroscience*, 15, 60. <https://doi.org/10.3389/FNINS.2021.616667>
- Jie, F., Yin, G., Yang, W., Yang, M., Gao, S., Lv, J., & Li, B. (2018). Stress in Regulation of GABA Amygdala System and Relevance to Neuropsychiatric Diseases. *Frontiers in Neuroscience*, 12, 562. <https://doi.org/10.3389/FNINS.2018.00562>
- Jung, P., Baumgärtner, U., Stoeter, P., & Treede, R.-D. (2009). Structural and functional asymmetry in the human parietal opercular cortex. *J Neurophysiol*, 101(6), 3246–3257. <https://doi.org/10.1152/jn.91264.2008>
- Kähkönen, S., Komssi, S., Wilenius, J., & Ilmoniemi, R. J. (2005). Prefrontal TMS produces smaller EEG responses than motor-cortex TMS: Implications for rTMS treatment in depression. *Psychopharmacology*, 181(1), 16–20. <https://doi.org/10.1007/s00213-005-2197-3>
- Kaiser, D. A. (2010). Special Issue - Cortical Cartography. *Biofeedback*, 38(1), 9–12. <https://doi.org/https://doi.org/10.5298/1081-5937-38.1.9>
- Kammer, T., Beck, S., Thielscher, A., Laubis-Herrmann, U., & Topka, H. (2001). Motor thresholds in humans: a transcranial magnetic stimulation study comparing different pulse waveforms, current directions and stimulator types. *Clinical Neurophysiology : Official Journal of the International Federation of Clinical Neurophysiology*, 112(2), 250–258. [https://doi.org/10.1016/S1388-2457\(00\)00513-7](https://doi.org/10.1016/S1388-2457(00)00513-7)
- Kammer, T., & Thielscher, U. A. (2018). Physikalische und physiologische Grundlagen der transkraniellen Magnetstimulation. *Nervenheilkunde*, 22(4), 168–176. <https://doi.org/10.1055/S-0038-1624397>
- Kemp, W. J., Tubbs, R. S., Cohen-Gadol, A. A., & Cohen-Gadol, A. A. (2011). The innervation of the scalp: A comprehensive review including anatomy, pathology, and neurosurgical correlates. *Surgical Neurology International*, 2, 178. <https://doi.org/10.4103/2152-7806.90699>
- Kerwin, L. J., Keller, C. J., Wu, W., Narayan, M., & Etkin, A. (2018). Test-retest reliability of transcranial magnetic stimulation EEG evoked potentials. *Brain Stimulation*, 11(3), 536–544. <https://doi.org/10.1016/j.brs.2017.12.010>
- Kessler, R. C., Berglund, P., Demler, O., Jin, R., Merikangas, K. R., & Walters, E. E. (2005). Lifetime prevalence and age-of-onset distributions of DSM-IV disorders in the National Comorbidity Survey Replication. *Arch Gen Psychiatry*, 62(6), 593–602. <https://doi.org/10.1001/archpsyc.62.6.593>
- Kessler, R. C., Ruscio, A. M., Shear, K., & Wittchen, H.-U. (2009). Epidemiology of anxiety disorders. In *Behavioral neurobiology of anxiety and its treatment* (pp. 21–35). Springer.
- Khedr, E. M., El Fetoh, N. A., El Bieh, E., Ali, A. M., & Karim, A. A. (2014). Altered cortical excitability in anorexia nervosa. *Neurophysiologie Clinique/Clinical Neurophysiology*, 44(3), 291–299. <https://doi.org/10.1016/j.neucli.2014.08.002>

- Kida, T., Nishihira, Y., Wasaka, T., Sakajiri, Y., & Tazoe, T. (2004). Differential modulation of the short- and long-latency somatosensory evoked potentials in a forewarned reaction time task. *Clinical Neurophysiology*, *115*(10), 2223–2230. <https://doi.org/10.1016/J.CLINPH.2004.04.017>
- Kirschstein, T., & Köhling, R. (2009). What is the Source of the EEG?: *Clinical EEG and Neuroscience*, *40*(3), 146–149. <https://doi.org/10.1177/155005940904000305>
- Knight, R. T., Scabini, D., Woods, D. L., & Clayworth, C. (1988). The effects of lesions of superior temporal gyrus and inferior parietal lobe on temporal and vertex components of the human AEP. *Electroencephalography and Clinical Neurophysiology*, *70*(6), 499–509. [https://doi.org/10.1016/0013-4694\(88\)90148-4](https://doi.org/10.1016/0013-4694(88)90148-4)
- Komssi, S., & Kähkönen, S. (2006). The novelty value of the combined use of electroencephalography and transcranial magnetic stimulation for neuroscience research. *Brain Research Reviews*, *52*(1), 183–192. <https://doi.org/10.1016/J.BRAINRESREV.2006.01.008>
- Kushner, M. G., Abrams, K., & Borchardt, C. (2000). The relationship between anxiety disorders and alcohol use disorders: A review of major perspectives and findings. *Clinical Psychology Review*, *20*(2), 149–171. [https://doi.org/10.1016/S0272-7358\(99\)00027-6](https://doi.org/10.1016/S0272-7358(99)00027-6)
- Lachance, B., Wang, Z., Badjatia, N., & Jia, X. (2020). Somatosensory Evoked Potentials and Neuroprognostication After Cardiac Arrest. *Neurocritical Care*, *32*(3), 847–857. <https://doi.org/10.1007/s12028-019-00903-4>
- Langers, D. R. M., Van Dijk, P., & Backes, W. H. (2005). Lateralization, connectivity and plasticity in the human central auditory system. *NeuroImage*, *28*(2), 490–499. <https://doi.org/10.1016/j.neuroimage.2005.06.024>
- LeDoux, J. E. (2000). Emotion circuits in the brain. *Annual Review of Neuroscience*, *23*(1), 155–184. <https://doi.org/10.1146/annurev.neuro.23.1.155>
- LeDoux, J. E., & Pine, D. S. (2016). Using Neuroscience to Help Understand Fear and Anxiety: A Two-System Framework. *Am J Psychiatry*, *173*(11), 1083–1093. <https://doi.org/10.1176/APPI.AJP.2016.16030353>
- Lightfoot, G. (2016). Summary of the N1-P2 Cortical Auditory Evoked Potential to Estimate the Auditory Threshold in Adults. *Seminars in Hearing*, *37*(1), 1–8. <https://doi.org/10.1055/s-0035-1570334>
- Linares, I. M., Trzesniak, C., Chagas, M. H., Hallak, J. E., Nardi, A. E., & Crippa, J. A. (2012). Neuroimaging in specific phobia disorder: a systematic review of the literature. *Braz J Psychiatry*, *34*(1), 101–111. <https://pubmed.ncbi.nlm.nih.gov/22392396/>
- Lioumis, P., Kicić, D., Savolainen, P., Mäkelä, J. P., & Kähkönen, S. (2009). Reproducibility of TMS-Evoked EEG responses. *Hum Brain Mapp*, *30*(4), 1387–1396. <https://doi.org/10.1002/hbm.20608>
- Lioumis, P., Kičić, D., Savolainen, P., Mäkelä, J. P., & Kähkönen, S. (2009). Reproducibility of TMS - Evoked EEG responses. *Human Brain Mapping*, *30*(4), 1387–1396. <https://doi.org/10.1002/hbm.20608>
- Lioumis, P., Zomorodi, R., Hadas, I., Daskalakis, Z. J., & Blumberger, D. M. (2018). Combined transcranial magnetic stimulation and electroencephalography of the dorsolateral prefrontal cortex. *Journal of Visualized Experiments*, *2018*(138), e57983. <https://doi.org/10.3791/57983>
- Loheswaran, G., Barr, M. S., Zomorodi, R., Rajji, T. K., Blumberger, D. M., Le Foll, B., & Daskalakis, Z. J. (2018). Alcohol Impairs N100 Response to Dorsolateral Prefrontal Cortex Stimulation. *Scientific Reports*, *8*(1), 1–6. <https://doi.org/10.1038/s41598-018-21457-z>

- Lueken, U., Kruschwitz, J., Muehlhan, M., Siegert, Hoyer, J., & Wittchen, H. (2011). How specific is specific phobia? Different neural response patterns in two subtypes of specific phobia. *NeuroImage*, *56*(1), 363–372. <https://doi.org/10.1016/J.NEUROIMAGE.2011.02.015>
- MacDonald, A. W., Cohen, J. D., Stenger, V. A., & Carter, C. S. (2000). Dissociating the role of the dorsolateral prefrontal and anterior cingulate cortex in cognitive control. *Science*, *288*(5472), 1835–1838. <https://doi.org/10.1126/science.288.5472.1835>
- Magee, W. J., Eaton, W. W., Wittchen, H. U., McGonagle, K. A., & Kessler, R. C. (1996). Agoraphobia, simple phobia, and social phobia in the National Comorbidity Survey. *Archives of General Psychiatry*, *53*(2), 159–168. <https://doi.org/10.1001/ARCHPSYC.1996.01830020077009>
- Mahajan, Y., & McArthur, G. (2012). Maturation of auditory event-related potentials across adolescence. *Hearing Research*, *294*(1–2), 82–94. <https://doi.org/10.1016/J.HEARES.2012.10.005>
- Malizia, A. L., Cunningham, V. J., Bell, C. J., Liddle, P. F., Jones, T., & Nutt, D. J. (1998). Decreased brain GABA(A)-benzodiazepine receptor binding in panic disorder. Preliminary results from a quantitative PET study. *Archives of General Psychiatry*, *55*(8), 715–720. <https://doi.org/10.1001/archpsyc.55.8.715>
- Marowsky, A., Yanagawa, Y., Obata, K., & Vogt, K. E. (2005). A specialized subclass of interneurons mediates dopaminergic facilitation of amygdala function. *Neuron*, *48*(6), 1025–1037. <https://doi.org/10.1016/J.NEURON.2005.10.029>
- Massimini, M., Ferrarelli, F., Huber, R., Esser, S. K., Singh, H., & Tononi, G. (2005). Breakdown of cortical effective connectivity during sleep. *Science (New York, N.Y.)*, *309*(5744), 2228–2232. <https://doi.org/10.1126/science.1117256>
- McCallum, W. C., & Curry, S. H. (1980). The Form and Distribution of Auditory Evoked Potentials and CNVs when Stimuli and Responses are Lateralized. *Progress in Brain Research*, *54*(C), 767–775. [https://doi.org/10.1016/S0079-6123\(08\)61701-X](https://doi.org/10.1016/S0079-6123(08)61701-X)
- McClelland, J., Kekic, M., Bozhilova, N., Nestler, S., Dew, T., Van Den Eynde, F., David, A. S., Rubia, K., Campbell, I. C., & Schmidt, U. (2016). A Randomised Controlled Trial of Neuronavigated Repetitive Transcranial Magnetic Stimulation (rTMS) in Anorexia Nervosa. *PLOS ONE*, *11*(3), e0148606. <https://doi.org/10.1371/JOURNAL.PONE.0148606>
- McDonald, A. J., Mascagni, F., & Muller, J. F. (2004). Immunocytochemical localization of GABABR1 receptor subunits in the basolateral amygdala. *Brain Research*, *1018*(2), 147–158. <https://doi.org/10.1016/J.BRAINRES.2004.05.053>
- McLean, C. P., Asnaani, A., Litz, B. T., & Hofmann, S. G. (2011). Gender differences in anxiety disorders: prevalence, course of illness, comorbidity and burden of illness. *J Psychiatr Res*, *45*(8), 1027–1035. <https://doi.org/10.1016/j.jpsychires.2011.03.006>
- Meermann, E., & Okon, R. (2005). *Angststörungen: Agoraphobie, Panikstörung, spezifische Phobien* (A. Batra & G. Buchkremer (eds.)). Kohlhammer.
- Menzies, R. G., & Clarke, J. C. (1995). The etiology of phobias: a nonassociative account. *Clinical Psychology Review*, *15*(1), 23–48. [https://doi.org/10.1016/0272-7358\(94\)00039-5](https://doi.org/10.1016/0272-7358(94)00039-5)
- Merton, P. A., & Morton, H. B. (1980). Stimulation of the cerebral cortex in the intact human subject. *Nature*, *285*(5762), 227. <https://doi.org/10.1038/285227a0>
- Meuret, A. E., Wolitzky-Taylor, K. B., Twohig, M. P., & Craske, M. G. (2012). Coping Skills and Exposure Therapy in Panic Disorder and Agoraphobia: Latest Advances and Future Directions. *Behavior Therapy*, *43*(2), 271. <https://doi.org/10.1016/J.BETH.2011.08.002>

- Mineka, S., & Oehlberg, K. (2008). The relevance of recent developments in classical conditioning to understanding the etiology and maintenance of anxiety disorders. *Acta Psychologica*, *127*(3), 567–580. <https://doi.org/10.1016/J.ACTPSY.2007.11.007>
- Möhler, H. (2012). The GABA system in anxiety and depression and its therapeutic potential. *Neuropharmacology*, *62*(1), 42–53. <https://doi.org/10.1016/j.neuropharm.2011.08.040>
- Moliadze, V., Lyzhko, E., Schmanke, T., Andreas, S., Freitag, C. M., & Siniatchkin, M. (2018). 1 mA cathodal tDCS shows excitatory effects in children and adolescents: Insights from TMS evoked N100 potential. *Brain Research Bulletin*, *140*, 43–51. <https://doi.org/10.1016/J.BRAINRESBULL.2018.03.018>
- Mombereau, C., Kaupmann, K., Froestl, W., Sansig, G., van der Putten, H., & Cryan, J. F. (2004). Genetic and pharmacological evidence of a role for GABA(B) receptors in the modulation of anxiety- and antidepressant-like behavior. *Neuropsychopharmacology*, *29*(6), 1050–1062. <https://doi.org/10.1038/sj.npp.1300413>
- Mowrer, O. H. (1939). A stimulus-response analysis of anxiety and its role as a reinforcing agent. *Psychological Review*, *46*(6), 553–565. <https://doi.org/10.1037/H0054288>
- Mowrer, O. H. (1947). On the dual nature of learning—a re-interpretation of “conditioning” and “problem-solving.” *Harvard Educational Review*, *17*, 102–148. <https://psycnet.apa.org/record/1950-03076-001>
- Mowrer, O. H. (1956). Two-factor learning theory reconsidered, with special reference to secondary reinforcement and the concept of habit. *Psychological Review*, *63*(2), 114–128. <https://doi.org/10.1037/H0040613>
- Mowrer, O. H. (1960). Learning theory and behavior. In *Learning theory and behavior*. Wiley. <https://doi.org/10.1037/10802-000>
- Muris, P., Merckelbach, H., De Jong, P. J., & Ollendick, T. H. (2002). The etiology of specific fears and phobias in children: a critique of the non-associative account. *Behaviour Research and Therapy*, *40*(2), 185–195. [https://doi.org/10.1016/S0005-7967\(01\)00051-1](https://doi.org/10.1016/S0005-7967(01)00051-1)
- Mutanen, T., Mäki, H., & Ilmoniemi, R. J. (2013). The Effect of Stimulus Parameters on TMS–EEG Muscle Artifacts. *Brain Stimulation*, *6*(3), 371–376. <https://doi.org/10.1016/J.BRS.2012.07.005>
- Nakata, H., Sakamoto, K., Yumoto, M., & Kakigi, R. (2011). The relationship in gating effects between short-latency and long-latency somatosensory-evoked potentials. *Neuroreport*, *22*(18), 1000–1004. <https://doi.org/10.1097/WNR.0b013e32834dc296>
- Nevalainen, P., Ramstad, R., Isotalo, E., Haapanen, M. L., & Lauronen, L. (2006). Trigeminal somatosensory evoked magnetic fields to tactile stimulation. *Clinical Neurophysiology*, *117*(9), 2007–2015. <https://doi.org/10.1016/j.clinph.2006.05.019>
- Nikolaus, S., Antke, C., Beu, M., & Müller, H.-W. (2010). Cortical GABA, Striatal Dopamine and Midbrain Serotonin as the Key Players in Compulsive and Anxiety Disorders - Results from In Vivo Imaging Studies. *Reviews in the Neurosciences*, *21*(2), 119–140. <https://doi.org/10.1515/REVNEURO.2010.21.2.119>
- Nikouline, V., Ruohonen, J., & Ilmoniemi, R. J. (1999). The role of the coil click in TMS assessed with simultaneous EEG. *Clinical Neurophysiology*, *110*(8), 1325–1328. [https://doi.org/10.1016/S1388-2457\(99\)00070-X](https://doi.org/10.1016/S1388-2457(99)00070-X)
- Nikulin, V. V., Kicić, D., Kähkönen, S., & Ilmoniemi, R. J. (2003). Modulation of electroencephalographic responses to transcranial magnetic stimulation: evidence for changes in cortical excitability related to movement. *Eur J Neurosci*, *18*(5), 1206–1212.

<https://doi.org/10.1046/j.1460-9568.2003.02858.x>

- Noda, Y., Cash, R. F. H., Zomorodi, R., Dominguez, L. G., Farzan, F., Rajji, T. K., Barr, M. S., Chen, R., Daskalakis, Z. J., & Blumberger, D. M. (2016). A combined TMS-EEG study of short-latency afferent inhibition in the motor and dorsolateral prefrontal cortex. *Journal of Neurophysiology*, *116*(3), 938–948. <https://doi.org/10.1152/jn.00260.2016>
- Noda, Y., Zomorodi, R., Cash, R. F. H., Barr, M. S., Farzan, F., Rajji, T. K., Chen, R., Daskalakis, Z. J., & Blumberger, D. M. (2017). Characterization of the influence of age on GABAA and glutamatergic mediated functions in the dorsolateral prefrontal cortex using paired-pulse TMS-EEG. *Aging*, *9*(2), 556–572. <https://doi.org/10.18632/aging.101178>
- Nuss, P. (2015). Anxiety disorders and GABA neurotransmission: a disturbance of modulation. *Neuropsychiatric Disease and Treatment*, *11*, 165–175. <https://doi.org/10.2147/NDT.S58841>
- Oberndorfer, T. A., Kaye, W. H., Simmons, A. N., Strigo, I. A., & Matthews, S. C. (2011). Demand-specific alteration of medial prefrontal cortex response during an inhibition task in recovered anorexic women. *The International Journal of Eating Disorders*, *44*(1), 1–8. <https://doi.org/10.1002/EAT.20750>
- Öhman, A., & Mineka, S. (2001). Fears, phobias, and preparedness: Toward an evolved module of fear and fear learning. *Psychological Review*, *108*(3), 483–522. <https://doi.org/10.1037/0033-295X.108.3.483>
- Oldfield, R. C. (1971). The assessment and analysis of handedness: The Edinburgh inventory. *Neuropsychologia*, *9*(1), 97–113. [https://doi.org/10.1016/0028-3932\(71\)90067-4](https://doi.org/10.1016/0028-3932(71)90067-4)
- Owen, A. M., McMillan, K. M., Laird, A. R., & Bullmore, E. (2005). N-back working memory paradigm: a meta-analysis of normative functional neuroimaging studies. *Hum Brain Mapp*, *25*(1), 46–59. <https://doi.org/10.1002/hbm.20131>
- Paes, F., Baczynski, T., Novaes, F., Marinho, T., Arias-Carrión, O., Budde, H., Sack, A. T., Huston, J. P., Almada, L. F., Carta, M., Silva, A. C., Nardi, A. E., & Machado, S. (2013). Repetitive Transcranial Magnetic Stimulation (rTMS) to Treat Social Anxiety Disorder: Case Reports and a Review of the Literature. *Clinical Practice & Epidemiology in Mental Health*, *9*(1), 180–188. <https://doi.org/10.2174/1745017901309010180>
- Pape, H.-C., & Pare, D. (2010). Plastic Synaptic Networks of the Amygdala for the Acquisition, Expression, and Extinction of Conditioned Fear. *Physiol Rev*, *90*, 419–463. <https://doi.org/10.1152/physrev.00037.2009>
- Paré, D., Quirk, G. J., & LeDoux, J. E. (2004). New vistas on amygdala networks in conditioned fear. *Journal of Neurophysiology*, *92*(1), 1–9. <https://doi.org/10.1152/JN.00153.2004>
- Paus, T., Keshavan, M., & Giedd, J. N. (2008). Why do many psychiatric disorders emerge during adolescence? *Nature Reviews Neuroscience*, *9*, 947–957. <https://doi.org/10.1038/nrn2513>
- Paus, T., Sipila, P. K., & Strafella, A. P. (2001). Synchronization of neuronal activity in the human primary motor cortex by transcranial magnetic stimulation: an EEG study. *Journal of Neurophysiology*, *86*(4), 1983–1990. <https://doi.org/10.1152/jn.2001.86.4.1983>
- Perera, T., George, M. S., Grammer, G., Janicak, P. G., Pascual-Leone, A., & Wirecki, T. S. (2016). The Clinical TMS Society Consensus Review and Treatment Recommendations for TMS Therapy for Major Depressive Disorder. *Brain Stimulation*, *9*(3), 336–346. <https://doi.org/10.1016/J.BRS.2016.03.010>
- Phelps, E. A. (2006). Emotion and cognition: Insights from studies of the human amygdala. *Annual Review of Psychology*, *57*, 27–53. <https://doi.org/10.1146/annurev.psych.56.091103.070234>

- Pollack, M. H., Roy-Byrne, P. P., Van Ameringen, M., Snyder, H., Brown, C., Ondrasik, J., & Rickels, K. (2005). The selective GABA reuptake inhibitor tiagabine for the treatment of generalized anxiety disorder: Results of a placebo-controlled study. *Journal of Clinical Psychiatry, 66*(11), 1401–1408. <https://doi.org/10.4088/JCP.v66n1109>
- Poulton, R., & Menzies, R. G. (2002). Non-associative fear acquisition: a review of the evidence from retrospective and longitudinal research. *Behaviour Research and Therapy, 40*(2), 127–149. [https://doi.org/10.1016/S0005-7967\(01\)00045-6](https://doi.org/10.1016/S0005-7967(01)00045-6)
- Powers, M. B., & Emmelkamp, P. M. (2008). Virtual reality exposure therapy for anxiety disorders: A meta-analysis. *J Anxiety Disord, 22*(3), 561–569. <https://doi.org/10.1016/j.janxdis.2007.04.006>
- Premoli, I., Castellanos, N., Rivolta, D., Belardinelli, P., Bajo, R., Zipser, C., Espenhahn, S., Heidegger, T., Müller-Dahlhaus, F., & Ziemann, U. (2014). TMS-EEG signatures of GABAergic neurotransmission in the human cortex. *Journal of Neuroscience, 34*(16), 5603–5612. <https://doi.org/10.1523/JNEUROSCI.5089-13.2014>
- Premoli, I., Király, J., Müller-Dahlhaus, F., Zipser, C. M., Rossini, P., Zrenner, C., Ziemann, U., & Belardinelli, P. (2018). Short-interval and long-interval intracortical inhibition of TMS-evoked EEG potentials. *Brain Stimulation, 11*(4), 818–827. <https://doi.org/10.1016/j.BRS.2018.03.008>
- Premoli, I., Rivolta, D., Espenhahn, S., Castellanos, N., Belardinelli, P., Ziemann, U., & Müller-Dahlhaus, F. (2014). Characterization of GABAB-receptor mediated neurotransmission in the human cortex by paired-pulse TMS-EEG. *NeuroImage, 103*, 152–162. <https://doi.org/10.1016/J.NEUROIMAGE.2014.09.028>
- Quirk, G. J., & Mueller, D. (2008). Neural mechanisms of extinction learning and retrieval. *Neuropsychopharmacology, 33*(1), 56–72. <https://doi.org/10.1038/sj.npp.1301555>
- Rachman, S. (1977). The conditioning theory of fear-acquisition: a critical examination. *Behaviour Research and Therapy, 15*(5), 375–387. [https://doi.org/10.1016/0005-7967\(77\)90041-9](https://doi.org/10.1016/0005-7967(77)90041-9)
- Rahko, J., Paakki, J., Starck, T., Nikkinen, J., & Remes, J. (2010). Functional Mapping of Dynamic Happy and Fearful Facial Expression Processing in Adolescents. *Brain Imaging and Behavior, 4*, 164–176. <https://doi.org/10.1007/s11682-010-9096-x>
- Raymond, J. G., Steele, J. D., & Seriès, P. (2017). Modeling trait anxiety: From computational processes to personality. *Frontiers in Psychiatry, 8*(1), 1–19. <https://doi.org/10.3389/fpsy.2017.00001>
- Reti, I. M. (2015). *Brain stimulation : methodologies and interventions*. Wiley-Blackwell. <https://www.wiley.com/en-us/Brain+Stimulation:+Methodologies+and+Interventions-p-9781118568293>
- Rocchi, L., Di Santo, A., Brown, K., Ibáñez, J., Casula, E., Rawji, V., Di Lazzaro, V., Koch, G., & Rothwell, J. (2021). Disentangling EEG responses to TMS due to cortical and peripheral activations. *Brain Stimulation, 14*(1), 4–18. <https://doi.org/10.1016/j.brs.2020.10.011>
- Rogasch, N. C., Daskalakis, Z. J., & Fitzgerald, P. B. (2015). Cortical inhibition of distinct mechanisms in the dorsolateral prefrontal cortex is related to working memory performance: a TMS-EEG study. *Cortex, 64*, 68–77. <https://doi.org/10.1016/j.cortex.2014.10.003>
- Rogasch, N. C., & Fitzgerald, P. B. (2013). Assessing cortical network properties using TMS-EEG. *Human Brain Mapping, 34*(7), 1652–1669. <https://doi.org/10.1002/hbm.22016>
- Rogasch, N. C., Thomson, R. H., Farzan, F., Fitzgibbon, B. M., Bailey, N. W., Hernandez-Pavon, J. C., Daskalakis, Z. J., & Fitzgerald, P. B. (2014). Removing artefacts from TMS-EEG recordings using independent component analysis: Importance for assessing prefrontal and motor cortex

- network properties. *NeuroImage*, *101*, 425–439.  
<https://doi.org/10.1016/j.neuroimage.2014.07.037>
- Rogasch, N. C., Zipser, C., Darmani, G., Mutanen, T. P., Biabani, M., Zrenner, C., Desideri, D., Belardinelli, P., Müller-Dahlhaus, F., & Ziemann, U. (2020). The effects of NMDA receptor blockade on TMS-evoked EEG potentials from prefrontal and parietal cortex. *Scientific Reports*, *10*(1), 3168. <https://doi.org/10.1038/s41598-020-59911-6>
- Roos, D., Biermann, L., Jarczok, T. A., & Bender, S. (2021). Local Differences in Cortical Excitability – A Systematic Mapping Study of the TMS-Evoked N100 Component. *Frontiers in Neuroscience*, *15*(623692), 1–17. <https://doi.org/10.3389/FNINS.2021.623692>
- Rosanova, M., Casali, A., Bellina, V., Resta, F., Mariotti, M., & Massimini, M. (2009). Natural Frequencies of Human Corticothalamic Circuits. *Journal of Neuroscience*, *29*(24), 7679–7685. <https://doi.org/10.1523/JNEUROSCI.0445-09.2009>
- Rosenkranz, J. A., & Grace, A. A. (2001). Dopamine attenuates prefrontal cortical suppression of sensory inputs to the basolateral amygdala of rats. *The Journal of Neuroscience : The Official Journal of the Society for Neuroscience*, *21*(11), 4090–4103. <https://doi.org/10.1523/JNEUROSCI.21-11-04090.2001>
- Rossi, S., Hallett, M., Rossini, P. M., Pascual-Leone, A., & Group, T. S. of T. C. (2009). Safety, ethical considerations, and application guidelines for the use of transcranial magnetic stimulation in clinical practice and research. *Clinical Neurophysiology : Official Journal of the International Federation of Clinical Neurophysiology*, *120*(12), 2008–2039. <https://doi.org/10.1016/j.clinph.2009.08.016>
- Rossini, P. M., Barker, A. T., Berardelli, A., Caramia, M. D., Caruso, G., Cracco, R. Q., Dimitrijević, M. R., Hallett, M., Katayama, Y., Lücking, C. H., Maertens de Noordhout, A. L., Marsden, C. D., Murray, N. M. F., Rothwell, J. C., Swash, M., & Tomberg, C. (1994). Non-invasive electrical and magnetic stimulation of the brain, spinal cord and roots: basic principles and procedures for routine clinical application. Report of an IFCN committee. *Electroencephalography and Clinical Neurophysiology*, *91*(2), 79–92. [https://doi.org/10.1016/0013-4694\(94\)90029-9](https://doi.org/10.1016/0013-4694(94)90029-9)
- Rothwell, J., Hallett, M., Berardelli, A., Eisen, A., Rossini, P., & Paulus, W. (1999). Magnetic stimulation: motor evoked potentials. *Electroencephalogr Clin Neurophysiol Suppl.*, *52*, 97–103. <https://pubmed.ncbi.nlm.nih.gov/10590980/>
- Rusjan, P. M., Barr, M. S., Farzan, F., Arenovich, T., Maller, J. J., Fitzgerald, P. B., & Daskalakis, Z. J. (2010). Optimal Transcranial Magnetic Stimulation Coil Placement for Targeting the Dorsolateral Prefrontal Cortex Using Novel Magnetic Resonance Image-Guided Neuronavigation. *Hum Brain Mapp*, *31*(11), 1643–1652. <https://doi.org/10.1002/hbm.20964>
- Russo, S., Sarasso, S., Puglisi, G. E., Dal Palù, D., Pigorini, A., Casarotto, S., D’Ambrosio, S., Astolfi, A., Massimini, M., Rosanova, M., & Fecchio, M. (2022). TAAC - TMS Adaptable Auditory Control: a universal tool to mask TMS click. *Journal of Neuroscience Methods*, 109491. <https://doi.org/10.1016/J.JNEUMETH.2022.109491>
- Sagliano, L., D’Olimpio, F., Panico, F., Gagliardi, S., & Trojano, L. (2016). The role of the dorsolateral prefrontal cortex in early threat processing: A TMS study. *Social Cognitive and Affective Neuroscience*, *11*(12), 1992–1998. <https://doi.org/10.1093/scan/nsw105>
- Samaha, J., Gosseries, O., & Postle, B. R. (2017). Distinct Oscillatory Frequencies Underlie Excitability of Human Occipital and Parietal Cortex. *Journal of Neuroscience*, *37*(11), 2824–2833. <https://doi.org/10.1523/JNEUROSCI.3413-16.2017>
- Schandry, R. (2016). *Biologische Psychologie* (4th ed.). Beltz Verlag.

[https://www.beltz.de/produkt\\_detailansicht/8082-biologische-psychologie.html](https://www.beltz.de/produkt_detailansicht/8082-biologische-psychologie.html)

- Schiele, M. A., Herzog, K., Kollert, L., Schartner, C., Leehr, E. J., Böhnlein, J., Repple, J., Rosenkranz, K., Lonsdorf, T. B., Dannlowski, U., Zwanzger, P., Reif, A., Pauli, P., Deckert, J., & Domschke, K. (2020). Extending the vulnerability–stress model of mental disorders: three-dimensional NPSR1 × environment × coping interaction study in anxiety. *The British Journal of Psychiatry*, *217*(5), 645–650. <https://doi.org/10.1192/BJP.2020.73>
- Schienze, A., Schäfer, A., Walter, B., Stark, R., & Vaitl, D. (2005). Brain activation of spider phobics towards disorder-relevant, generally disgust-and fear-inducing pictures. *Neuroscience Letters*, *388*(1), 1–6. <https://doi.org/10.1016/j.neulet.2005.06.025>
- Seligman, M. E. P. (1971). Phobias and preparedness. *Behavior Therapy*, *2*(3), 307–320. [https://doi.org/10.1016/S0005-7894\(71\)80064-3](https://doi.org/10.1016/S0005-7894(71)80064-3)
- Siebner, H. R., Conde, V., Tomasevic, L., Thielscher, A., & Bergmann, T. O. (2019). Distilling the essence of TMS-evoked EEG potentials (TEPs): A call for securing mechanistic specificity and experimental rigor. *Brain Stimulation*, *12*(4), 1051–1054. <https://doi.org/10.1016/j.brs.2019.03.076>
- Skinner, B. F. (1938). *The behavior of organisms: an experimental analysis*. <https://psycnet.apa.org/record/1939-00056-000>
- Smeets, E., Roefs, A., Van Furth, E., & Jansen, A. (2008). Attentional bias for body and food in eating disorders: Increased distraction, speeded detection, or both? *Behaviour Research and Therapy*, *46*, 229–238. <https://doi.org/10.1016/j.brat.2007.12.003>
- Sotres-Bayon, F., & Quirk, G. J. (2010). Prefrontal control of fear: More than just extinction. *Current Opinion in Neurobiology*, *20*(2), 231–235. <https://doi.org/10.1016/j.conb.2010.02.005>
- Stinson, F. S., Dawson, D. A., Chou, S. P., Smith, S., Goldstein, R. B., Ruan, W. J., & Grant, B. F. (2007). The epidemiology of DSM-IV specific phobia in the USA: results from the National Epidemiologic Survey on Alcohol and Related Conditions. *Psychological Medicine*, *37*(7), 1047–1059. <https://doi.org/10.1017/S0033291707000086>
- Straube, T., Mentzel, H. J., Glauer, M., & Miltner, W. H. R. (2004). Brain activation to phobia-related words in phobic subjects. *Neuroscience Letters*, *372*(3), 204–208. <https://doi.org/10.1016/j.neulet.2004.09.050>
- Stujenske, J. M., & Likhtik, E. (2017). Fear from the bottom up: amygdala inputs to the prefrontal cortex. *Nature Neuroscience*, *20*(6), 765–767. <https://doi.org/10.1038/NN.4578>
- Tallus, J., Lioumis, P., Hämäläinen, H., Kähkönen, S., & Tenovuo, O. (2013). Transcranial magnetic stimulation-electroencephalography responses in recovered and symptomatic mild traumatic brain injury. *Journal of Neurotrauma*, *30*(14), 1270–1277. <https://doi.org/10.1089/neu.2012.2760>
- Tao, D., He, Z., Lin, Y., Liu, C., & Tao, Q. (2021). Where does fear originate in the brain? A coordinate-based meta-analysis of explicit and implicit fear processing. *NeuroImage*, *227*(117686), 1–11. <https://doi.org/10.1016/j.NEUROIMAGE.2020.117686>
- Taquet, M., Holmes, E. A., & Harrison, P. J. (2021). Depression and anxiety disorders during the COVID-19 pandemic: knowns and unknowns. *The Lancet*, *398*(10312), 1665–1666. [https://doi.org/10.1016/S0140-6736\(21\)02221-2](https://doi.org/10.1016/S0140-6736(21)02221-2)
- Teng, S., Guo, Z., Peng, H., Xing, G., Chen, H., He, B., McClure, M. A., & Mu, Q. (2017). High-frequency repetitive transcranial magnetic stimulation over the left DLPFC for major depression: Session-dependent efficacy: A meta-analysis. *European Psychiatry*, *41*, 75–84.

<https://doi.org/10.1016/j.eurpsy.2016.11.002>

- ter Braack, E. M., de Vos, C. C., & van Putten, M. J. A. M. (2015). Masking the Auditory Evoked Potential in TMS–EEG: A Comparison of Various Methods. *Brain Topography*, *28*(3), 520–528. <https://doi.org/10.1007/s10548-013-0312-z>
- Thomson, A. M., & Destexhe, A. (1999). Dual intracellular recordings and computational models of slow inhibitory postsynaptic potentials in rat neocortical and hippocampal slices. *Neuroscience*, *92*(4), 1193–1215. [https://doi.org/10.1016/S0306-4522\(99\)00021-4](https://doi.org/10.1016/S0306-4522(99)00021-4)
- Thut, G., Veniero, D., Romei, V., Miniussi, C., Schyns, P., & Gross, J. (2011). Rhythmic TMS causes local entrainment of natural oscillatory signatures. *Current Biology*, *21*(14), 1176–1185. <https://doi.org/10.1016/j.cub.2011.05.049>
- Tonnquist-Uhlen, I., Ponton, C. W., Eggermont, J. J., Kwong, B., & Don, M. (2003). Maturation of human central auditory system activity: The T-complex. *Clinical Neurophysiology*, *114*(4), 685–701. [https://doi.org/10.1016/S1388-2457\(03\)00005-1](https://doi.org/10.1016/S1388-2457(03)00005-1)
- Tremblay, S., Rogasch, N. C., Premoli, I., Blumberger, D. M., Casarotto, S., Chen, R., Lazzaro, V. Di, Farzan, F., Fitzgerald, P. B., Hui, J., Ilmoniemi, R. J., & Vasilios, K. (2019). Clinical utility and prospective of TMS-EEG. *Clinical Neurophysiology*, *130*(5), 802–844. <https://doi.org/10.1016/j.clinph.2019.01.001>
- Trepel, M. (2017). *Neuroanatomie: Struktur und Funktion* (7th ed.). Urban & Fischer Verlag/Elsevier GmbH.
- Vagg, P. R., Spielberger, C. D., & O’Hearn, T. P. (1980). Is the state-trait anxiety inventory multidimensional? *Personality and Individual Differences*, *1*(3), 207–214. [https://doi.org/10.1016/0191-8869\(80\)90052-5](https://doi.org/10.1016/0191-8869(80)90052-5)
- Van Houtem, C. M., Laine, M. L., Boomsma, D. I., Ligthart, L., van Wijk, A. J., & De Jongh, A. (2013). A review and meta-analysis of the heritability of specific phobia subtypes and corresponding fears. *Journal of Anxiety Disorders*, *27*(4), 379–388. <https://doi.org/10.1016/J.JANXDIS.2013.04.007>
- Veniero, D., Bortoletto, M., & Miniussi, C. (2009). TMS-EEG co-registration: on TMS-induced artifact. *Clin Neurophysiol*, *120*(7), 1392–1399. <https://doi.org/10.1016/j.clinph.2009.04.023>
- Venkatasubramanian, G., & Narayanaswamy, J. C. (2019). Transcranial direct current stimulation in psychiatry. *The Lancet Psychiatry*, *6*(1), 8–9. [https://doi.org/10.1016/S2215-0366\(18\)30468-1](https://doi.org/10.1016/S2215-0366(18)30468-1)
- Voineskos, D., Blumberger, D. M., Zomorodi, R., Rogasch, N. C., Farzan, F., Foussias, G., Rajji, T. K., & Daskalakis, Z. J. (2018). Altered Transcranial Magnetic Stimulation–Electroencephalographic Markers of Inhibition and Excitation in the Dorsolateral Prefrontal Cortex in Major Depressive Disorder. *Biological Psychiatry*, *85*(6), 477–486. <https://doi.org/10.1016/j.biopsych.2018.09.032>
- Wardenaar, K. J., Lim, C. C. W., Al-Hamzawi, A. O., Alonso, J., Andrade, L. H., Benjet, C., Bunting, B., de Girolamo, G., Demyttenaere, K., Florescu, S. E., Gureje, O., Hisateru, T., Hu, C., Huang, Y., Karam, E., Kiejna, A., Lepine, J. P., Navarro-Mateu, F., Oakley Browne, M., ... de Jonge, P. (2017). The cross-national epidemiology of specific phobia in the World Mental Health Surveys. *Psychol Med*, *47*(10), 1744–1760. <https://doi.org/10.1017/s0033291717000174>
- Westin, G. G., Bassi, B. D., Lisanby, S. H., & Luber, B. (2014). Determination of motor threshold using visual observation overestimates transcranial magnetic stimulation dosage: Safety implications. *Clinical Neurophysiology*, *125*(1), 142–147. <https://doi.org/10.1016/J.CLINPH.2013.06.187>
- Weyh, T., & Siebner, H. R. (2007). Hirnstimulation — Technische Grundlagen. In H. Siebner & U. Ziemann (Eds.), *Das TMS-Buch* (pp. 17–26). Springer Medizin Verlag.

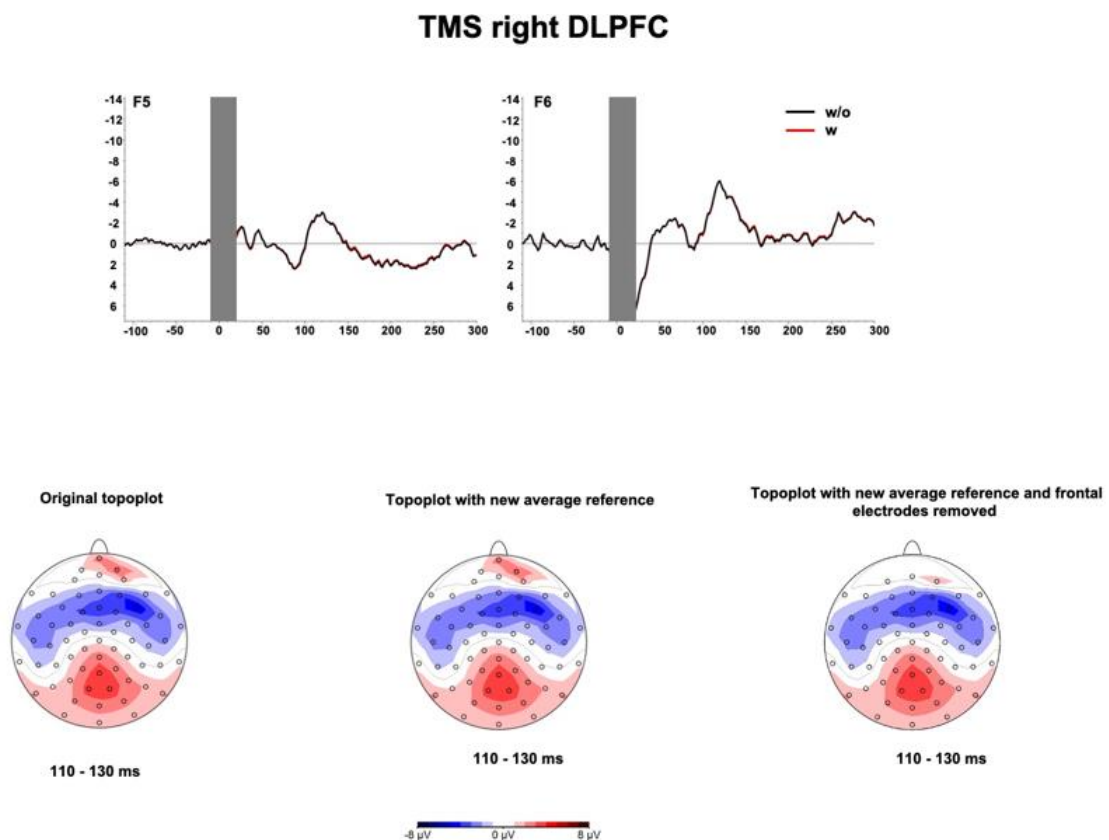
[https://doi.org/10.1007/978-3-540-71905-2\\_2](https://doi.org/10.1007/978-3-540-71905-2_2)

- Whalen, P. J. (1998). Fear, Vigilance, and Ambiguity: Initial Neuroimaging Studies of the Human Amygdala. *Current Directions in Psychological Science*, 7(6), 177–188.  
<https://doi.org/https://doi.org/10.1111/1467-8721.ep10836912>
- Williams, J. B. W. (1988). A structured interview guide for the Hamilton Depression Rating Scale. *Archives of General Psychiatry*, 45(8), 742–747.  
<https://doi.org/10.1001/ARCHPSYC.1988.01800320058007>
- Wittchen, H.-U., & Hoyer, J. (2011). *Klinische Psychologie & Psychotherapie* (Vol. 2). Springer-Verlag Berlin Heidelberg. <https://link.springer.com/book/10.1007/978-3-642-13018-2>
- Wu, D., Xiong, W., Jia, X., Geocadin, R. G., & Thakor, N. V. (2012). Short-and long-latency somatosensory neuronal responses reveal selective brain injury and effect of hypothermia in global hypoxic ischemia. *J Neurophysiol*, 107, 1164–1171.  
<https://doi.org/10.1152/jn.00681.2011.-Evoked>
- Yamanaka, K., Kadota, H., & Nozaki, D. (2013). Long-latency TMS-evoked potentials during motor execution and inhibition. *Frontiers in Human Neuroscience*, 7(751), 1–11.  
<https://doi.org/10.3389/FNHUM.2013.00751/BIBTEX>
- Yang, T., Menon, V., Eliez, S., Blasey, C., White, C., Reid, A., Gotlib, I., & Reiss, A. (2002). Amygdalar activation associated with positive and negative facial expressions. *Neuroreport*, 13(14), 1737–1741. <https://doi.org/10.1097/00001756-200210070-00009>
- Yu, Y., Yang, J., Ejima, Y., Fukuyama, H., & Wu, J. (2018). Asymmetric Functional Connectivity of the Contra- and Ipsilateral Secondary Somatosensory Cortex during Tactile Object Recognition. *Frontiers in Human Neuroscience*, 11(662), 1–7. <https://doi.org/10.3389/fnhum.2017.00662>
- Ziemann, U. (2003). Pharmacology of TMS. *Supplements to Clinical Neurophysiology*, 56, 226–231.  
[https://doi.org/10.1016/S1567-424X\(09\)70226-0](https://doi.org/10.1016/S1567-424X(09)70226-0)
- Zimmermann, K. S., Richardson, R., & Baker, K. D. (2019). Maturation changes in prefrontal and amygdala circuits in adolescence: implications for understanding fear inhibition during a vulnerable period of development. *Brain Sciences*, 9(65), 1–20.  
<https://doi.org/10.3390/brainsci9030065>

## 6 Supplementary Material

### Supplmenetary Material Study 1: Single-Pulse TMS to the Temporo-Occipital and Dorsolateral Prefrontal Cortex Evokes Lateralized Long Latency EEG Responses at the Stimulation Site

The Supplementary Material for this article can be found online at: <https://www.frontiersin.org/articles/10.3389/fnins.2021.616667/full#supplementary-material>



Image\_1\_Single-Pulse TMS to the Temporo-Occipital and Dorsolateral Prefrontal Cortex Evokes Lateralized Long Latency EEG Responses at the Stimulation

#### 1. Procedure for determining the stimulation site for temporo-occipital cortex TMS

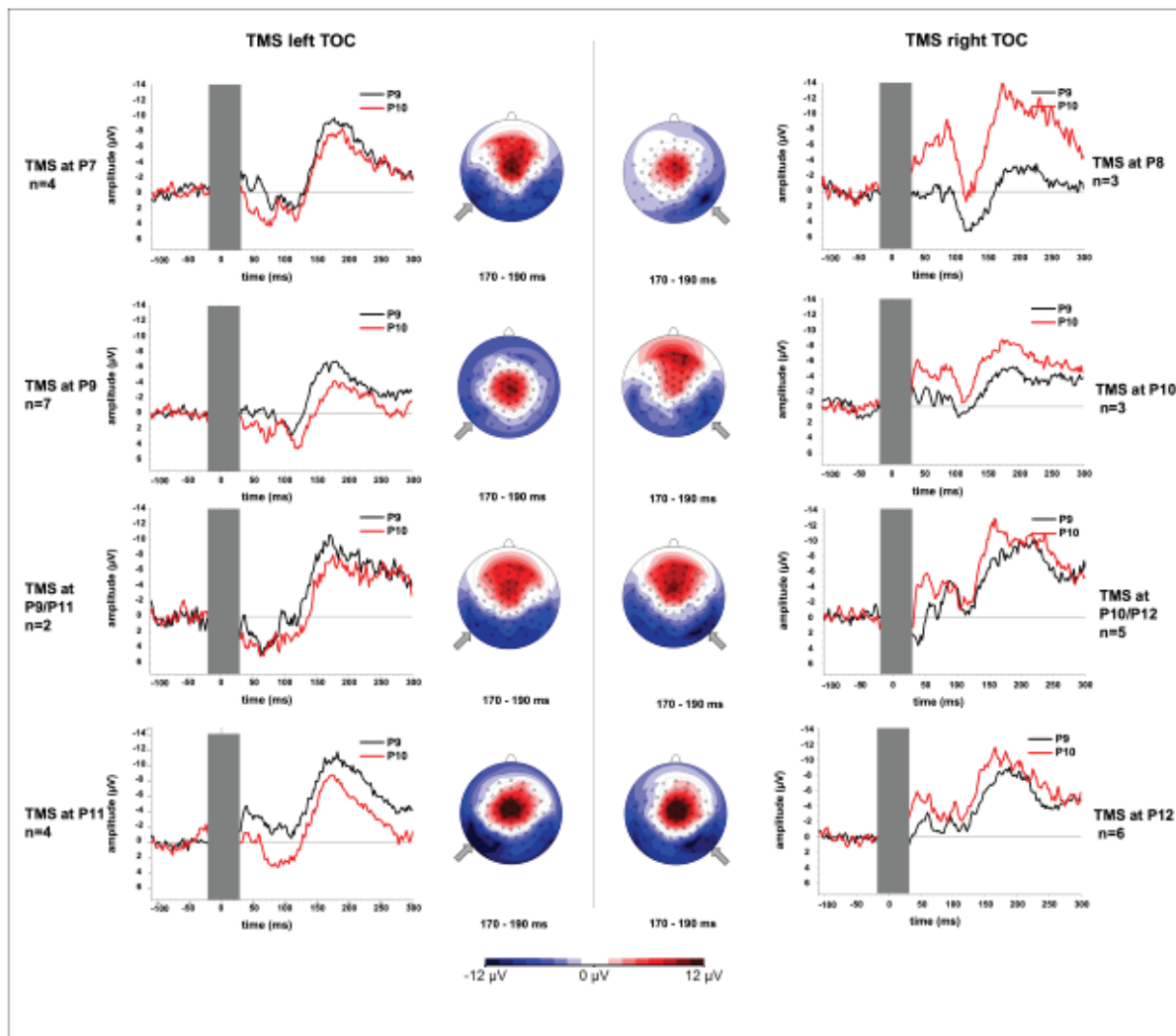
The exact site of stimulation for temporo-occipital cortex stimulation was determined by localizing the visual N700 event-related potential (ERP) component (Bender et al., 2008). To this end subjects performed a visual working memory task (change detection task) before the transcranial magnetic stimulation (TMS) procedure. In this task an initial visual stimulus (S1) consisting of colored squares distributed equally over both visual hemifields (5 in each hemifield) had to be compared to a second stimulus (S2). S2 was presented to either the right

or the left visual hemifield. In 50% of trials S2 was identical to the same hemifield presented in S1. Subjects were instructed to indicate whether S2 differed from the corresponding hemifield in S1 or not by pressing one of two buttons. A version of task with minor variations is described in detail by Hecht et al. (2016). The differences to that task were a shorter interval between S1 and S2 (900 ms), less trials (32 stimulus pairs) and a shorter inter-stimulus interval (varying between 6 and 10 ms) in the task used here. ERPs were analysed immediately after with Brain Vision Analyzer 2.1 software (Brain Products GmbH, München) in order to determine the electrode with the highest N700 peak amplitude in each individual participant, which was then chosen as the stimulation site for this person. The locus of stimulation was determined separately for each hemisphere.

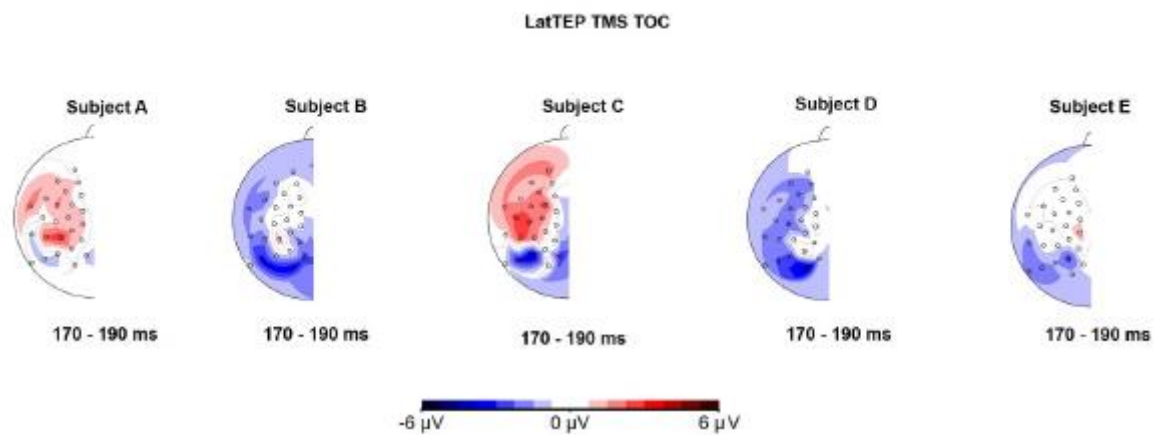
Therefore, S2 was averaged separately for left and the right visual hemifield presentation. The visual N700 component has its modality specific maximum amplitude contralateral to the side of the presentation of S2 over the visual association cortex (Bender et al., 2010). If no N700 component was detectable in a participant, TMS was performed at electrodes P9 for the left hemisphere and P10 for the right hemisphere.

## **2. Effects of the exact coil position on TEP topography**

TMS was administered at electrodes P7 (n=4), P9 (n=7), between P9 and P11 (n=2) or at P11 (n=4) for TMS to the left temporo-occipital cortex (TOC) and at P8 (n=3), P10 (n=3) between P10 and P12 (n=5) or at P12 (n=6). TEP grand averages calculated separately for each exact coil location in the temporooccipital cortex (TOC) stimulation condition revealed only a small non-systematic effect on the topography. The lateralization effect found for the overall group with higher N180 amplitudes ipsilateral to the stimulated hemisphere was present in each of the sub-groups (Supplementary Figure 1). LatTEPs on a single subject level show a robust negative maximum at temporo-occipital electrodes in individual averages (examples in Supplementary Figure 2).



**Supplementary Figure 1:** TEP grand averages for each sub-group that was stimulated at a specific location in the temporo-occipital cortex. In each of the sub-groups TEP time courses at electrodes P9 and P10 show higher N180 amplitudes in the electrode ipsilateral to the stimulated hemisphere (i.e., P9 higher than P10 for TMS to the left temporo-occipital cortex, P10 higher than P10 for TMS to the right temporo-occipital cortex). A negative ipsilateral maximum can be observed in the corresponding topoplots in temporo-occipital electrodes in the time window 170 to 190 ms.



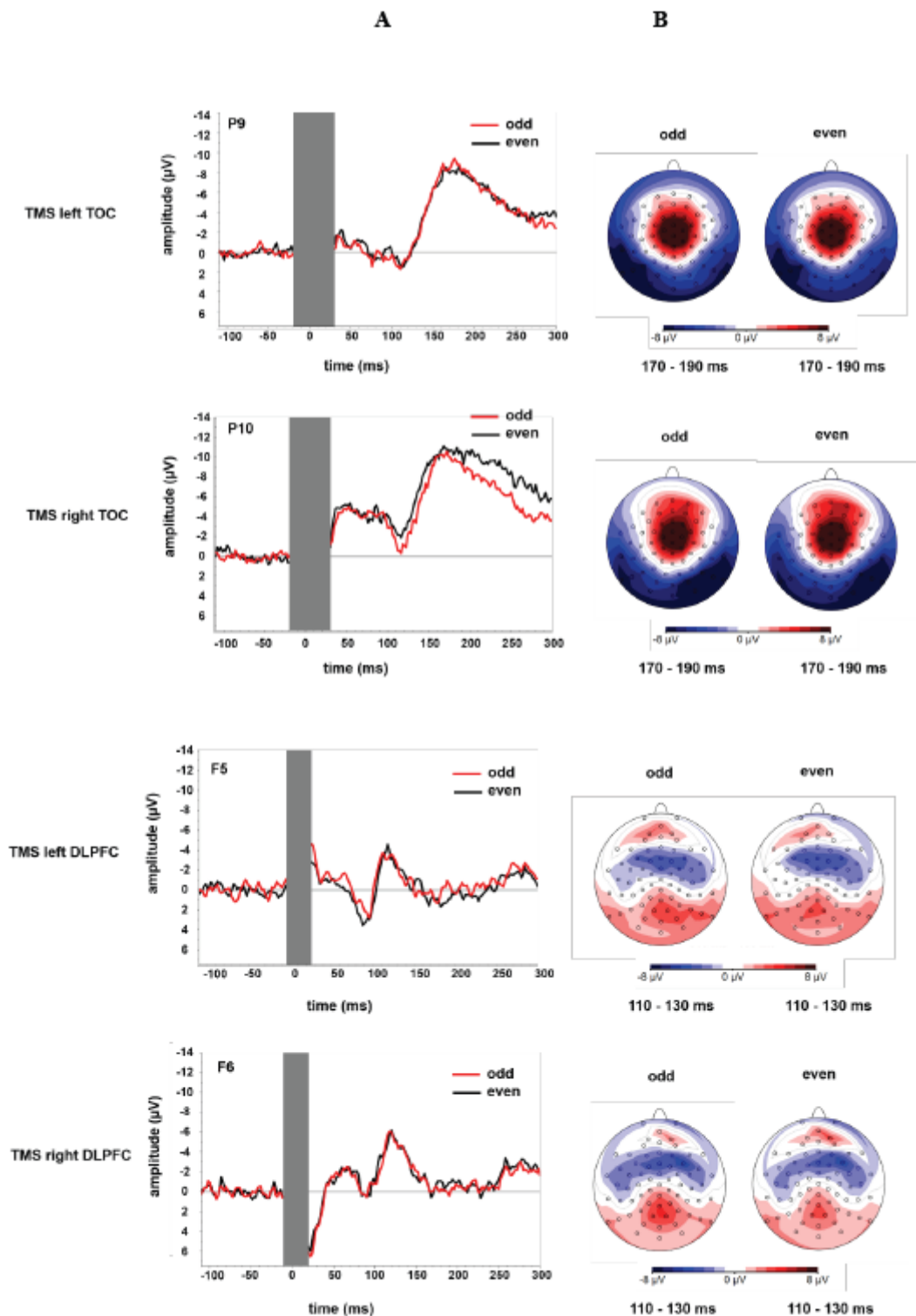
**Supplementary Figure 2:** Examples of individual LatTEP averages for five subjects. The negative maximum in electrodes around the stimulation site in the temporo-occipital cortex can be observed on a single subject level.

### 3. Assessment of Reliability

**Supplementary Table 1:** Intraclass correlation of the peak amplitudes of TEP averages of odd and even trials.

Electrode (Stimulation Site)	ICC	CI 95%	
F5 (DLPFC left)	0.89	0.76	0.95
F6 (DLPFC right)	0.95	0.89	0.98
P9 (TOC left)	0.98	0.93	0.99
P10 (TOC right)	0.78	0.42	0.92

*ICC* intraclass correlation coefficient



**Supplementary Figure 3:** Time course of TEPs at the site of stimulation (A) and topoplots (B) for split-half averages in each stimulation condition. Odd and even trials were averaged separately to assess the reliability of the measurements. Topoplots present the time window corresponding to the peak latency of the TEP in the respective condition. A high reliability was found across the time course of the TEP and in particular at the latency of long latency negative peak.

### References Supplementary Material Study 1:

- Bender, S., Behringer, S., Freitag, C.M., Resch, F., Weisbrod, M., 2010. Transmodal comparison of auditory, motor, and visual post-processing with and without intentional short-term memory maintenance. *Clin. Neurophysiol.* 121, 2044–2064.
- Bender, S., Oelkers-Ax, R., Hellwig, S., Resch, F., Weisbrod, M., 2008. The topography of the scalp-recorded visual N700. *Clin. Neurophysiol.* 119, 587–604.
- Hecht, M., Thiemann, U., Freitag, C.M., Bender, S., 2016. Time-resolved neuroimaging of visual short term memory consolidation by post-perceptual attention shifts. *NeuroImage* 125, 964–977.

## Supplementary Material Study 2: Topography and lateralization of long-latency trigeminal somatosensory evoked potentials

The Supplementary Material for this article can be found online at: <https://doi.org/10.1016/j.clinph.2021.11.073>

### A. Sample details

Table A1: Demographical and stimulation parameters of the sample.

	Subjects (N = 14, plus 1 single-subject)
Age (years)	22.8 ± 1.6
Sex (f/m)	11/4
Handedness (r/l)	13/2
Occupation	
Student (N)	14
Pupil (N)	1
Volume White Noise for auditory masking (dB)	91.7 ± 4.3
TMS stimulation parameters (% MSO)	
Resting Motor Threshold (% MSO)	53.4 ± 11.6
Electrical nerve stimulation parameters	
Perception threshold intensity (mA)	1.1 ± 0.2
Electrical stimulation intensity (mA)	4.4 ± 2.6

Note. TMS = Transcranial magnetic stimulation; MSO = maximum stimulator output.

### B. Lateralized activity calculation

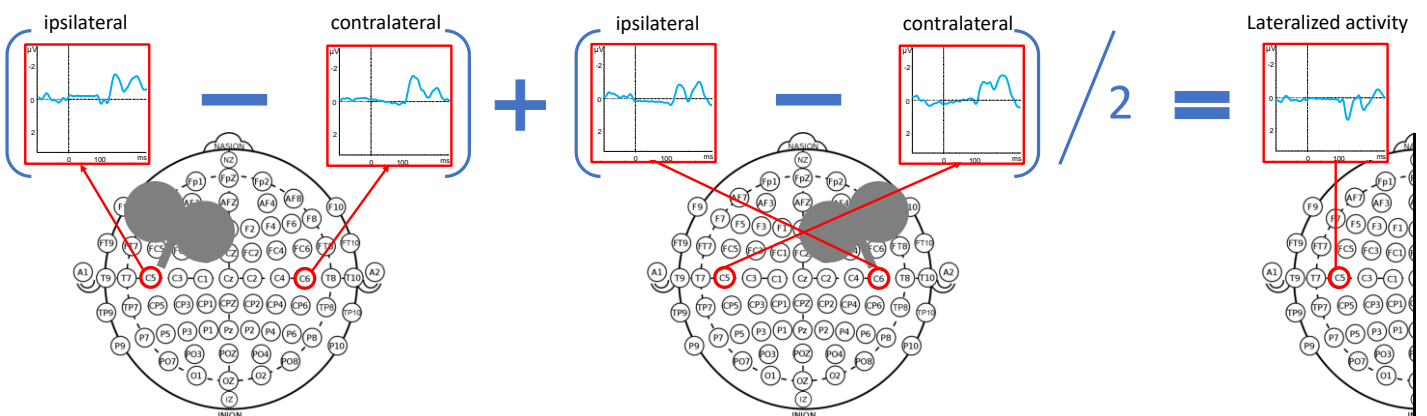


Figure B1. Visualization of the calculation procedure of the lateralized activity. The contralateral hemisphere was subtracted from the ipsilateral hemisphere.

## **Supplementary Material Study 3: Fearful facial expressions reduce inhibition levels in the dorsolateral prefrontal cortex in subjects with specific phobia**

The Supplementary Material for this article can be found online at:  
<https://onlinelibrary.wiley.com/doi/full/10.1002/da.23217>

### **A. Analyses of subtypes of specific phobia**

#### **A.1 Statistics**

In order to explore possible influences of different subtypes of specific phobia, a further analysis was calculated including only subjects with animal phobias (rest condition: 15 subjects, 1-back-task condition: 14 subjects) since this was the largest subgroup in our sample. This analysis was analogous to the described calculations with all subjects with specific phobia. To investigate possible differences between different subtypes within the group of specific phobia, a 2x2 ANOVA at rest with the within-subject factor SIDE and the between-subject factor SUBTYPE and the 3x2 ANOVA in the emotional 1-back-task with the factors EMOTION and SUBTYPE were repeated only for the group of specific phobia without control subjects (rest condition: 15 subjects with animal phobias vs. 7 subjects with other specific phobia subtypes, 1-back-task: 14 subjects with animal phobias vs. 7 subjects with other specific phobia subtypes).

#### **A.2 Results of TMS-evoked N100 at rest**

The 2x2 ANOVA comparing subjects with animal phobias and the control group (15 subjects with animal phobias vs. 24 controls) showed a trend towards a main effect of GROUP ( $F(1,37)=3.62$ ,  $p=.07$ , partial  $\eta^2=.09$ ) with animal phobias showing smaller N100 amplitudes compared to controls (Table 1). No other main effect or interaction was obtained (main effect SIDE:  $F(1,37)=3.03$ ,  $p=.09$ , partial  $\eta^2=.08$ ; interaction SIDE x GROUP:  $F(1,37)=.10$ ,  $p=.75$ , partial  $\eta^2=.003$ ).

Within the group of specific phobias, the 2x2 ANOVA comparing subjects with animal phobias and subjects with other subtypes of phobias (15 subjects with animal phobias vs. 7 subjects with other specific phobia subtypes) showed no main effect of SUBTYPE ( $F(1,20)<.001$ ,  $p=1.0$ ,

partial  $\eta^2 < .001$ ). Thus, there was no difference in the N100 amplitude over both stimulation sides between the groups of subtypes.

### **A.3 Results of TMS-evoked N100: effect of emotional facial expression**

The 3x2 ANOVA comparing subjects with animal phobias and the control group showed a significant main effect of EMOTION ( $F(1.70, 59.50) = 4.19, p = .03^*$ , partial  $\eta^2 = .11$ ) with smallest DLPFC N100 amplitudes for fearful facial expressions (Table 1). Moreover, there was a significant main effect of GROUP ( $F(1,35) = 5.01, p = .03^*$ , partial  $\eta^2 = .13$ ) with subjects with animal phobias presenting lower DLPFC N100 amplitudes. EMOTION and GROUP did not interact (EMOTION x GROUP:  $F(1.70, 59.50) = 1.70, p = .19$ , partial  $\eta^2 = .05$ ).

Considering the specific phobic group alone, the 3x2 ANOVA comparing subjects with animal phobias to subjects with other specific phobia subtypes (14 subjects with animal phobias vs. 7 subjects with other specific phobia subtypes) showed no difference in the N100 amplitude between the subtype groups (main effect SUBTYPE:  $F(1,19) = .03, p = .87$ , partial  $\eta^2 = .001$ ). There was a main effect in EMOTION ( $F(1.53, 29.06) = 3.94, p = .04^*$ , partial  $\eta^2 = .17$ ). There was no difference in the N100 amplitude between the subtype groups (main effect SUBTYPE:  $F(1,19) = .03, p = .87$ , partial  $\eta^2 = .001$ ). EMOTION and SUBTYPE did not interact ( $F(1.53, 29.06) = .20, p = .82$ , partial  $\eta^2 = .01$ ).

### **A.4 Further discussion on the subtype analysis**

Few studies exist that examine possible differences in functional cortical activation patterns between different subtypes of specific phobia (Lueken et al., 2011). In the literature, specific phobic subjects of the blood-injection-injury type show differences in their sustained reactions in the emotional processing (Caseras, Giampietro, et al., 2010; Caseras, Mataix-Cols, et al., 2010; Lueken et al., 2011). We only had one subject with this subtype.

### **B. Lateralized activity: description and calculation**

Lateralized activity was extracted from the data to visualize lateralized potentials. The calculation results in one channel encompassing signals from both stimulation sides and both hemispheres. The calculation was analogous to the calculation of lateralized readiness potentials (Coles, 1989).

The following is an example calculation:

*lateralized F5/F6*

$$= \frac{F5(TMS\ left) - F6(TMS\ left) + F6(TMS\ right) - F5(TMS\ right)}{2}$$

Each electrode pair of homologous electrodes for both stimulation sides were treated in this fashion. Ipsilaterally lateralized potential components thus appear with their original polarity when the lateralized activity is calculated (i.e. ipsilateral negative potentials lead to negative deflections in the lateralized activity). While the transcranially evoked cortical response occurs at the stimulation site, peripherally evoked auditory or somatosensory responses are lateralized to the contralateral hemisphere and include negativity over fronto-temporal areas (Jarczok et al., 2021; Rocchi et al., 2021). Contralateral negativities lead in this calculation to positive deflections in the lateralized activity due to the subtraction procedure ipsilateral minus contralateral potentials. Symmetrical components that are not lateralized, like early auditory evoked potentials are subtracted.

In conclusion, lateralized activity results are well suited to isolate potential components which systematically depend on the stimulation site, like the TMS-evoked N100. However, they always need to be analyzed together with the “original data” maps for left- and right-sided stimulation. This is necessary to determine whether lateralized activity reflects ipsi- or contralateral activity.

### C. Confidence intervals for partial $\eta^2$

Table C1. *Effect sizes and confidence intervals for the resulting main effects, interactions, and mean differences.*

	ANOVAs		t-tests	
	Part. $\eta^2$	90%-CI [LL;UL]	Cohen's <i>d</i>	95%-CI [LL;UL]
<b>ANOVAs</b>				
N100: rest				
GROUP*	.091	[.002;.236]		
SIDE	.083	[.000;.226]		
SIDE x GROUP	.005	[.000;.084]		
N100: 1-back task				
CONDITION	.041	[.000;.170]		
GROUP *	.127	[.013;.283]		
CONDITION x GROUP	.004	[.000;.083]		
N100: effect of emotional facial expressions				
EMOTION*	.087	[.005;.192]		
EMOTION x GROUP	.034	[.000;.114]		
EMOTION* (specific phobia group)	.197	[.012;.366]		
EMOTION (control group)	.015	[.000;.081]		
Reaction time: effect of emotional facial expressions				
RT EMOTION**	.431	[.283;.529]		
GROUP	.001	[.000;.046]		
RT EMOTION x GROUP	.012	[.000;.058]		
Subtype Analysis: effect of different subtypes of phobia				
N100(animal vs. control): rest				
GROUP	.089	[.000;.247]		
SIDE	.076	[.000;.230]		
SIDE x GROUP	.003	[.000;.079]		
N100(animal vs. other phobias): rest				
SUBTYPE	<.001	[.000;.000]		
SIDE	.057	[.000;.256]		
SIDE x GROUP	.002	[.000;.070]		

N100(animal vs. control): effect of emotional facial expressions		
GROUP*	.125	[.006;.294]
EMOTION*	.107	[.008;.225]
SIDE x GROUP	.046	[.000;.142]

N100(animal vs. other phobias): effect of emotional facial expressions		
SUBTYPE	.001	[.000;.055]
EMOTION*	.172	[.004;.345]
SIDE x GROUP	.010	[.000;.097]

#### **t-tests**

N100: Fearful vs. neutral facial expressions*	.464	[.151;.773]
N100: Fearful vs. angry facial expressions	.245	[-.056;.544]
N100: Angry vs. neutral facial expressions	.119	[-.178;.415]
Error rate: specific phobia vs. control group*	-.710	[-1.338;-.073]
Reaction time: Fearful vs. neutral facial expressions**	-.713	[-1.053;-.366]
Reaction time: Angry vs. neutral facial expressions**	-1.090	[-1.473;-.698]
Reaction time: Angry vs. fearful facial expressions**	.582	[.248;.912]

---

LL=lower limit; UL=upper limit

\* significant main effect or interaction

\*\* highly significant main effect or interaction

#### **D. Detailed discussion on the sample size and power of results**

Our result of a smaller N100 in the specific phobia group with a medium effect size of partial  $\eta^2=.09$  is in good agreement with meta-analytic results on short-interval cortical inhibition (a measure of inhibition in the motor cortex) in other psychiatric populations (Radhu et al., 2013). In addition, we found a significant main effect of GROUP, suggesting a sufficiently large sample size to examine our main outcome, a difference in N100 between specific phobia and controls at rest (Hoenig & Heisey, 2001).

In the 1-back-task condition, two additional subjects had to be excluded from the analyses. We obtained a significant N100 GROUP difference during the task with 44 subjects as well. We

also obtained a significant effect of EMOTION. However, we could not find a significant EMOTION x GROUP interaction. With our sample size, we cannot resolve the question of whether the emotion effect found in this study is specific to people with an anxiety disorder or whether it is a general effect that can also be found in control subjects (or can be found in control subjects to a lesser extent). It is therefore important for future studies with a larger sample size to clarify whether such an interaction exists.

### References Supplementary Material Study 3:

- Caseras, X., Giampietro, V., Lamas, A., Brammer, M., Vilarroya, O., Carmona, S., Rovira, M., Torrubia, R., & Mataix-Cols, D. (2010). The functional neuroanatomy of blood-injection-injury phobia: a comparison with spider phobics and healthy controls. *Psychological Medicine, 40*(1), 125–134. <https://doi.org/10.1017/S0033291709005972>
- Caseras, X., Mataix-Cols, D., Trasovares, M., López-Solà, M., Ortriz, H., Pujol, J., Soriano-Mas, C., Giampietro, V., Brammer, M., & Torrubia, R. (2010). Dynamics of brain responses to phobic-related stimulation in specific phobia subtypes. *The European Journal of Neuroscience, 32*(8), 1414–1422. <https://doi.org/10.1111/J.1460-9568.2010.07424.X>
- Coles, M. G. H. (1989). Modern Mind-Brain Reading: Psychophysiology, Physiology, and Cognition. *Psychophysiology, 26*(3), 251–269. <https://doi.org/10.1111/J.1469-8986.1989.TB01916.X>
- Hoenig, J. M., & Heisey, D. M. (2001). The abuse of power: The pervasive fallacy of power calculations for data analysis. *American Statistician, 55*(1), 19–24. <https://doi.org/10.1198/000313001300339897>
- Jarczok, T. A., Roebruck, F., Pokorny, L., Biermann, L., Roessner, V., Klein, C., & Bender, S. (2021). Single pulse TMS to the temporo-occipital and dorsolateral prefrontal cortex evokes lateralized long latency EEG responses at the stimulation site. *Frontiers in Neuroscience, 15*, 60. <https://doi.org/10.3389/FNINS.2021.616667>
- Lueken, U., Kruschwitz, J., Muehlhan, M., Siegert, Hoyer, J., & Wittchen, H. (2011). How specific is specific phobia? Different neural response patterns in two subtypes of specific phobia. *NeuroImage, 56*(1), 363–372. <https://doi.org/10.1016/J.NEUROIMAGE.2011.02.015>
- Radhu, N., de Jesus, D. R., Ravindran, L. N., Zanjani, A., Fitzgerald, P. B., & Daskalakis, Z. J. (2013). A meta-analysis of cortical inhibition and excitability using transcranial magnetic stimulation in psychiatric disorders. *Clinical Neurophysiology, 124*(7), 1309–1320. <https://doi.org/10.1016/j.clinph.2013.01.014>
- Rocchi, L., Di Santo, A., Brown, K., Ibáñez, J., Casula, E., Rawji, V., Di Lazzaro, V., Koch, G., & Rothwell, J. (2021). Disentangling EEG responses to TMS due to cortical and peripheral activations. *Brain Stimulation, 14*(1), 4–18. <https://doi.org/10.1016/j.brs.2020.10.011>